TRANSCRIPTIONAL TARGETS AND PROTEIN INTERACTIONS OF NKX2-2 IN EWING SARCOMA

by

John Phillip Lorenzo Fadul

A dissertation submitted to the faculty of
The University of Utah
in partial fulfillment of the requirements for the degree of

Doctor of Philosophy

Department of Oncological Sciences

The University of Utah

August 2015

The University of Utah Graduate School

STATEMENT OF DISSERTATION APPROVAL

The dissertation of **John Phillip Lorenzo Fadul**

has been approved by the following supervisory committee members:

Stephen L. Lessnick	, Chair	**May 26, 2015** Date Approved
Bradley R. Cairns	, Member	**May 26, 2015** Date Approved
Michael E. Engel	, Member	**May 26, 2015** Date Approved
Laura M. Hoffman	, Member	**May 26, 2015** Date Approved
Rodney A. Stewart	, Member	**May 26, 2015** Date Approved

and by **Bradley R. Cairns** , Chair/Dean of

the Department/College/School of **Oncological Sciences**

and by David B. Kieda, Dean of The Graduate School.

ABSTRACT

Ewing sarcoma is a bone-associated malignancy of children and adolescents caused by EWS/FLI, an oncogenic transcription factor encoded by a chromosomal translocation. EWS/FLI causes massive transcriptional dysregulation. A critical upregulated target, NKX2-2, is a homeodomain transcription factor required for Ewing sarcomagenesis; however, its specific role in this disease is unknown. We addressed this question using a twofold approach. First, using RNA sequencing, we found that NKX2-2 represses genes important for cell adhesion and ECM organization. We also show that it inhibits mesenchymal features of Ewing sarcoma cells: actin stress fiber organization, focal adhesion assembly, cell spreading—phenocopying EWS/FLI knockdown. NKX2-2-depleted cells also display increased cell adhesion and migration. Finally, we show that NKX2-2 and ZEB2 mediate anti-mesenchymalization and anti-epithelialization programs, respectively, in Ewing sarcoma to keep cells in a partially undifferentiated state. Second, we show that NKX2.2 binds MTG16 in an interaction that is disrupted by Notch. Presumably, these proteins comprise a repressor complex given the proper cellular context. Furthermore, NKX2.2 is capable of oligomerization; interestingly, both heterotypic and homotypic interactions are mediated by the transcriptional activation domain of NKX2.2. While the biological significance of the NKX2.2-MTG16 interaction is currently unknown, we propose that investigating this complex may be tractable in pancreatic β-islet cells. Importantly, defining the transcriptional targets and elucidating the molecular interactions of critical transcription factors in Ewing sarcoma, as well as in other cancers, may more fully define their function.

TABLE OF CONTENTS

ABSTRACT....iii

LIST OF FIGURES....v

LIST OF TABLES....vii

ACKNOWLEDGMENTS....viii

Chapter

1. INTRODUCTION....1

References....12

2. EWS/FLI UTILIZES NKX2-2 TO REPRESS MESENCHYMAL FEATURES OF EWING SARCOMA....18

Abstract....19
Introduction....19
Results....20
Discussion....28
Materials and Methods....29
References....31

3. NOVEL PROTEIN INTERACTIONS MEDIATED BY NKX2.2....47

Abstract....48
Introduction....48
Results....50
Discussion....53
Materials and Methods....55
References....65

4. CONCLUSION AND FUTURE DIRECTIONS....68

References....75

LIST OF FIGURES

Figure Page

2.1-RNA-seq transcriptional profiling of NKX2-2 in the Ewing sarcoma cell line A673...21

2.2-NKX2-2 impairs the capacity of A673 Ewing sarcoma cells to spread on the substrate and to form actin stress fibers and focal adhesions.....23

2.3-NKX2-2 represses mesenchymal features in two other Ewing sarcoma cell lines.....24

2.4-NKX2-2 is necessary but not sufficient for EWS/FLI-mediated repression of mesenchymal features of Ewing sarcoma cells.....25

2.5-NKX2-2 inhibits cell adhesion and migration.....26

2.6-The NKX2-2 and ZEB2 transcriptional profiles are inversely correlated.....27

2.7-Low expression of NKX2-2 may predict poor patient outcome.....28

2.S1-Key NKX2.2-regulated genes.....41

2.S2-: Immunofluorescence 40X fields of A673 cells harboring control, NKX2-2, or EWS/FLI shRNA.....42

2.S3-Immunofluorescence 40X fields of EWS502 cells harboring control, NKX2-2, or EWS/FLI shRNA.....43

2.S4-Immunofluorescence 40X fields of TC71 cells harboring control, NKX2-2, or EWS/FLI shRNA.....44

2.S5-qRT-PCR and western blots of EWS502 and TC71 cells.....45

2.S6-Immunofluorescence 40X fields of A673 knockdown-rescue cells.....46

3.1-Domain organization of wild-type and mutant human NKX2.2.....59

3.2-Domain organization of wild-type and mutant mouse MTG16.....60

3.3-NKX2.2 and MTG16 participate in a novel protein interaction that is mappable on both proteins.....61

3.4-NKX2.2 forms a homo-oligomer using TAD.....63

3.5-NKX2.2 and Notch1 intracellular domain compete for MTG16 binding.....64

LIST OF TABLES

Table Page

2.S1-List of NKX2-2 repressed and activated gene targets.....34

ACKNOWLEDGMENTS

I am grateful to Steve Lessnick for the opportunity to pursue graduate research with him, and for the training and support he has given me. In his lab, I learned a great deal about biology, cancer, and the conduct of scientific research. Many thanks to all the members of the Lessnick Lab for guidance and help both within and outside the realm of science. Thanks to my committee members: Brad Cairns and Rod Stewart for advice on research and career planning; Mike Engel for co-mentoring me and for sharing reagents and the expertise of his team; and Laura Hoffman for patiently guiding me through protocols and techniques, critically reading my manuscript, and for the afternoon pep talks that always got me ready for the next experiment. I acknowledge the Sydney's Incredible Defeat of Ewing Sarcoma (SIDES) Charity for scholarship funding. Seven years of graduate school is tough, and making it through would have been impossible without the support of numerous people from the MB/BC Program, OncSci and the Huntsman Cancer Institute, and the University of Utah. I really appreciate all your help.

My utmost thanks goes to my family and friends, from back home in Manila to here in Salt Lake City—your moral support and belief in me has kept me going. To my mom, Beth; my sister, Jackie; and my friends who by now are more like family: I share with you my successes as you've shared with me my trials. Maraming salamat.

CHAPTER 1

INTRODUCTION

Ewing sarcoma is a bone-associated malignancy that affects mostly children and young adults that was first described by James Ewing as a diffuse endothelioma of bone in 1921 [1]. It is a rare cancer, occurring at a rate of 3 per million per year in the United States [2]. Though usually occurring in bone, it arises in soft tissue as well, and is frequently described as a small, round, blue-cell tumor (SRBCT). Patient survival has steadily improved over the past few decades. Five- and ten-year survival rates currently stand at 68% and 63% for localized disease, and 39% and 32% for metastatic disease, respectively, according to Surveillance, Epidemiology, and End Results (SEER) data from 1973 through 2004 [2]. SEER data also indicate that the five-year conditional survival for localized disease increases with time: 72.9% at diagnosis to 91.4% five years after diagnosis. Predictably, these numbers are lower for metastatic disease, at 31.7% and 83.6%, respectively [3]. Furthermore, using California Cancer Registry data from 1989 to 2007, several factors that are correlated with significantly poorer outcome, such as large tumor size, pelvic involvement, lack of surgery, Hispanic ethnicity, and low socioeconomic status, were identified [4]. Thus, even if outcome has significantly advanced, there is still a lot that can be done, especially for patients who present with metastases at diagnosis. There is currently no molecularly targeted strategy available to treat Ewing sarcoma. A specific drug would potentially raise patient survival even further, while avoiding the undesirable side effects of the cytotoxic therapies presently being utilized.

Ewing sarcoma is characterized by a requisite reciprocal translocation between a FET (*FUS*, *EWSR1*, *TAF15*) gene and a member of the ETS (E26 transformation specific) family of transcription factors (reviewed in [5]). t(11;22)(q24;q12), the archetypal and by far the most common translocation (found in 85% of all Ewing sarcomas), fuses the transcriptional regulatory domain of EWS to the DNA binding domain of FLI [6-8]. EWS/FLI causes massive transcriptional dysregulation in Ewing sarcoma [9-12]. Though

recent genomic sequencing studies of Ewing tumor samples and established cell lines identified a few recurrent mutations (*STAG2*, *CDKN2A*, and *TP53*), the majority of tumors are—with the exception of the EWS/FLI lesion itself—genetically quiet [13-15]. In the absence of other cooperating mutations, it is thought that the different arms of tumor pathogenesis in Ewing sarcoma are controlled exclusively by EWS/FLI [16].

Various EWS/FLI transcriptional targets have been identified previously [9, 10, 12, 17-27]. EWS/FLI is capable of directly activating targets by binding GGAA microsatellites [28, 29] and of directly repressing targets in a histone deacetylase (HDAC)-dependent fashion by binding an as yet uncharacterized consensus site [19]. Both activation and repression mechanisms require the recruitment of lysine-specific demethylase 1 (LSD1) [30]. We and others have shown that several of the identified EWS/FLI transcriptional targets are necessary for the transformed phenotype. Interestingly, a number of these targets are transcription factors themselves, implying that EWS/FLI may amplify its regulatory effects by causing subsequent waves of transcription. One of these EWS/FLI-upregulated transcription factors is NKX2-2 [9, 31].

NKX2-2 belongs to a family of evolutionarily ancient homeobox-binding transcription factors [32, 33]. The *Drosophila melanogaster* ortholog *vnd* (ventral nervous system defective) was identified in the late 1970s and early 1980s as a deletion of the tip of the fly X chromosome. Deletion of or mutations in this region are lethal, and examination of fly embryos revealed a near-absence of a ventral nervous system [34-36]. The gene responsible for the defect was isolated and sequenced in 1989, along with three other related genes, and were collectively named the NK homeobox genes, after the authors Marshall Nirenberg and Yongsok Kim [37]. The primary protein structure of human NKX2.2 has since been defined. (Nomenclature of human genes dictates using "NKX2-2" for the gene and "NKX2.2" for protein.) It has four important domains; from

the N to the C termini, they lie: tinman (TN), homeodomain (HD), specific domain (SD), and transcriptional activation domain (TAD) (Fig. 3.1) [38-40]. Sequencing of the gene and of the protein it encodes then allowed the dissection of the physiological function of NKX2-2 in development.

A host of studies using mouse models have defined the role of *Nkx2.2* in mammalian development. While heterozygous littermates survive to adulthood, mice with constitutive homozygous deletion of *Nkx2.2* die shortly after birth due to a complete lack of functional, insulin-producing β-cells and a reduced number of glucagon-producing α-cells and pancreatic polypeptide (PP)-producing γ-cells, resulting in severe hyperglycemia. In this model, most markers of β-islet differentiation are lost, suggesting that the loss of Nkx2.2 traps β-cells in a partially differentiated state [41]. Interestingly, several transcription factors were demonstrated to functionally bind the promoter of the insulin gene in vivo: Nkx2.2; Pax6, with which Nkx2.2 defines the dorsoventral axis of the developing neural tube; Pdx1, a homeobox factor and pancreas-specific marker; and Beta2 [42]. Furthermore, using Nkx2.2-HD fusions with the Engrailed repressor or VP16 activator, it was demonstrated that, while Nkx2.2-repressor activity is sufficient to specify α-cells and a reduced number of β-cells, Nkx2.2-activator activity seems to be required for full β-cell maturation. In addition, the interaction of Nkx2.2 with Grg3, a Groucho/transducin-like enhancer of split (Gro/TLE) family member that is highly expressed in the embryonic pancreas, is lost when TN is deleted [43]. To further investigate the role of the NKX2.2 transcriptional repressor activity, Papizan and colleagues demonstrated that a homozygous TN mutation disrupts Grg3 interaction and β-cell specification, causes hyperglycemia, and induces ectopic expression of the Aristaless homeobox (*Arx*) gene in β-cells, leading to β-to-α-cell reprogramming [44]. Somewhat relatedly, Nkx2.2 is required for the development of enteroendocrine cells in

the intestine, though it is dispensable for the development of enterocytes, paneth cells, and goblet cells [45].

In the realm of central nervous system (CNS) development, the related genes *Nkx2.2*, *Nkx2.9*, and *Nkx6.1* in concert control the differentiation of neural progenitors that give rise to motor neurons and interneurons [46-50]. In particular, while Nkx2.2 is not required for the establishment of progenitor cell populations in the ventral neural tube—due to possible redundancy with Nkx2.9—it is required for the maintenance of V3 interneurons. Moreover, Nkx2.2 suppresses the development of somatic motor neurons [46]. Lastly, Nkx2.2 also regulates oligodendrocyte differentiation [51, 52].

In Ewing sarcoma, NKX2-2 was identified as a top EWS/FLI-activated gene in the cell line A673 in early microarray transcriptional profiling studies [9]. Smith and colleagues demonstrated that depletion of NKX2-2, while not adversely affecting cell growth in culture, completely ablated the ability of Ewing sarcoma cells to form colonies in soft agar; anchorage-independent growth is a measure of transformation. This phenotype is rescued by expressing an RNAi-resistant NKX2-2 cDNA, demonstrating that the loss of transformation is specifically attributable to the loss of NKX2-2. Similarly, NKX2-2 knockdown cells were unable to form tumors in a xenograft mouse model. Tumors eventually grew in some mice, but it was demonstrated that these originated from cells that had lost the knockdown and started to re-express NKX2-2. Collectively, these data show that NKX2-2 is absolutely required for the maintenance of transformation in Ewing sarcoma. However, re-expression of NKX2-2 upon EWS/FLI knockdown did not rescue transformation, demonstrating that NKX2-2 is insufficient for EWS/FLI-mediated transformation and suggesting that many other transcriptional targets of EWS/FLI are jointly responsible for the transformed phenotype [9].

The regulation of NKX2-2 by EWS/FLI is an area of active research. In the developing neural tube, a gradient of Hedgehog (Hh) signal activates the Gli family of

transcription factors, which in turn activate Nkx2.2 [53-55]. Since EWS/FLI also upregulates GLI1, albeit in a Hh-independent fashion [18, 20, 23], one possibility is that the GLI1-NKX2-2 regulation node is conserved in Ewing sarcoma [22]. Furthermore, it has been demonstrated that GLI1 is a direct transcriptional target of EWS/FLI, further suggesting that NKX2.2 upregulation by EWS/FLI occurs indirectly [22]. However, recent ChIP-seq data revealed an EWS/FLI-bound microsatellite region ~40 kb upstream of the NKX2-2 transcription start that may serve as an enhancer element, suggesting that EWS/FLI directly activates NKX2-2 ([56]; Jason Tanner et al., unpublished data). Further studies need to be performed to determine whether this microsatellite facilitates active transcription of the NKX2-2 gene in Ewing sarcoma.

The work of Smith et al. in the Lessnick Lab paved the way for investigating NKX2-2 function in Ewing sarcoma. In a subsequent study in our lab, Owen et al. performed NKX2-2 microarray transcriptional profiling in A673 cells [31]. It was found that NKX2-2 controlled a small but significant subset of EWS/FLI-repressed genes. Moreover, it was shown that enforced expression of AES (amino enhancer of split), a dominant-negative Gro/TLE protein, or treatment with the pan-HDAC inhibitor vorinostat, abrogated transformation in a soft agar assay. This suggested that Gro/TLE and HDAC function are essential to transformation, as could be expected if these co-repressors are recruited by NKX2.2 to its target loci. Strikingly, treatment of Ewing sarcoma cells with vorinostat completely reversed the NKX2-2 transcriptional profile, suggesting that indeed NKX2-2 represses its targets via a histone deacetylation-dependent mechanism [31].

EWS/FLI controls the regulation of multiple genes with vastly different functions. Transcriptional profiles generated through microarray and RNA-seq, as well as DAVID gene ontology and KEGG pathway analyses, reveal that EWS/FLI represses genes that are important for focal adhesion (FA), extracellular matrix (ECM) receptor

function, and regulation of actin cytoskeleton, among others [30, 31, 57]. Chaturvedi et al. showed that, strikingly, knockdown of EWS/FLI results in cells that assemble more FAs, form thicker and more organized actin stress fibers, and spread better on a fibronectin substrate, compared to control. Moreover, these EWS/FLI-depleted Ewing sarcoma cells also display reduced adhesion to substrate in vitro, reduced adhesion to lung parenchyma in vivo in a tail vein injection model, and dramatically increased migration in a scratch assay [58]. Some transcriptional targets of EWS/FLI that control mesenchymalization were also identified [57]. For instance, EWS/FLI represses zyxin, which stabilizes actin stress fibers, and α5 integrin, which attaches as a heterodimer with β1 integrin to fibronectin in the ECM. Individual re-expression of these genes results in manifestation of a subset of mesenchymal traits. Meanwhile, double re-expression of zyxin and α5 integrin is sufficient to capture the full complement of mesenchymal traits controlled by EWS/FLI and also reduces colony growth in soft agar, while having a negligible effect on the proliferation of cells in culture [57]. Taken together, these data suggest that EWS/FLI represses mesenchymal features of Ewing sarcoma [58].

More recently, the Lessnick Lab demonstrated that the zinc finger E-box-binding homeobox 2 (ZEB2) gene is expressed at high levels in Ewing sarcoma cell lines, human neural crest stem cells, and bone marrow-derived mesenchymal stem cells [59, 60]. ZEB2 RNA-seq transcriptional profiling using two independent siRNAs revealed that ZEB2 represses genes important in epithelial cell differentiation, actin binding, cell junctions, etc., suggesting that this transcription factor may repress epithelial features of Ewing sarcoma [60]. Indeed, when ZEB2 is depleted from Ewing sarcoma cells, they assume epithelial features: a cobblestone morphology with an actin ring structure around the cell periphery, and slower migration in a scratch assay compared to control knockdown cells. Moreover, enforced expression in Ewing sarcoma cells of a miR-200 cluster, known to repress both ZEB2 and the related ZEB1, causes de-repression of the

epithelial genes keratin 8 and desmoplakin and reduces migration capacity compared to a miR control. Importantly, ZEB2 knockdown impairs the metastatic capacity of Ewing cells in an intratibial xenograft model. Collectively, these data show that ZEB2 represses epithelial features of Ewing sarcoma [60].

These studies performed by our group and Mary Beckerle's group again bring forth the question of the Ewing sarcoma cell-of-origin, which is yet to be definitively determined. Early work showed that enforced expression of EWS/FLI in heterologous cells had disparate results: soft agar colony growth and transformation in mouse embryonic fibroblasts [8] and p53-dependent growth arrest in primary human foreskin fibroblasts [61]. Because of the demonstrated differences in gene expression profiles between the Ewing sarcoma cell line A673 and the hitherto preferred EWS/FLI-transduced NIH3T3 model [62], our lab and others moved to a system in which EWS/FLI was RNAi-depleted in Ewing cell lines [9, 10, 63].

Of the various potential cells-of-origin proposed, neural crest cells and mesenchymal stem cells (MSCs) have been the most favored [16]. Ewing tumor cells are known to express neuroectodermal markers and can be induced to display features of neural differentiation [64-66]. Enforced EWS/FLI expression in a rhabdomyosarcoma cell line results in a Ewing sarcoma-like morphology and induction of genes highly expressed in Ewing sarcoma and in the neural crest [67]. Likewise, transcriptional profiles of Ewing tumors and A673 cells cluster strongly with those from brain tissue and human vascular endothelial cells [68]. However, as had been pointed out before, these lines of evidence cannot distinguish between a neural crest origin and a model in which the EWS/FLI translocation occurs in a cell type permissive to the induction of neuronal features [21, 67, 68].

The proposal that MSC is the Ewing sarcoma cell-of-origin is more recent. For example, both EWS/FLI and EWS/ERG blocked the differentiation of murine bone

marrow-derived stromal cells along the osteogenic and adipogenic pathways, two lineages arising from MSCs [69]. Viable SRBCTs are produced in murine primary bone-derived cells grafted into immunocompetent mice [70] or in murine primary bone marrow-derived mesenchymal progenitor cells grafted into SCID mice [71]. Using a loss-of-function approach, Tirode and colleagues demonstrated that EWS/FLI-depleted Ewing cells mimicked the transcriptional profile of MSCs and can be induced towards adipogenic differentiation, suggesting a mesenchymal origin [72]. Ectopic EWS/FLI expression in mesenchymal cells of the developing mouse limb bud gives rise to SRBCTs, but only with an accompanying p53 deletion [73]. To more accurately model Ewing sarcoma, Riggi and colleagues expressed EWS/FLI in human MSCs. However, while the gene expression of these derivative MSCs closely and specifically approached that of Ewing sarcoma, xenografts in immunocompromised mice failed to generate tumors [74]. Interestingly, the neural crest and MSC models may not be mutually exclusive; Ewing sarcoma initiation has been demonstrated both in human neural crest stem cells and the MSCs that derive from them [59, 75]. These key studies represent only a subset of the current literature; extensive reviews have previously been published [16, 76].

As a manner of summary, I offer here three reasons why studying Ewing sarcoma is vastly important. First, it is a devastating disease that affects children and adolescents. Although the overall outcome has risen, patients with metastatic or recurrent disease face very poor prognoses. Our goal in the Lessnick Lab is to understand the disease biology to aid in identifying therapeutically targetable genes or pathways. Such a directed treatment, while bettering patient survival, also will hopefully reduce adverse side effects of currently available nonspecific chemotherapeutics. The importance of this cannot be overstated in pediatric malignancies where young survivors look forward to many years of fruitful life after cancer.

Secondly, Ewing sarcoma is an important model for studying genomically silent malignancies. While cancers are generally driven by a primary genetic aberration, many of these co-opt secondary hits, usually the result of a mutation in p53 or another gene that compromises genetic stability, that are necessary for tumor maintenance and/or metastasis. The singularity of EWS/FLI as a genetic lesion that controls myriad aspects of oncogenesis is rare. In the absence of confounding cancer "engines," Ewing sarcoma and its EWS/FLI "driver" are an excellent platform in which to study how transcriptional dysregulation can solely drive runaway cell proliferation, escape from cell death, drug resistance, and avoidance of terminal differentiation.

Lastly, Ewing sarcoma is unique in that, until now, its cell-of-origin has yet to be definitively characterized. Correct identification of this permissive cell type will allow genetic models to be constructed; these, in turn, will aid in understanding basic biology and in testing of possible drug leads. Moreover, this difficulty has underscored the importance of cellular context during transformation. Perhaps EWS/FLI can also be used as a model to study other neural crest- or MSC-derived cancers, sarcomas, or other cancers of uncertain origin.

Goals of the thesis

While NKX2-2 is one of the most highly upregulated and earliest identified EWS/FLI transcriptional targets, we do not know its biological function in Ewing sarcoma. As had been discussed above, NKX2-2 is critical for transformation and the individual contributions of its domains to this phenotype have been elucidated. However, there were key unknowns as well. We therefore identified two major related goals for my doctoral research, which I briefly discuss here.

The first goal of my thesis is to make biologic sense of the transcriptional program mediated by NKX2-2 in Ewing sarcoma. To this end, we performed NKX2-2

transcriptional profiling by RNA-seq and found that NKX2-2 represses genes important for cell adhesion and ECM organization. This became the impetus for testing whether NKX2-2 represses mesenchymal features of Ewing sarcoma, as EWS/FLI does. We found that this is indeed the case, and that Ewing sarcoma cells depleted of NKX2-2 show increased organization of actin stress fibers, increased FA assembly and cell spreading, and de-repression of the cytoskeletal and FA protein zyxin, which stabilizes actin stress fibers. Functionally, this translated to greater cell adhesion and faster cell migration. Importantly, we found that the NKX2-2 and ZEB2 transcriptional profiles are inverses of each other—exactly what is expected since these two programs represent "mesenchymalized" and "epithelialized" Ewing sarcoma cells, respectively. Lastly, we show that NKX2-2 expression level in tumors stratify outcome, with low expressors having a nearly significant decreased survival, suggesting that there is a "sweet spot" level of NKX2-2 expression that allows maintenance of transformation while providing cells with sufficient mesenchymal features that might promote establishment at distal sites. This work is published in *Genes & Cancer* and is detailed in Chapter 2.

The second goal of my thesis is to identify the protein interaction partners of NKX2.2 to better understand the transcriptional mechanisms it employs. This information will give valuable clues on NKX2.2 function that a transcriptional profile would be unable to reveal. We undertook a candidate approach and identified MTG16 as a novel protein interaction partner of NKX2.2; the interaction domains were mapped on both NKX2.2 and MTG16. Details of this interaction led to the hypothesis and demonstration that NKX2.2 is capable of homo-oligomerization. Both the heterotypic and homotypic interactions map to the NKX2.2-TAD, demonstrating that this region is a competent protein-binding motif. This work is detailed in Chapter 3.

Finally, I state our conclusions and identify future directions in Chapter 4.

References

1. Ewing J. Classics in oncology. Diffuse endothelioma of bone. James Ewing. Proceedings of the New York Pathological Society, 1921. CA Cancer J Clin. 1972;22(2):95-8.

2. Esiashvili N, Goodman M, Marcus RB, Jr. Changes in incidence and survival of Ewing sarcoma patients over the past 3 decades: Surveillance Epidemiology and End Results data. J Pediatr Hematol Oncol. 2008;30(6):425-30.

3. Miller BJ, Lynch CF, Buckwalter JA. Conditional survival is greater than overall survival at diagnosis in patients with osteosarcoma and Ewing's sarcoma. Clin Orthop Relat Res. 2013;471(11):3398-404.

4. Lee J, Hoang BH, Ziogas A, Zell JA. Analysis of prognostic factors in Ewing sarcoma using a population-based cancer registry. Cancer. 2010;116(8):1964-73.

5. Sankar S, Lessnick SL. Promiscuous partnerships in Ewing's sarcoma. Cancer Genet. 2011;204(7):351-65.

6. Turc-Carel C, Aurias A, Mugneret F, Lizard S, Sidaner I, Volk C, et al. Chromosomes in Ewing's sarcoma. I. An evaluation of 85 cases of remarkable consistency of t(11;22)(q24;q12). Cancer Genet Cytogenet. 1988;32(2):229-38.

7. Delattre O, Zucman J, Plougastel B, Desmaze C, Melot T, Peter M, et al. Gene fusion with an ETS DNA-binding domain caused by chromosome translocation in human tumours. Nature. 1992;359(6391):162-5.

8. May WA, Gishizky ML, Lessnick SL, Lunsford LB, Lewis BC, Delattre O, et al. Ewing sarcoma 11;22 translocation produces a chimeric transcription factor that requires the DNA-binding domain encoded by FLI1 for transformation. Proc Natl Acad Sci U S A. 1993;90(12):5752-6.

9. Smith R, Owen LA, Trem DJ, Wong JS, Whangbo JS, Golub TR, et al. Expression profiling of EWS/FLI identifies NKX2.2 as a critical target gene in Ewing's sarcoma. Cancer Cell. 2006;9(5):405-16.

10. Kinsey M, Smith R, Lessnick SL. NR0B1 is required for the oncogenic phenotype mediated by EWS/FLI in Ewing's sarcoma. Mol Cancer Res. 2006;4(11):851-9.

11. Patel M, Simon JM, Iglesia MD, Wu SB, McFadden AW, Lieb JD, et al. Tumor-specific retargeting of an oncogenic transcription factor chimera results in dysregulation of chromatin and transcription. Genome Res. 2012;22(2):259-70.

12. Prieur A, Tirode F, Cohen P, Delattre O. EWS/FLI-1 silencing and gene profiling of Ewing cells reveal downstream oncogenic pathways and a crucial role for repression of insulin-like growth factor binding protein 3. Mol Cell Biol. 2004;24(16):7275-83.

13. Brohl AS, Solomon DA, Chang W, Wang J, Song Y, Sindiri S, et al. The genomic landscape of the Ewing Sarcoma family of tumors reveals recurrent STAG2 mutation. PLoS Genet. 2014;10(7):e1004475.

14. Crompton BD, Stewart C, Taylor-Weiner A, Alexe G, Kurek KC, Calicchio ML, et al. The genomic landscape of pediatric Ewing sarcoma. Cancer Discov. 2014;4(11):1326-41.

15. Tirode F, Surdez D, Ma X, Parker M, Le Deley MC, Bahrami A, et al. Genomic landscape of Ewing sarcoma defines an aggressive subtype with co-association of STAG2 and TP53 mutations. Cancer Discov. 2014;4(11):1342-53.

16. Toomey EC, Schiffman JD, Lessnick SL. Recent advances in the molecular pathogenesis of Ewing's sarcoma. Oncogene. 2010;29(32):4504-16.

17. Luo W, Gangwal K, Sankar S, Boucher KM, Thomas D, Lessnick SL. GSTM4 is a microsatellite-containing EWS/FLI target involved in Ewing's sarcoma oncogenesis and therapeutic resistance. Oncogene. 2009;28(46):4126-32.

18. Zwerner JP, Joo J, Warner KL, Christensen L, Hu-Lieskovan S, Triche TJ, et al. The EWS/FLI1 oncogenic transcription factor deregulates GLI1. Oncogene. 2008;27(23):3282-91.

19. Sankar S, Bell R, Stephens B, Zhuo R, Sharma S, Bearss DJ, et al. Mechanism and relevance of EWS/FLI-mediated transcriptional repression in Ewing sarcoma. Oncogene. 2013;32(42):5089-100.

20. Sankar S, Tanner JM, Bell R, Chaturvedi A, Randall RL, Beckerle MC, et al. A novel role for keratin 17 in coordinating oncogenic transformation and cellular adhesion in Ewing sarcoma. Mol Cell Biol. 2013;33(22):4448-60.

21. Wiles ET, Lui-Sargent B, Bell R, Lessnick SL. BCL11B is up-regulated by EWS/FLI and contributes to the transformed phenotype in Ewing sarcoma. PLoS One. 2013;8(3):e59369.

22. Joo J, Christensen L, Warner K, States L, Kang HG, Vo K, et al. GLI1 is a central mediator of EWS/FLI1 signaling in Ewing tumors. PLoS One. 2009;4(10):e7608.

23. Beauchamp E, Bulut G, Abaan O, Chen K, Merchant A, Matsui W, et al. GLI1 is a direct transcriptional target of EWS-FLI1 oncoprotein. J Biol Chem. 2009;284(14):9074-82.

24. Richter GH, Plehm S, Fasan A, Rossler S, Unland R, Bennani-Baiti IM, et al. EZH2 is a mediator of EWS/FLI1 driven tumor growth and metastasis blocking endothelial and neuro-ectodermal differentiation. Proc Natl Acad Sci U S A. 2009;106(13):5324-9.

25. Riggi N, Suva ML, De Vito C, Provero P, Stehle JC, Baumer K, et al. EWS-FLI-1 modulates miRNA145 and SOX2 expression to initiate mesenchymal stem cell reprogramming toward Ewing sarcoma cancer stem cells. Genes Dev. 2010;24(9):916-32.

26. Takahashi A, Higashino F, Aoyagi M, Yoshida K, Itoh M, Kyo S, et al. EWS/ETS fusions activate telomerase in Ewing's tumors. Cancer Res. 2003;63(23):8338-44.

27. Tirado OM, Mateo-Lozano S, Villar J, Dettin LE, Llort A, Gallego S, et al. Caveolin-1 (CAV1) is a target of EWS/FLI-1 and a key determinant of the oncogenic phenotype and tumorigenicity of Ewing's sarcoma cells. Cancer Res. 2006;66(20):9937-47.

28. Gangwal K, Sankar S, Hollenhorst PC, Kinsey M, Haroldsen SC, Shah AA, et al. Microsatellites as EWS/FLI response elements in Ewing's sarcoma. Proc Natl Acad Sci U S A. 2008;105(29):10149-54.

29. Guillon N, Tirode F, Boeva V, Zynovyev A, Barillot E, Delattre O. The oncogenic EWS-FLI1 protein binds in vivo GGAA microsatellite sequences with potential transcriptional activation function. PLoS One. 2009;4(3):e4932.

30. Sankar S, Theisen ER, Bearss J, Mulvihill T, Hoffman LM, Sorna V, et al. Reversible LSD1 inhibition interferes with global EWS/ETS transcriptional activity and impedes Ewing sarcoma tumor growth. Clin Cancer Res. 2014;20(17):4584-97.

31. Owen LA, Kowalewski AA, Lessnick SL. EWS/FLI mediates transcriptional repression via NKX2.2 during oncogenic transformation in Ewing's sarcoma. PLoS One. 2008;3(4):e1965.

32. Larroux C, Fahey B, Degnan SM, Adamski M, Rokhsar DS, Degnan BM. The NK homeobox gene cluster predates the origin of Hox genes. Curr Biol. 2007;17(8):706-10.

33. Stanfel MN, Moses KA, Schwartz RJ, Zimmer WE. Regulation of organ development by the NKX-homeodomain factors: an NKX code. Cell Mol Biol (Noisy-le-grand). 2005;Suppl 51:OL785-99.

34. White K, DeCelles NL, Enlow TC. Genetic and developmental analysis of the locus vnd in Drosophila melanogaster. Genetics. 1983;104(3):433-48.

35. Jimenez F, Campos-Ortega JA. A region of the Drosophila genome necessary for CNS development. Nature. 1979;282(5736):310-2.

36. White K. Defective neural development in Drosophila melanogaster embryos deficient for the tip of the X chromosome. Dev Biol. 1980;80(2):332-44.

37. Kim Y, Nirenberg M. Drosophila NK-homeobox genes. Proc Natl Acad Sci U S A. 1989;86(20):7716-20.

38. Hartigan DJ, Rubenstein JL. The cDNA sequence of murine Nkx-2.2. Gene. 1996;168(2):271-2.

39. Price M, Lazzaro D, Pohl T, Mattei MG, Ruther U, Olivo JC, et al. Regional expression of the homeobox gene Nkx-2.2 in the developing mammalian forebrain. Neuron. 1992;8(2):241-55.

40. Watada H, Mirmira RG, Kalamaras J, German MS. Intramolecular control of transcriptional activity by the NK2-specific domain in NK-2 homeodomain proteins. Proc Natl Acad Sci U S A. 2000;97(17):9443-8.

41. Sussel L, Kalamaras J, Hartigan-O'Connor DJ, Meneses JJ, Pedersen RA, Rubenstein JL, et al. Mice lacking the homeodomain transcription factor Nkx2.2 have diabetes due to arrested differentiation of pancreatic beta cells. Development. 1998;125(12):2213-21.

42. Cissell MA, Zhao L, Sussel L, Henderson E, Stein R. Transcription factor occupancy of the insulin gene in vivo. Evidence for direct regulation by Nkx2.2. J Biol Chem. 2003;278(2):751-6.

43. Doyle MJ, Loomis ZL, Sussel L. Nkx2.2-repressor activity is sufficient to specify alpha-cells and a small number of beta-cells in the pancreatic islet. Development. 2007;134(3):515-23.

44. Papizan JB, Singer RA, Tschen SI, Dhawan S, Friel JM, Hipkens SB, et al. Nkx2.2 repressor complex regulates islet beta-cell specification and prevents beta-to-alpha-cell reprogramming. Genes Dev. 2011;25(21):2291-305.

45. Desai S, Loomis Z, Pugh-Bernard A, Schrunk J, Doyle MJ, Minic A, et al. Nkx2.2 regulates cell fate choice in the enteroendocrine cell lineages of the intestine. Dev Biol. 2008;313(1):58-66.

46. Briscoe J, Sussel L, Serup P, Hartigan-O'Connor D, Jessell TM, Rubenstein JL, et al. Homeobox gene Nkx2.2 and specification of neuronal identity by graded Sonic hedgehog signalling. Nature. 1999;398(6728):622-7.

47. Briscoe J, Pierani A, Jessell TM, Ericson J. A homeodomain protein code specifies progenitor cell identity and neuronal fate in the ventral neural tube. Cell. 2000;101(4):435-45.

48. McMahon AP. Neural patterning: the role of Nkx genes in the ventral spinal cord. Genes Dev. 2000;14(18):2261-4.

49. Holz A, Kollmus H, Ryge J, Niederkofler V, Dias J, Ericson J, et al. The transcription factors Nkx2.2 and Nkx2.9 play a novel role in floor plate development and commissural axon guidance. Development. 2010;137(24):4249-60.

50. Jarrar W, Dias JM, Ericson J, Arnold HH, Holz A. Nkx2.2 and nkx2.9 are the key regulators to determine cell fate of branchial and visceral motor neurons in caudal hindbrain. PLoS One. 2015;10(4):e0124408.

51. Qi Y, Cai J, Wu Y, Wu R, Lee J, Fu H, et al. Control of oligodendrocyte differentiation by the Nkx2.2 homeodomain transcription factor. Development. 2001;128(14):2723-33.

52. Tochitani S, Hayashizaki Y. Nkx2.2 antisense RNA overexpression enhanced oligodendrocytic differentiation. Biochem Biophys Res Commun. 2008;372(4):691-6.

53. Briscoe J, Therond PP. The mechanisms of Hedgehog signalling and its roles in development and disease. Nat Rev Mol Cell Biol. 2013;14(7):416-29.

54. Stamataki D, Ulloa F, Tsoni SV, Mynett A, Briscoe J. A gradient of Gli activity mediates graded Sonic Hedgehog signaling in the neural tube. Genes Dev. 2005;19(5):626-41.

55. Lei Q, Jeong Y, Misra K, Li S, Zelman AK, Epstein DJ, et al. Wnt signaling inhibitors regulate the transcriptional response to morphogenetic Shh-Gli signaling in the neural tube. Dev Cell. 2006;11(3):325-37.

56. Riggi N, Knoechel B, Gillespie SM, Rheinbay E, Boulay G, Suva ML, et al. EWS-FLI1 utilizes divergent chromatin remodeling mechanisms to directly activate or repress enhancer elements in Ewing sarcoma. Cancer Cell. 2014;26(5):668-81.

57. Chaturvedi A, Hoffman LM, Jensen CC, Lin YC, Grossmann AH, Randall RL, et al. Molecular dissection of the mechanism by which EWS/FLI expression compromises actin cytoskeletal integrity and cell adhesion in Ewing sarcoma. Mol Biol Cell. 2014;25(18):2695-709.

58. Chaturvedi A, Hoffman LM, Welm AL, Lessnick SL, Beckerle MC. The EWS/FLI oncogene drives changes in cellular morphology, adhesion, and migration in Ewing sarcoma. Genes Cancer. 2012;3(2):102-16.

59. von Levetzow C, Jiang X, Gwye Y, von Levetzow G, Hung L, Cooper A, et al. Modeling initiation of Ewing sarcoma in human neural crest cells. PLoS One. 2011;6(4):e19305.

60. Wiles ET, Bell R, Thomas D, Beckerle M, Lessnick SL. ZEB2 represses the epithelial phenotype and facilitates metastasis in Ewing sarcoma. Genes Cancer. 2013;4(11-12):486-500.

61. Lessnick SL, Dacwag CS, Golub TR. The Ewing's sarcoma oncoprotein EWS/FLI induces a p53-dependent growth arrest in primary human fibroblasts. Cancer Cell. 2002;1(4):393-401.

62. Braunreiter CL, Hancock JD, Coffin CM, Boucher KM, Lessnick SL. Expression of EWS-ETS fusions in NIH3T3 cells reveals significant differences to Ewing's sarcoma. Cell Cycle. 2006;5(23):2753-9.

63. Hu-Lieskovan S, Heidel JD, Bartlett DW, Davis ME, Triche TJ. Sequence-specific knockdown of EWS-FLI1 by targeted, nonviral delivery of small interfering RNA inhibits tumor growth in a murine model of metastatic Ewing's sarcoma. Cancer Res. 2005;65(19):8984-92.

64. Lipinski M, Hirsch MR, Deagostini-Bazin H, Yamada O, Tursz T, Goridis C. Characterization of neural cell adhesion molecules (NCAM) expressed by Ewing and neuroblastoma cell lines. Int J Cancer. 1987;40(1):81-6.

65. Lipinski M, Braham K, Philip I, Wiels J, Philip T, Goridis C, et al. Neuroectoderm-associated antigens on Ewing's sarcoma cell lines. Cancer Res. 1987;47(1):183-7.

66. Cavazzana AO, Miser JS, Jefferson J, Triche TJ. Experimental evidence for a neural origin of Ewing's sarcoma of bone. Am J Pathol. 1987;127(3):507-18.

67. Hu-Lieskovan S, Zhang J, Wu L, Shimada H, Schofield DE, Triche TJ. EWS-FLI1 fusion protein up-regulates critical genes in neural crest development and is responsible for the observed phenotype of Ewing's family of tumors. Cancer Res. 2005;65(11):4633-44.

68. Staege MS, Hutter C, Neumann I, Foja S, Hattenhorst UE, Hansen G, et al. DNA microarrays reveal relationship of Ewing family tumors to both endothelial and fetal neural crest-derived cells and define novel targets. Cancer Res. 2004;64(22):8213-21.

69. Torchia EC, Jaishankar S, Baker SJ. Ewing tumor fusion proteins block the differentiation of pluripotent marrow stromal cells. Cancer Res. 2003;63(13):3464-8.

70. Castillero-Trejo Y, Eliazer S, Xiang L, Richardson JA, Ilaria RL, Jr. Expression of the EWS/FLI-1 oncogene in murine primary bone-derived cells Results in EWS/FLI-1-dependent, ewing sarcoma-like tumors. Cancer Res. 2005;65(19):8698-705.

71. Riggi N, Cironi L, Provero P, Suva ML, Kaloulis K, Garcia-Echeverria C, et al. Development of Ewing's sarcoma from primary bone marrow-derived mesenchymal progenitor cells. Cancer Res. 2005;65(24):11459-68.

72. Tirode F, Laud-Duval K, Prieur A, Delorme B, Charbord P, Delattre O. Mesenchymal stem cell features of Ewing tumors. Cancer Cell. 2007;11(5):421-9.

73. Lin PP, Pandey MK, Jin F, Xiong S, Deavers M, Parant JM, et al. EWS-FLI1 induces developmental abnormalities and accelerates sarcoma formation in a transgenic mouse model. Cancer Res. 2008;68(21):8968-75.

74. Riggi N, Suva ML, Suva D, Cironi L, Provero P, Tercier S, et al. EWS-FLI-1 expression triggers a Ewing's sarcoma initiation program in primary human mesenchymal stem cells. Cancer Res. 2008;68(7):2176-85.

75. Riggi N, Suva ML, Stamenkovic I. Ewing's sarcoma origin: from duel to duality. Expert Rev Anticancer Ther. 2009;9(8):1025-30.

76. Lin PP, Wang Y, Lozano G. Mesenchymal stem cells and the origin of Ewing's sarcoma. Sarcoma. 2011;2011:276463.

CHAPTER 2

EWS/FLI UTILIZES NKX2-2 TO REPRESS MESENCHYMAL FEATURES OF EWING SARCOMA

Fadul J, Bell R, Hoffman LM, Beckerle MC, Engel ME, and Lessnick SL. EWS/FLI utilizes NKX2-2 to repress mesenchymal features of Ewing sarcoma. 2015. *Genes Cancer* 6(3-4):129-143.

www.impactjournals.com/Genes&Cancer Genes & Cancer, Vol. 6 (3-4), March 2015

EWS/FLI utilizes NKX2-2 to repress mesenchymal features of Ewing sarcoma

John Fadul[1,2], Russell Bell[1,2], Laura M. Hoffman[1,3], Mary C. Beckerle[1,2,3], Michael E. Engel[1,2,4,5] and Stephen L. Lessnick[1,2,4,5]

[1] Huntsman Cancer Institute, School of Medicine, University of Utah, Salt Lake City, Utah, USA

[2] Department of Oncological Sciences, School of Medicine, University of Utah, Salt Lake City, Utah, USA

[3] Department of Biology, School of Medicine, University of Utah, Salt Lake City, Utah, USA

[4] Center for Children's Cancer Research, School of Medicine, University of Utah, Salt Lake City, Utah, USA

[5] Division of Pediatric Hematology and Oncology, School of Medicine, University of Utah, Salt Lake City, Utah, USA

Correspondence to: *Stephen L. Lessnick,* ***email:*** *stephen.lessnick@hci.utah.edu*

Keywords: Ewing sarcoma, NKX2-2, EWS/FLI, mesenchymal, adhesion

Received: *February 25, 2015* ***Accepted:*** *April 16, 2015* ***Published:*** *April 17, 2015*

ABSTRACT

In Ewing sarcoma, NKX2-2 is a critical activated target of the oncogenic transcription factor EWS/FLI that is required for transformation. However, its biological function in this malignancy is unknown. Here we provide evidence that NKX2-2 mediates the EWS/FLI-controlled block of mesenchymal features. Transcriptome-wide RNA sequencing revealed that NKX2-2 represses cell adhesion and extracellular matrix organization genes. NKX2-2-depleted cells form more focal adhesions and organized actin stress fibers, and spread over a wider area—hallmarks of mesenchymally derived cells. Furthermore, NKX2-2 represses the actin-stabilizing protein zyxin, suggesting that these morphological changes are attributable to zyxin de-repression. In addition, NKX2-2-knockdown cells display marked increases in migration and substrate adhesion. However, only part of the EWS/FLI phenotype is NKX2-2-dependent; consequently, NKX2-2 is insufficient to rescue EWS/FLI repression of mesenchymalization. Strikingly, we found that EWS/FLI- and NKX2-2-repressed genes are activated by ZEB2, which was previously shown to block Ewing sarcoma epithelialization. Together, these data support an emerging theme wherein Ewing sarcoma cells highly express transcription factors that maintain an undifferentiated state. Importantly, co-opting epithelial and mesenchymal traits by Ewing sarcoma cells may explain how the primary tumor grows rapidly while also "passively" metastasizing, without the need for transitions toward differentiated states, as in carcinomas.

INTRODUCTION

Translocation fusions between the various FET (FUS-EWS-TAF15) and ETS (E twenty-six) genes are the causative agent of Ewing sarcoma [1, 2]. Of these, the t(11;22)(q24;q12) lesion that encodes the oncogenic fusion protein EWS/FLI is by far the most common, being present in 85% of all Ewing sarcoma tumors [2]. The fusion of the DNA-binding domain of *FLI1* with the strong transactivation domain of *EWSR1* yields an aberrant transcription factor. Although genomic sequencing of tumor samples revealed occasional loss of *STAG2* and *CDKN2A*, as well as mutations in *TP53*, this pediatric malignancy is largely genomically stable, suggesting that transcriptional dysregulation by EWS/FLI is the primary oncogenic driver [3-5]. We have previously shown that EWS/FLI is able to directly activate genes by binding GGAA microsatellite-rich promoters, while others demonstrated its binding with the transcriptional co-activator CBP/p300, or phosphorylation-dependent interaction with the C-terminal domain of RNA PolII itself [6-12]. Recently, we found that EWS/FLI directly

represses genes by binding an as yet uncharacterized consensus sequence and recruiting histone deacetylases (HDACs) and lysine-specific demethylase 1 (LSD1) [13, 14]. We realize, however, the importance of a "second wave" of gene regulation that occurs when EWS/FLI modulates the expression of other transcription factors; for instance, we previously identified the homeobox transcription factor NKX2-2 as a critical upregulated target of EWS/FLI [15].

NKX2-2 has well-characterized roles in normal development. Deletion of its fly ortholog *vnd* (ventral nervous system defective) results to a complete loss of the ventral region of the central nervous system (CNS) and embryonic lethality [16, 17]. In the mammalian CNS, NKX2-2 specifies V3 interneurons, controls oligodendrocyte differentiation, and guides floor plate development [18-22]. It is critical in the fate specification of enteroendocrine cells in the small intestine and insulin-producing β-islet cells in the pancreas, where several of its transcriptional targets have been identified and characterized [23-32]. Mice homozygous for a null *Nkx2.2* mutation die postnatally due to a complete loss of β-islet cells and severe hyperglycemia [24]. Mechanistically, NKX2-2 has been shown to bind Gro/TLE co-repressors, which can then recruit HDACs, to effect transcriptional repression [33, 34]. Conversely, a C-terminal transactivation domain is unraveled when the neighboring NK2-specific domain is deleted, suggesting that NKX2-2 may also function as a transcriptional activator in some contexts [35, 36].

In Ewing sarcoma, we demonstrated that NKX2-2 is necessary for the maintenance of transformation *in vitro* and *in vivo* [15, 37]. Transcriptional profiling of NKX2-2 and EWS/FLI using microarrays revealed that they share a repressed geneset. Furthermore, Ewing sarcoma cells overexpressing AES (amino enhancer of split), a dominant-negative Gro/TLE protein, or treated with the HDAC inhibitor vorinostat display diminished transformation, consistent with NKX2-2 recruitment of Gro/TLE co-repressors and HDACs. Strikingly, vorinostat treatment completely reverses the transcriptional profile of NKX2-2, suggesting that NKX2-2 represses genes via modification of histone acetyl-lysine marks in Ewing sarcoma cells. Further analysis using domain deletion mutants demonstrated that DNA binding, transcriptional repression, and inhibition of transcriptional activation are necessary for the transformed phenotype [37]. Importantly, NKX2-2 was shown to be a sensitive and specific diagnostic marker of Ewing sarcoma versus other look-alike small round blue-cell tumors (SRBCTs), both at the RNA and protein levels [15, 38, 39].

In this current work, we perform unbiased transcriptional profiling of NKX2-2 using RNA-seq, which revealed that NKX2-2 downregulates genes critical for cell adhesion. This led to the discovery that EWS/FLI represses cell adhesion and other mesenchymal characteristics through upregulation of NKX2-2.

RESULTS

We previously reported that NKX2-2 is a critical upregulated target of EWS/FLI, and that it is necessary for the maintenance of transformation. Since it is a member of the NK family of homeobox-binding transcription factors and has been demonstrated to control gene expression in many developmental contexts, we reasoned that NKX2-2 depletion and transcriptional profiling would best reveal its function in Ewing sarcoma. We had previously determined the NKX2-2 transcriptional profile using microarrays [37]; to reduce bias, capture the full transcriptional profile, and enable direct comparison with our recent EWS/FLI dataset [14] we elected to perform RNA-seq. To this end we knocked down NKX2-2 expression in the Ewing sarcoma cell line A673 using retrovirally delivered shRNA (Fig. 1a). We then performed Illumina deep sequencing of mRNA isolated from these derivative polyclonal lines. Differential gene expression was determined with USeq tools. Using cutoff parameters of 1.5-fold change and FDR ≥ 50, we found 189 genes repressed and 49 genes activated by NKX2-2 (Table S1, Fig. 1c). The top regulated genes and heat maps are shown in Fig. S1a. We proceeded to validate select repressed and activated targets by qRT-PCR (Fig. S1b).

Gene set enrichment analyses (GSEA) revealed that NKX2-2-repressed genes are enriched in the EWS/FLI-repressed dataset, and NKX2-2-activated genes are enriched in the EWS/FLI-activated dataset (Fig. 1b). We also show that the NKX2-2- and EWS/FLI-repressed genesets, as well as the NKX2-2- and EWS/FLI-activated genesets, significantly overlap, consistent with GSEA data (Fig. 1c). This confirms microarray data we previously published and suggests that modulation of NKX2-2, and indeed any other transcription factor, can be utilized by EWS/FLI to amplify its transcriptional effect [37]. In addition, the NKX2-2-repressed and activated genesets are also appropriately well-represented in the dataset of EWS/ERG, a variant translocation harbored by TTC466 cells, suggesting that regulation of genes through NKX2-2 is translocation type-independent (Fig. 1b, Fig. S1c) [14]. Further GSEA analyses indicated that the NKX2-2-regulated genesets are not enriched in transcriptional profiles of rhabdomyosarcomas driven by PAX-FKHR fusions (data not shown) [40]. Thus, the NKX2-2 signature is specific for Ewing sarcoma.

Gene ontology (GO) analysis is widely used to determine the biological functions and cell processes for which a gene is important. We used DAVID functional annotation clustering for GO analysis, and found that NKX2-2 repressed genes important for cell adhesion, wound healing, and extracellular matrix (ECM) organization, among other GO terms identified (Fig. 1d). This suggested that NKX2-2 may contribute to EWS/

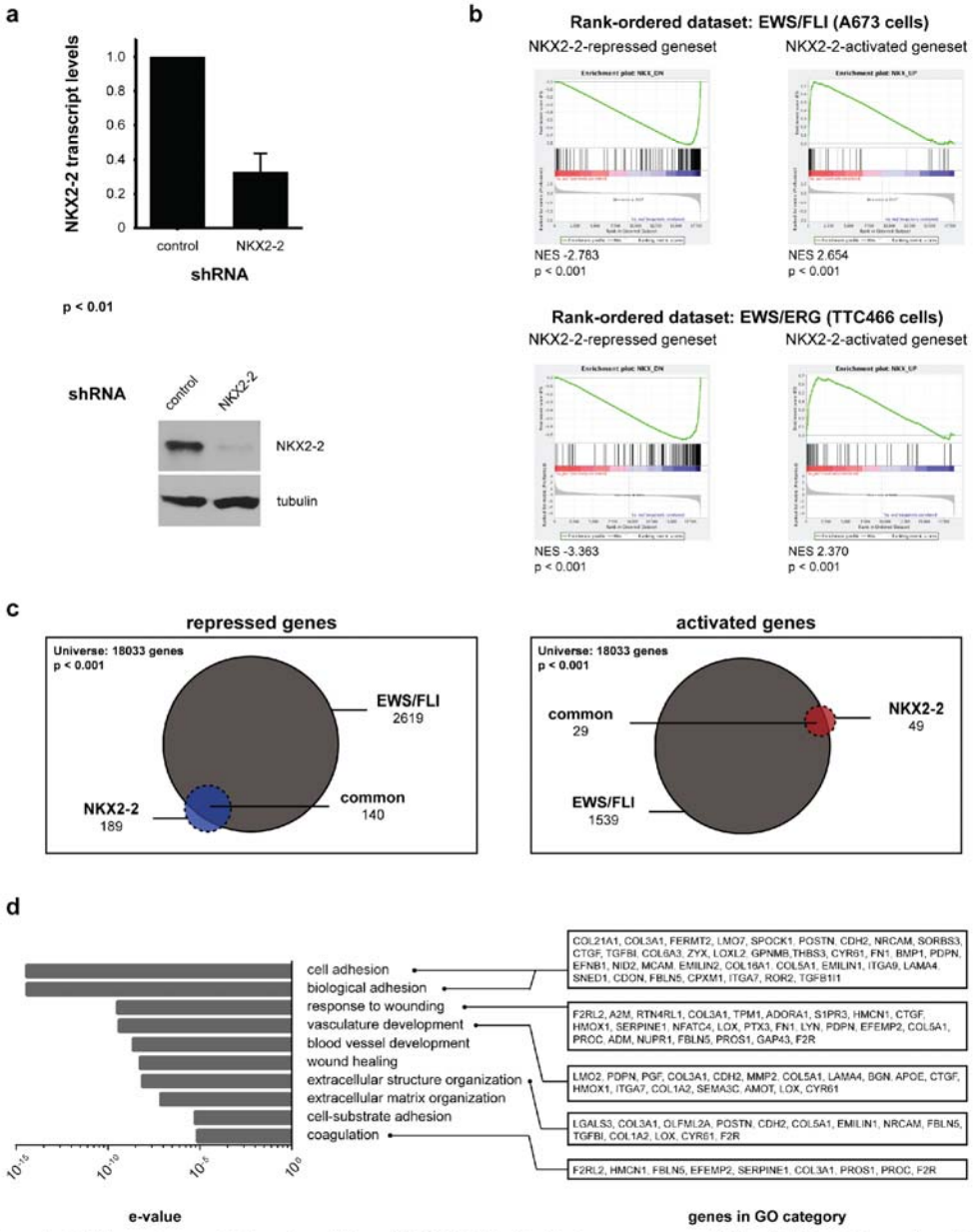

Figure 1: RNA-seq transcriptional profiling of NKX2-2 in the Ewing sarcoma cell line A673. (a) Expression of NKX2-2 is knocked down using retrovirally delivered shRNA specific to the 3'-UTR, as shown by qRT-PCR for NKX2-2 transcript levels (normalized to GAPDH levels) and western blot for protein levels (tubulin, loading control). (b) GSEA shows that NKX2-2-activated or repressed genes are enriched in the EWS/FLI-upregulated or downregulated dataset, respectively, from A673 cells. The same is true for the EWS/ERG-dataset from TTC466 cells. (c) Venn diagram analysis of the NKX2-2 and EWS/FLI repressed and activated genesets. The 140 common repressed genes and 29 common activated genes are highlighted in Table S1. (d) DAVID gene ontology analysis reveals that the NKX2-2-repressed geneset is enriched for cell adhesion genes. Genes from key GO terms are listed on the right.

FLI-mediated impairment of mesenchymal features of Ewing sarcoma cells, which was previously reported [41, 42]. Indeed, NKX2-2 knockdown in A673 cells (Fig. 2a) resulted in spreading over a significantly wider area on a fibronectin substrate compared to cells expressing a control shRNA, phenocopying loss of EWS/FLI (Fig. 2b, 2c; Fig. S2) [41]. Furthermore, while in control knockdown cells there is a diffuse signal of phalloidin staining, indicating short fragments of filamentous actin, upon NKX2-2 or EWS/FLI depletion actin organizes into long, thick stress fibers (Fig. 2b). Using a previously reported metric called stress fiber thickness index (SFTI), we determined that these increases in actin organization are indeed significant (Fig. 2e) [43, 44].

Cell spreading is a prominent feature of mesenchymally derived cells and occurs due to increased substrate adhesion. Adhesion is a complex process involving binding of various integrins to their cognate motifs in ECM proteins, signaling through adaptor proteins, and consequent organization of attached cytoskeletal elements. As predicted, we observed that significantly more focal adhesions (FA) form upon NKX2-2 or EWS/FLI knockdown, as shown by immunofluorescence staining for paxillin, one of the myriad proteins that populate FAs (Fig. 2b, 2d). Importantly, with all morphological phenotypes observed, the effect with NKX2-2 loss is less dramatic than EWS/FLI loss. This is not surprising because the NKX2-2-repressed geneset, while significantly overlapping with that of EWS/FLI, is only a small subset (Fig. 1c). Presumably EWS/FLI activates or represses the expression of other genes that control different aspects of formation of FAs and actin stress fibers, leading to increases in cell area.

An EWS/FLI-repressed gene that has been shown to have an effect on mesenchymal traits is zyxin. This protein is a FA component and has been demonstrated to aid in the stabilization of actin stress fibers [45]. The de-repression of *ZYX* might partially explain how NKX2-2 or EWS/FLI knockdown allows Ewing sarcoma cells to manifest mesenchymal characteristics. Predictably, when we knock down NKX2-2, zyxin is upregulated, as shown both by western blot (Fig. 2a) or by RNA-seq reads mapping to the *ZYX* locus (Fig. 2f).

Notably, these morphological changes were recapitulated in EWS502 and TC71, two other Ewing sarcoma lines with EWS/FLI translocations, demonstrating that this phenomenon is not cell line-specific (Fig 3a,c; Fig. S3, S4). Specifically, cell area and number of focal adhesions increase when NKX2-2 or EWS/FLI is knocked down in these cells (Fig 3b, 3d). In addition, while F-actin signals remain diffuse in EWS502 and TC71 control knockdown cells, actin stress fibers form upon NKX2-2 or EWS/FLI depletion in either cell line, with thicker and more pronounced fibers in the EWS/FLI knockdown condition (Fig. 3a, 3c). Though less efficient than in A673 cells, we were able to achieve appreciable knockdown of NKX2-2 in EWS502 cells as shown by protein levels, and in TC71 cells as shown by both mRNA and protein levels (Fig. S5). In addition, in these two cell lines zyxin is de-repressed slightly upon NKX2-2 depletion, and markedly upon EWS/FLI depletion, mirroring our initial findings in A673 cells (Fig. S5). Taken together, these data suggest that the underlying transcriptional networks leading to cell adhesion are conserved in all three cell lines used, and may be representative of Ewing sarcoma tumors.

To attribute increases in cell area and number of focal adhesions specifically to depletion of NKX2-2 either by an NKX2-2-specific shRNA or by knocking down EWS/FLI, we performed rescue experiments in A673 cells (Fig. 4a). The increase in cell area due to NKX2-2 knockdown was partially rescued by the RNAi-resistant cDNA construct of NKX2-2, confirming that our shRNA has few off-target effects (Fig. 4b, 4c; Fig. S6). There is also partial rescue of the increase in number of FAs (Fig. 4d). As had been shown before, EWS/FLI re-expression completely rescues EWS/FLI knockdown [41]. However, NKX2-2 re-expression upon EWS/FLI knockdown does not rescue phenotype, demonstrating that NKX2-2 is not sufficient to mediate the full complement of EWS/FLI repression of mesenchymal features (Fig. 4b-4d). This is not unexpected because we already observed that NKX2-2 confers only a partial phenotype in three cell lines. Moreover, it also supports our previous data showing that NKX2-2 is necessary but not sufficient for the transformation of Ewing sarcoma cells [37].

Since Ewing sarcoma cells form more focal adhesions upon depletion of NKX2-2, we reasoned that they also adhere more effectively to the substrate. Indeed we found that more NKX2-2-knockdown cells adhere after a 2-h incubation than control-knockdown cells, again phenocopying EWS/FLI knockdown, albeit to a less degree (Fig. 5a) [41].

A hallmark feature of mesenchymal cells is their pronounced capacity to migrate. In addition to impairing cell spreading and adhesion, it was previously demonstrated that EWS/FLI impedes the migration of Ewing sarcoma cells [41]. We therefore asked whether NKX2-2 also contributes to this phenotype. Indeed, in a monolayer scratch assay, depletion of NKX2-2 allows cells to more rapidly heal the wound than control-knockdown cells, but more slowly than EWS/FLI-knockdown cells (Fig. 5b, 5c). Importantly, this is not due to disparities in cell proliferation, as we have previously shown that these shRNAs do not profoundly impact growth in tissue culture [15, 37]. Upon closer examination of the monolayer edge we observed that NKX2-2- and EWS/FLI-knockdown cells migrate actively by elongating and spreading into the wound a feature that is absent in control knockdown cells, where wound healing seems to occur mainly by proliferation (Fig. 5d).

Recently, we showed that the transcription factor

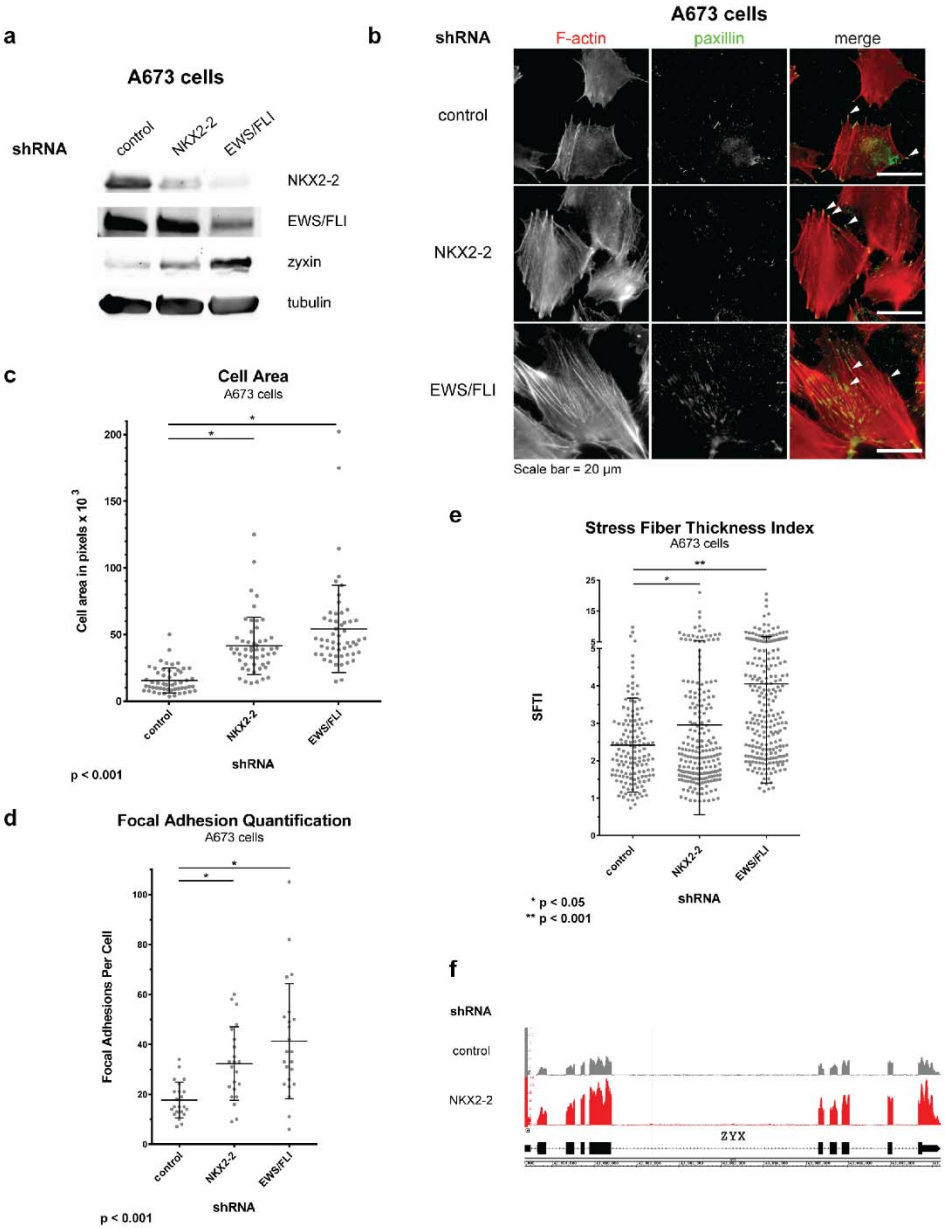

Figure 2: NKX2-2 impairs the capacity of A673 Ewing sarcoma cells to spread on the substrate and to form actin stress fibers and focal adhesions. (a) Western blots showing EWS/FLI, NKX2.2, zyxin, and tubulin protein levels for each condition. (b) NKX2-2 or EWS/FLI knockdown significantly increases cell area and organizes the actin cytoskeleton compared to control knockdown. At least 10 fields were taken for each condition. White arrowheads indicate paxillin-positive focal adhesions in the merged channel. (c-e) Quantification of (c) cell area, (d) number of focal adhesions, and (e) stress fiber thickness index in A673 cells. Scatter dot plot indicates individual measurements; mean ± SD is shown over the dot plots. Experiments were done in triplicate at least thrice; shown here is a single representative experiment. (f) Zyxin is de-repressed upon NKX2-2 knockdown. Shown is an Integrated Genome Browser snapshot of the *ZYX* locus (chr7:143,078,360-143,088,206; hg19) from the NKX2-2 RNA-seq differential expression analysis; there are significantly more reads in the NKX2-2 knockdown track than in control knockdown track.

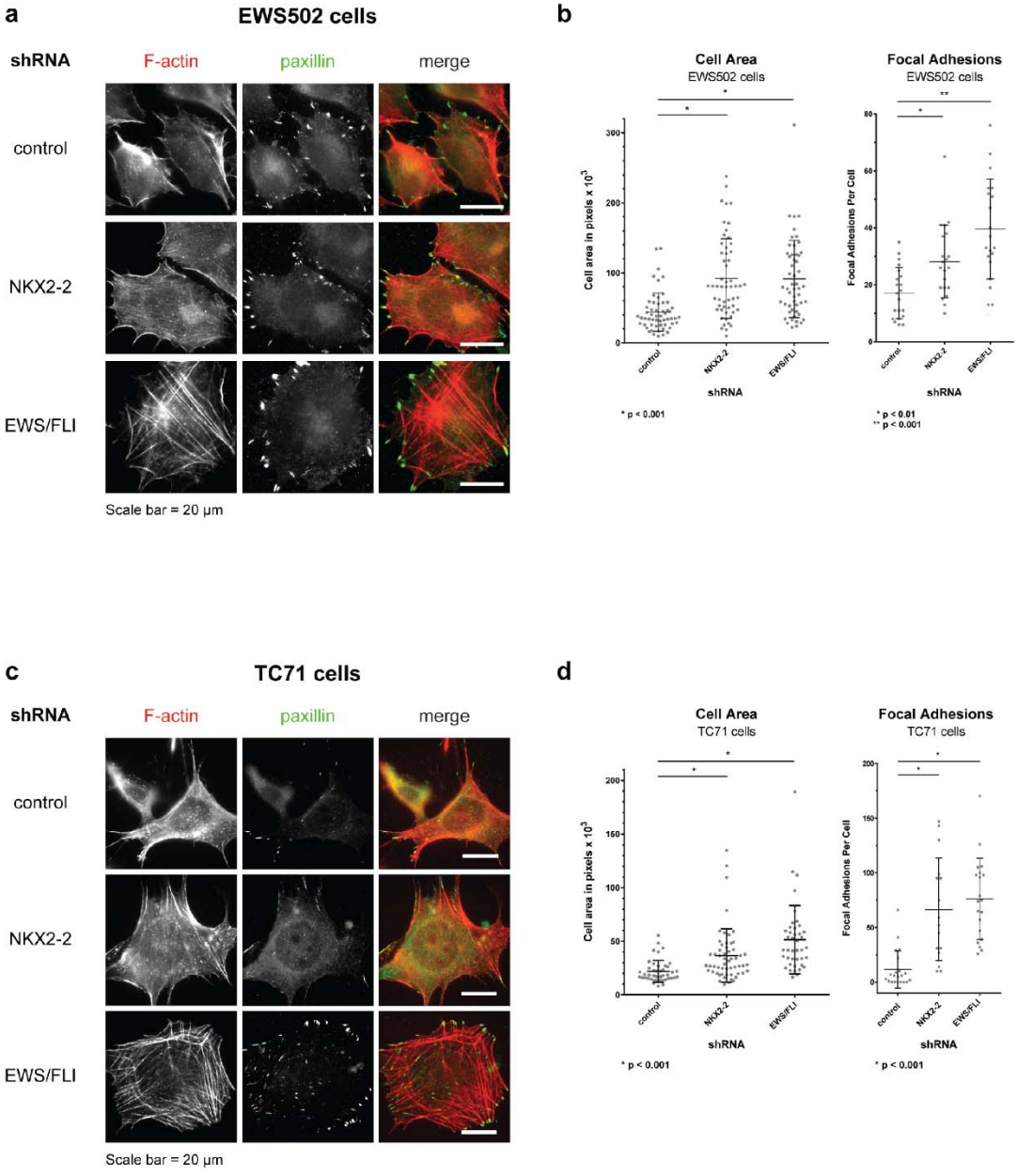

Figure 3: NKX2-2 represses mesenchymal features in two other Ewing sarcoma cell lines. (a,c) NKX2-2 or EWS/FLI deficiency significantly increases cell area and organizes the actin cytoskeleton compared to control in (a) EWS502 and (c) TC71 cells. At least 10 fields were taken for each condition. (b,d) Quantification of cell area and number of focal adhesions in (b) EWS502 and (d) TC71 cells.

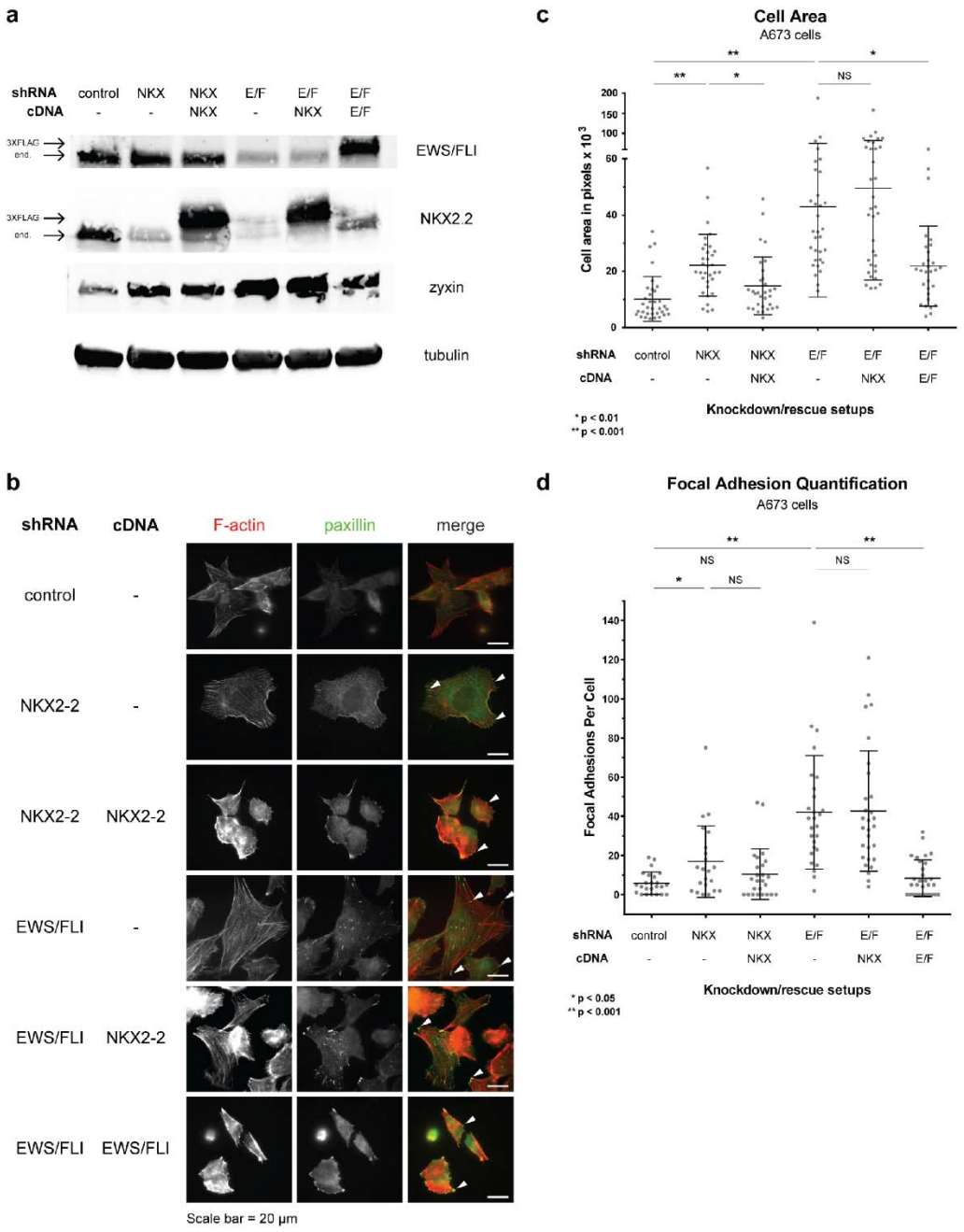

Figure 4: NKX2-2 is necessary but not sufficient for EWS/FLI-mediated repression of mesenchymal features of Ewing sarcoma cells. (a) Western blots showing EWS/FLI, NKX2.2, zyxin, and tubulin protein levels for all knockdown-rescue conditions. The bands for endogenous and exogenous 3XFLAG-tagged versions of EWS/FLI and NKX2.2 are indicated by arrows on the left. (b) Immunofluorescence experiments on re-expression studies. At least 10 fields were taken for each condition. White arrowheads indicate paxillin-positive focal adhesions in the merged channel. (c) Quantification of cell area in (b). (d) Quantification of focal adhesions in (b).

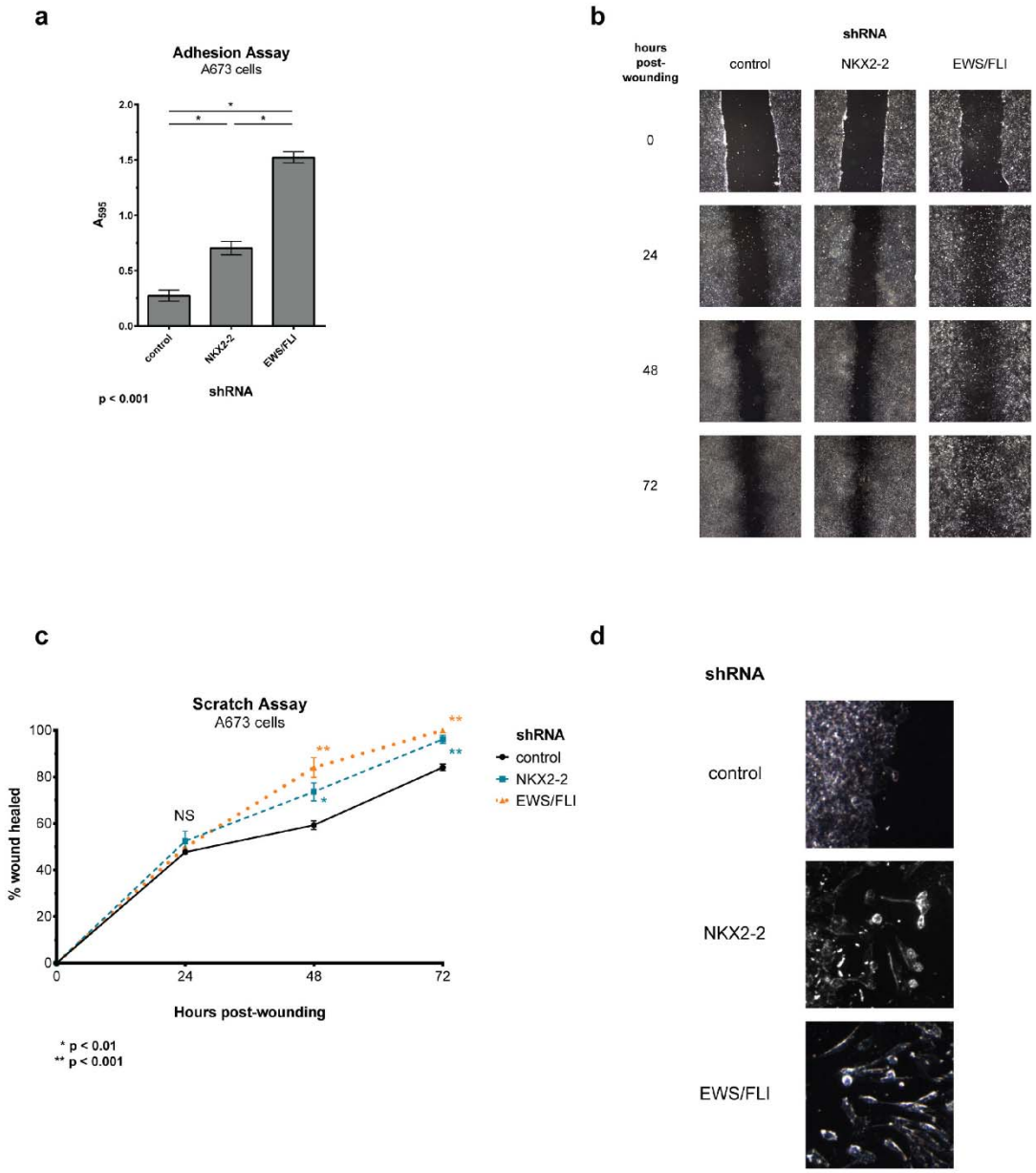

Figure 5: NKX2-2 inhibits cell adhesion and migration. (a) NKX2-2- or EWS/FLI-knockdown cells adhere more efficiently to the substrate than control cells. (b) NKX2-2 deficiency increases migration capacity in a scratch assay. Experiments were done at least thrice in A673 cells line using nine replicate fields per treatment. Shown is a single representative experiment. (c) Quantification of (b). Migration is shown as percentage of wound healed compared to the original area of scratch. Error bars indicate SEM. (d) Closer inspection of the monolayer edge reveals cells with mesenchymal features in NKX2-2- or EWS/FLI-knockdown cells, but not in control cells.

a **NKX2-2-repressed geneset**

siZEB2-5 dataset

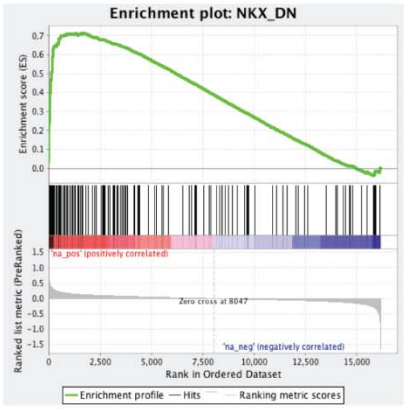

NES 3.141
p < 0.001

siZEB2-6 dataset

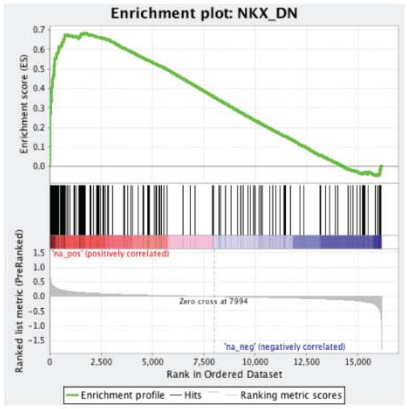

NES 2.844
p < 0.001

b **NKX2-2-activated geneset**

siZEB2-5 dataset

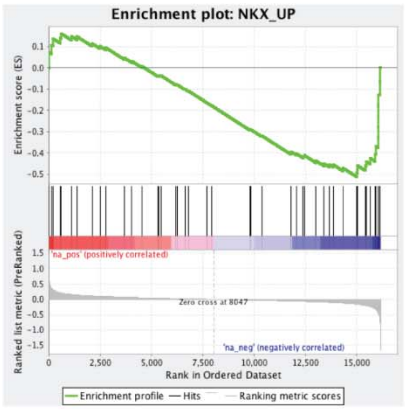

NES -1.741
p < 0.01

siZEB2-6 dataset

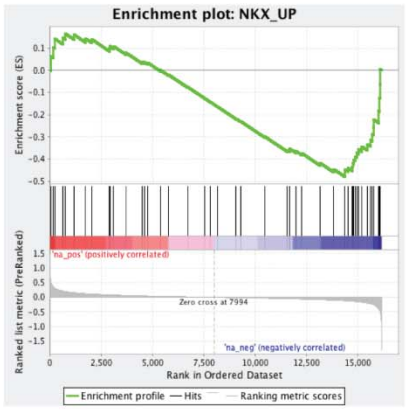

NES -1.652
p < 0.01

Figure 6: The NKX2-2 and ZEB2 transcriptional profiles are inversely correlated. (a) The NKX2-2 repressed geneset is enriched in the ZEB2 upregulated dataset, using two independent siRNAs against ZEB2. (b) The NKX2-2 activated geneset is enriched in the ZEB2 downregulated dataset.

and mesenchymal differentiation gene ZEB2 was highly expressed in both mesenchymal stem cells and Ewing sarcoma cell lines. Knockdown of ZEB2 in Ewing sarcoma cells induced morphological changes, such as a pronounced actin ring around the cell periphery, a cobblestone cell shape, and hampered cell migration in a scratch assay. These are in stark contrast to the EWS/FLI-depleted phenotype and strongly suggested that ZEB2 repressed epithelial features of Ewing sarcoma [46]. We reasoned that, since NKX2-2 loss phenocopied EWS/FLI loss, the NKX2-2 and ZEB2 transcriptional profiles must be inversely correlated, and this is indeed the case (Fig. 6). Using datasets previously generated with two independent siRNAs against ZEB2 in A673 cells [46], we found that the NKX2-2-repressed geneset, which contains the genes important for cell adhesion and ECM organization, is enriched in the ZEB2-upregulated dataset (Fig. 6a). Conversely, the NKX2-2-activated geneset is enriched in the ZEB2-downregulated dataset, but with lower normalized enrichment scores (Fig. 6b). Thus, the ZEB2 transcriptional profile which represents an "epithelialized" Ewing sarcoma, and the NKX2-2 transcriptional profile which represents a "mesenchymalized" Ewing sarcoma, antagonize each other. We therefore propose that EWS/FLI, through upregulation of NKX2-2, and ZEB2 act to repress differentiation in opposite directions along the epithelial-mesenchymal spectrum; together, they maintain Ewing sarcoma cells in a partially differentiated state.

DISCUSSION

NKX2-2 is one of the most highly upregulated genes by EWS/FLI [15]. It has been shown to have diagnostic significance, and may predict patient outcome (Fig. 7), but has thus far been used in the literature only as a marker for EWS/FLI transcriptional activation [47-50]. Our current work fills in this gap and identifies the importance of NKX2-2 as a tool of EWS/FLI in repressing salient mesenchymal characteristics of Ewing sarcoma cells, first displayed by unbiased transcriptional profiling. In summary, we show here that NKX2-2 assists in inhibiting cell spreading and formation of focal adhesions, as well as adhesion and migration in functional assays, and consequently mediates a block in mesenchymal differentiation.

Perhaps one of the most interesting findings of this current study is that NKX2-2 effects only a partial phenotype compared to EWS/FLI-this is true for all characteristics assayed. This underscores the enormity of the role of EWS/FLI, modulating a multitude of genes that each contribute partially to an attribute of tumorigenesis and/or metastasis. Because of the particularly low frequency of other genetic alterations, EWS/FLI acts as a "master regulator" of tumor growth and spread. Consequently, it was not surprising that NKX2-2 re-expression was insufficient for the EWS/FLI-mediated block of mesenchymalization. That several EWS/FLI transcriptional targets, such as NR0B1, GLI1, and indeed NKX2-2 itself, determined to be necessary for transformation are insufficient implies that such a genetic relationship could also be true for other phenotypes, such as cell adhesion and migration [15, 51, 52].

Recently, it was shown that zyxin and α5 integrin are repressed targets of EWS/FLI [42]. Specifically, when EWS/FLI is knocked down, expression of these two proteins go up, concomitant with the display of increased

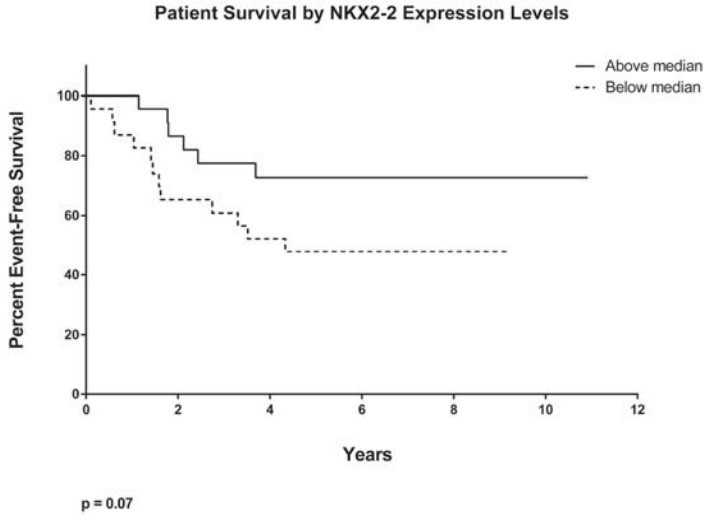

Figure 7: Low expression of NKX2-2 may predict poor patient outcome. Kaplan-Meier curve showing patient survival data for above- and below-median NKX2-2 expression (p = 0.07).

actin stress fiber organization, cell area, and number of FAs. Furthermore, when they are re-expressed individually without EWS/FLI depletion, the same mesenchymal traits manifest. Interestingly, zyxin and α5 integrin double re-expression is sufficient to capture the full EWS/FLI phenotype. Importantly, double re-expression also reduces colony growth in soft agar, suggesting that these two genes somehow contribute to transformation, while simultaneously shortening the latency of metastatic lesions in an intratibial xenograft model [42]. That enforced expression of zyxin and α5 integrin in concert is sufficient to counter the repression of mesenchymal features by EWS/FLI explains the part of the phenotype that cannot be attributed to NKX2-2. However, zyxin and α5 integrin double re-expression does not cause the full loss of transformation that depletion of NKX2-2 does [37], suggesting that there are additional, uncharacterized transcriptional targets of NKX2-2 that contribute to other arms of tumorigenesis.

During normal development, the differentiation state of a cell dictates many aspects of its life: proliferative capacity, interaction with other cells and with its microenvironment, and function. This also holds true for cells in a malignant context. While the cell-of-origin has been identified for the majority of carcinomas, this remains a challenge for Ewing sarcoma, nearly a century after it was first reported in the literature [53]. Neural crest cells and mesenchymal stem cells (MSCs) have had the most evidence for being the cell-of-origin for this disease, as reviewed previously [54]. In summary, Ewing sarcoma has been shown to express neural cell surface antigens; however, it has also been suggested that EWS/FLI has transcriptional control over neurogenesis and that this has little to do with the permissive cell type in which the translocation occurs [54-60]. On the other hand, when EWS/FLI is depleted from Ewing sarcoma cells, a transcriptional profile that closely mimics that of MSCs is adopted [50]. Enforced EWS/FLI expression in mesenchymal cells populating the developing mouse limb bud yields a SRBCT, but only upon p53 deletion [61]. However, while human MSCs expressing EWS/FLI displayed a transcriptional profile resembling that of Ewing sarcoma, injection into immunocompromised mice did not result in any viable tumors [49]. It has also been suggested that these two theories may not be mutually exclusive [54, 62, 63].

Although our work does not directly address the cell-of-origin question, it is consistent with an emerging theme whereby highly expressed proteins in Ewing sarcoma inhibits terminal differentiation. As was proposed before, the translocation perhaps occurs in a progenitor cell that is even less differentiated than MSCs [46]; EWS/FLI then upregulates NKX2-2 to repress mesenchymalization. ZEB2 and the interaction of endogenous EWS and RE1-silencing transcription factor (REST) then repress epithelialization and neuralization, respectively [46, 64]. Interestingly, using a dataset in a recent study of Ewing sarcoma patients from the Children's Oncology Group, we found that below-median expression of NKX2-2 correlates with decreased event-free survival (Fig. 7, $p = 0.07$) [65]. Volchenboum and colleagues further identified GO terms that are enriched in non-survivors versus survivors: migration, motility, and adhesion the very cell processes that EWS/FLI and NKX2-2 repress [65]. Collectively, our findings suggest that, while NKX2-2 is required for Ewing sarcomagenesis [37], there is a gradation of NKX2.2 levels in patient tumors that may contribute to outcome. Furthermore, high expression of ZEB2 also correlates with decreased survival [46]. Presumably, tumor cells in patients with low NKX2.2 levels and/or high ZEB2 levels are further along mesenchymal differentiation and may exhibit pronounced migratory characteristics, allowing them to metastasize to distal sites with enhanced capacity.

MATERIALS AND METHODS

Cell culture and knockdown-rescue infections

The Ewing sarcoma cell lines A673, EWS502, and TC71 were cultured, and retroviruses packaged in HEK293-EBNA cells, using standard techniques previously described [55, 56]. For RNA interference experiments, cells were infected with pMKO1.P retrovirus harboring shRNA constructs against luciferase (control), NKX2-2, or EWS/FLI. For cDNA rescue experiments, cells were infected with pMSCV-hygro retrovirus harboring cDNA for 3Xflag::NKX2-2 or 3Xflag::EWS/FLI, or an empty construct. The cloning strategy for these constructs and methods for retroviral infection and polyclonal selection are detailed elsewhere [15, 56].

Antibodies and western blotting

Standard western blot techniques were employed, using the following antibodies: goat α-NKX2.2 (Santa Cruz sc-15015, 1:200), rabbit α-FLI1 (Abcam ab15289, 1:1000), rabbit α-zyxin (kind gift from Mary Beckerle, 1:10000), mouse α-tubulin (Calbiochem CP06, 1:1000). HRP-conjugated secondary antibodies were used at 1:1000 dilution: donkey α-goat IgG (Santa Cruz sc-2020), sheep α-rabbit IgG (GE Healthcare NA934V), sheep α-mouse IgG (GE Healthcare NA931V). For western blots visualized using the Li-Cor Infrared Imaging System, their proprietary fluorophore-conjugated secondary antibodies were used at 1:2000 dilution: IRDye 680CW goat α-mouse IgG, IRDye 680CW donkey α-goat IgG, IRDye 800CW goat α-rabbit.

RNA sequencing and bioinformatic analyses

Total RNA was isolated from 5 x 10^6 cells using RNeasy Mini Kit (Qiagen) and quantified using NanoDrop. Knockdown was assessed using qRT-PCR (Bio-Rad iScript One-Step RT-PCR Kit with SYBR Green on a MyiQ/iQ5 system) and western blots, then libraries for mRNA sequencing were constructed with unique adapters for each of three biological replicates. The samples were run on the same sequencing lane on an Illumina HiSeq 2000 with 50-cycle single-end reads. Data from the NKX2-2 mRNA sequencing experiment were uploaded to the NCBI Sequence Read Archive (SUB237370) and is freely available. Raw sequence reads were aligned with Novoalign (Novocraft Technologies Sdn Bhd) to an hg19 index. This index is supplemented with small sequences representing splice junctions within the transcript model derived from Ensembl76, which was created by the MakeTranscription application from the USeq suite (http://useq.sourceforge.net). SAM files resulting from this step were processed with SamTranscriptomeParser from the same suite and used as input for the RNA-seq analysis. Differential expression was determined by using USeq's RNA-seq wrapper for the Bioconductor package DESeq [66]. Heat map and gene set enrichment analyses were performed using R and GenePattern, respectively. Venn diagrams were generated using VennMaster (http://sysbio.uni-ulm.de/?Software:VennMaster). Functional annotation clustering analysis was done using the Database for Annotation, Visualization and Integrated Discovery (DAVID v6.7, http://david.abcc.ncifcrf.gov/home.jsp).

Immunofluorescence studies

Staining of cells for immunofluorescence microscopy was performed using methods described previously [41], using the following reagents: normal goat serum (Santa Cruz sc-2043), mouse α-paxillin (BD Biosciences 610619), AlexaFluor-488 goat α-mouse IgG (Life Technologies A11029), AlexaFluor-568-phalloidin (Life Technologies A12380), DAPI (Life Technologies), Fluoromount-G (Southern Biotech 0100-01). Microscopy at 40X and 63X under oil immersion was performed using a Zeiss Axioskop 2 MOT Plus system, also previously described [41]. ImageJ was used to quantify cell area, while paxillin-positive focal adhesions were manually enumerated. Phalloidin-stained actin stress fibers were quantitated using an erosion decay method to generate a stress fiber thickness index (SFTI) as previously described [43, 44].

Adhesion assay

3 x 10^5 A673 cells from each condition were seeded in triplicate in 24-well plates and allowed to adhere for 2 h at 37°C and 5% CO_2. Wells were gently washed with PBS, fixed with 3.7% formaldehyde for 15 minutes, and again washed with PBS. Adherent cells were stained with 1% Toluidine Blue for 1 h. Wells were washed with dH_2O and allowed to dry overnight. Cells were lysed and the dye solubilized with 2% SDS. Absorbance readings were done at 595 nm, using 2% SDS as blank.

Migration assays

Scratch assays were performed as previously described [46]. Briefly, 2 x 10^6 cells were seeded in triplicate into 6-well tissue culture plates, and allowed to reach confluency. A micropipette tip was used to make a wound on the monolayer across the vertical diameter of the well. Each day wells were washed gently with PBS and replaced with culture media containing 5% serum. Phase-contrast images were taken of 9 fields at 0, 24, 48, and 72 hours post-wounding using a 5X objective on a Zeiss Axiovert100 microscope and QCapture Pro 7 software. Wound area was quantified with ImageJ and data presented as percent wound area healed per day.

Statistical analyses

Unpaired two-sample t-test analyses assuming unequal variance were performed in Microsoft Excel for qRT-PCR experiments and quantifications for cell area and focal adhesions. A log p rank test was performed for the Kaplan-Meier curve using GraphPad Prism 6.

ACKNOWLEDGMENTS

We are grateful to Beth Lawlor of the Department of Pediatrics and Communicable Diseases at the University of Michigan for providing clinical data and performing patient survival analysis. We thank Brian Dalley and the High Throughput Genomics core facility at the Huntsman Cancer Institute (HCI) for performing quality assessment, library preparation, and RNA-seq of our samples. We acknowledge David Nix of the Bioinformatics core facility and Ken Boucher of the Study Design and Biostatistics Center, both at HCI, for help with data analysis. JF acknowledges support from the SIDES (Sydney's Incredible Defeat of Ewing Sarcoma) Charity. This work was supported by NIH/NCI Grants R01 CA140394 (to SLL), K08 DK080190 (to MEE), GM50877 (to MCB), and P30 CA042014 (Cancer Center Support Grant to HCI); as well as funding from the Sunbeam Foundation and the CureSearch for Children's Cancer Foundation.

CONFLICT OF INTEREST

The authors have no conflict of interest to disclose.

REFERENCES

1. Delattre O, Zucman J, Plougastel B, Desmaze C, Melot T, Peter M, Kovar H, Joubert I, de Jong P, Rouleau G, Aurias A, Thomas G. Gene fusion with an ETS DNA-binding domain caused by chromosome translocation in human tumours. Nature. 1992; 359: 162-165.
2. Sankar S, Lessnick SL. Promiscuous partnerships in Ewing's sarcoma. Cancer Genet. 2011; 204: 351-365.
3. Brohl AS, Solomon DA, Chang W, Wang J, Song Y, Sindiri S, Patidar R, Hurd L, Chen L, Shern JF, Liao H, Wen X, Gerard J, et al. The genomic landscape of the Ewing Sarcoma family of tumors reveals recurrent STAG2 mutation. PLoS genetics. 2014; 10: e1004475.
4. Crompton BD, Stewart C, Taylor-Weiner A, Alexe G, Kurek KC, Calicchio ML, Kiezun A, Carter SL, Shukla SA, Mehta SS, Thorner AR, de Torres C, Lavarino C, et al. The Genomic Landscape of Pediatric Ewing Sarcoma. Cancer discovery. 2014.
5. Tirode F, Surdez D, Ma X, Parker M, Le Deley MC, Bahrami A, Zhang Z, Lapouble E, Grossetete-Lalami S, Rusch M, Reynaud S, Rio-Frio T, Hedlund E, et al. Genomic Landscape of Ewing Sarcoma Defines an Aggressive Subtype with Co-Association of STAG2 and TP53 Mutations. Cancer discovery. 2014.
6. Beck R, Monument MJ, Watkins WS, Smith R, Boucher KM, Schiffman JD, Jorde LB, Randall RL, Lessnick SL. EWS/FLI-responsive GGAA microsatellites exhibit polymorphic differences between European and African populations. Cancer Genet. 2012; 205: 304-312.
7. Gangwal K, Close D, Enriquez CA, Hill CP, Lessnick SL. Emergent Properties of EWS/FLI Regulation via GGAA Microsatellites in Ewing's Sarcoma. Genes Cancer. 2010; 1: 177-187.
8. Gangwal K, Sankar S, Hollenhorst PC, Kinsey M, Haroldsen SC, Shah AA, Boucher KM, Watkins WS, Jorde LB, Graves BJ, Lessnick SL. Microsatellites as EWS/FLI response elements in Ewing's sarcoma. Proc Natl Acad Sci U S A. 2008; 105: 10149-10154.
9. Guillon N, Tirode F, Boeva V, Zynovyev A, Barillot E, Delattre O. The oncogenic EWS-FLI1 protein binds in vivo GGAA microsatellite sequences with potential transcriptional activation function. PloS one. 2009; 4: e4932.
10. Monument MJ, Johnson KM, McIlvaine E, Abegglen L, Watkins WS, Jorde LB, Womer RB, Beeler N, Monovich L, Lawlor ER, Bridge JA, Schiffman JD, Krailo MD, et al. Clinical and biochemical function of polymorphic NR0B1 GGAA-microsatellites in Ewing sarcoma: a report from the Children's Oncology Group. PloS one. 2014; 9: e104378.
11. Ramakrishnan R, Fujimura Y, Zou JP, Liu F, Lee L, Rao VN, Reddy ES. Role of protein-protein interactions in the antiapoptotic function of EWS-Fli-1. Oncogene. 2004; 23: 7087-7094.
12. Kwon I, Kato M, Xiang S, Wu L, Theodoropoulos P, Mirzaei H, Han T, Xie S, Corden JL, McKnight SL. Phosphorylation-regulated binding of RNA polymerase II to fibrous polymers of low-complexity domains. Cell. 2013; 155: 1049-1060.
13. Sankar S, Bell R, Stephens B, Zhuo R, Sharma S, Bearss DJ, Lessnick SL. Mechanism and relevance of EWS/FLI-mediated transcriptional repression in Ewing sarcoma. Oncogene. 2013; 32: 5089-5100.
14. Sankar S, Theisen ER, Bearss J, Mulvihill T, Hoffman LM, Sorna V, Beckerle MC, Sharma S, Lessnick SL. Reversible LSD1 inhibition interferes with global EWS/ETS transcriptional activity and impedes Ewing sarcoma tumor growth. Clinical cancer research : an official journal of the American Association for Cancer Research. 2014; 20: 4584-4597.
15. Smith R, Owen LA, Trem DJ, Wong JS, Whangbo JS, Golub TR, Lessnick SL. Expression profiling of EWS/FLI identifies NKX2.2 as a critical target gene in Ewing's sarcoma. Cancer Cell. 2006; 9: 405-416.
16. Jimenez F, Campos-Ortega JA. A region of the Drosophila genome necessary for CNS development. Nature. 1979; 282: 310-312.
17. White K, DeCelles NL, Enlow TC. Genetic and developmental analysis of the locus vnd in Drosophila melanogaster. Genetics. 1983; 104: 433-448.
18. Briscoe J, Sussel L, Serup P, Hartigan-O'Connor D, Jessell TM, Rubenstein JL, Ericson J. Homeobox gene Nkx2.2 and specification of neuronal identity by graded Sonic hedgehog signalling. Nature. 1999; 398: 622-627.
19. Holz A, Kollmus H, Ryge J, Niederkofler V, Dias J, Ericson J, Stoeckli ET, Kiehn O, Arnold HH. The transcription factors Nkx2.2 and Nkx2.9 play a novel role in floor plate development and commissural axon guidance. Development. 2010; 137: 4249-4260.
20. McMahon AP. Neural patterning: the role of Nkx genes in the ventral spinal cord. Genes Dev. 2000; 14: 2261-2264.
21. Qi Y, Cai J, Wu Y, Wu R, Lee J, Fu H, Rao M, Sussel L, Rubenstein J, Qiu M. Control of oligodendrocyte differentiation by the Nkx2.2 homeodomain transcription factor. Development. 2001; 128: 2723-2733.
22. Tochitani S, Hayashizaki Y. Nkx2.2 antisense RNA overexpression enhanced oligodendrocytic differentiation. Biochem Biophys Res Commun. 2008; 372: 691-696.
23. Desai S, Loomis Z, Pugh-Bernard A, Schrunk J, Doyle MJ, Minic A, McCoy E, Sussel L. Nkx2.2 regulates cell fate choice in the enteroendocrine cell lineages of the intestine. Dev Biol. 2008; 313: 58-66.
24. Sussel L, Kalamaras J, Hartigan-O'Connor DJ, Meneses JJ, Pedersen RA, Rubenstein JL, German MS. Mice lacking

the homeodomain transcription factor Nkx2.2 have diabetes due to arrested differentiation of pancreatic beta cells. Development. 1998; 125: 2213-2221.

25. Cissell MA, Zhao L, Sussel L, Henderson E, Stein R. Transcription factor occupancy of the insulin gene in vivo. Evidence for direct regulation by Nkx2.2. J Biol Chem. 2003; 278: 751-756.
26. Raum JC, Gerrish K, Artner I, Henderson E, Guo M, Sussel L, Schisler JC, Newgard CB, Stein R. FoxA2, Nkx2.2, and PDX-1 regulate islet beta-cell-specific mafA expression through conserved sequences located between base pairs -8118 and -7750 upstream from the transcription start site. Mol Cell Biol. 2006; 26: 5735-5743.
27. Doyle MJ, Loomis ZL, Sussel L. Nkx2.2-repressor activity is sufficient to specify alpha-cells and a small number of beta-cells in the pancreatic islet. Development. 2007; 134: 515-523.
28. Doyle MJ, Sussel L. Nkx2.2 regulates beta-cell function in the mature islet. Diabetes. 2007; 56: 1999-2007.
29. Anderson KR, Torres CA, Solomon K, Becker TC, Newgard CB, Wright CV, Hagman J, Sussel L. Cooperative transcriptional regulation of the essential pancreatic islet gene NeuroD1 (beta2) by Nkx2.2 and neurogenin 3. J Biol Chem. 2009; 284: 31236-31248.
30. Anderson KR, White P, Kaestner KH, Sussel L. Identification of known and novel pancreas genes expressed downstream of Nkx2.2 during development. BMC Dev Biol. 2009; 9: 65.
31. Hill JT, Anderson KR, Mastracci TL, Kaestner KH, Sussel L. Novel computational analysis of protein binding array data identifies direct targets of Nkx2.2 in the pancreas. BMC Bioinformatics. 2011; 12: 62.
32. Papizan JB, Singer RA, Tschen SI, Dhawan S, Friel JM, Hipkens SB, Magnuson MA, Bhushan A, Sussel L. Nkx2.2 repressor complex regulates islet beta-cell specification and prevents beta-to-alpha-cell reprogramming. Genes Dev. 2011; 25: 2291-2305.
33. Hoffman BG, Zavaglia B, Beach M, Helgason CD. Expression of Groucho/TLE proteins during pancreas development. BMC Dev Biol. 2008; 8: 81.
34. Muhr J, Andersson E, Persson M, Jessell TM, Ericson J. Groucho-mediated transcriptional repression establishes progenitor cell pattern and neuronal fate in the ventral neural tube. Cell. 2001; 104: 861-873.
35. Watada H, Mirmira RG, Kalamaras J, German MS. Intramolecular control of transcriptional activity by the NK2-specific domain in NK-2 homeodomain proteins. Proc Natl Acad Sci U S A. 2000; 97: 9443-9448.
36. Yu Z, Syu LJ, Mellerick DM. Contextual interactions determine whether the Drosophila homeodomain protein, Vnd, acts as a repressor or activator. Nucleic Acids Res. 2005; 33: 1-12.
37. Owen LA, Kowalewski AA, Lessnick SL. EWS/FLI mediates transcriptional repression via NKX2.2 during oncogenic transformation in Ewing's sarcoma. PloS one. 2008; 3: e1965.
38. Baird K, Davis S, Antonescu CR, Harper UL, Walker RL, Chen Y, Glatfelter AA, Duray PH, Meltzer PS. Gene expression profiling of human sarcomas: insights into sarcoma biology. Cancer Res. 2005; 65: 9226-9235.
39. Yoshida A, Sekine S, Tsuta K, Fukayama M, Furuta K, Tsuda H. NKX2.2 is a useful immunohistochemical marker for Ewing sarcoma. Am J Surg Pathol. 2012; 36: 993-999.
40. Davicioni E, Finckenstein FG, Shahbazian V, Buckley JD, Triche TJ, Anderson MJ. Identification of a PAX-FKHR gene expression signature that defines molecular classes and determines the prognosis of alveolar rhabdomyosarcomas. Cancer Res. 2006; 66: 6936-6946.
41. Chaturvedi A, Hoffman LM, Welm AL, Lessnick SL, Beckerle MC. The EWS/FLI Oncogene Drives Changes in Cellular Morphology, Adhesion, and Migration in Ewing Sarcoma. Genes Cancer. 2012; 3: 102-116.
42. Chaturvedi A, Hoffman LM, Jensen CC, Lin YC, Grossmann AH, Randall RL, Lessnick SL, Welm AL, Beckerle MC. Molecular dissection of the mechanism by which EWS/FLI expression compromises actin cytoskeletal integrity and cell adhesion in Ewing sarcoma. Mol Biol Cell. 2014; 25: 2695-2709.
43. Hoffman LM, Jensen CC, Kloeker S, Wang CL, Yoshigi M, Beckerle MC. Genetic ablation of zyxin causes Mena/VASP mislocalization, increased motility, and deficits in actin remodeling. J Cell Biol. 2006; 172: 771-782.
44. Yoshigi M, Hoffman LM, Jensen CC, Yost HJ, Beckerle MC. Mechanical force mobilizes zyxin from focal adhesions to actin filaments and regulates cytoskeletal reinforcement. J Cell Biol. 2005; 171: 209-215.
45. Smith MA, Blankman E, Gardel ML, Luettjohann L, Waterman CM, Beckerle MC. A zyxin-mediated mechanism for actin stress fiber maintenance and repair. Developmental cell. 2010; 19: 365-376.
46. Wiles ET, Bell R, Thomas D, Beckerle M, Lessnick SL. ZEB2 Represses the Epithelial Phenotype and Facilitates Metastasis in Ewing Sarcoma. Genes Cancer. 2013; 4: 486-500.
47. Leacock SW, Basse AN, Chandler GL, Kirk AM, Rakheja D, Amatruda JF. A zebrafish transgenic model of Ewing's sarcoma reveals conserved mediators of EWS-FLI1 tumorigenesis. Disease models & mechanisms. 2012; 5: 95-106.
48. Patel M, Simon JM, Iglesia MD, Wu SB, McFadden AW, Lieb JD, Davis IJ. Tumor-specific retargeting of an oncogenic transcription factor chimera results in dysregulation of chromatin and transcription. Genome research. 2012; 22: 259-270.
49. Riggi N, Suva ML, Suva D, Cironi L, Provero P, Tercier S, Joseph JM, Stehle JC, Baumer K, Kindler V, Stamenkovic I. EWS-FLI-1 expression triggers a Ewing's sarcoma initiation program in primary human mesenchymal stem

cells. Cancer Res. 2008; 68: 2176-2185.

50. Tirode F, Laud-Duval K, Prieur A, Delorme B, Charbord P, Delattre O. Mesenchymal stem cell features of Ewing tumors. Cancer Cell. 2007; 11: 421-429.
51. Kinsey M, Smith R, Lessnick SL. NR0B1 is required for the oncogenic phenotype mediated by EWS/FLI in Ewing's sarcoma. Molecular cancer research : MCR. 2006; 4: 851-859.
52. Sankar S, Tanner JM, Bell R, Chaturvedi A, Randall RL, Beckerle MC, Lessnick SL. A novel role for keratin 17 in coordinating oncogenic transformation and cellular adhesion in Ewing sarcoma. Mol Cell Biol. 2013; 33: 4448-4460.
53. Ewing J. Classics in oncology. Diffuse endothelioma of bone. James Ewing. Proceedings of the New York Pathological Society, 1921. CA: a cancer journal for clinicians. 1972; 22: 95-98.
54. Toomey EC, Schiffman JD, Lessnick SL. Recent advances in the molecular pathogenesis of Ewing's sarcoma. Oncogene. 2010; 29: 4504-4516.
55. Hu-Lieskovan S, Zhang J, Wu L, Shimada H, Schofield DE, Triche TJ. EWS-FLI1 fusion protein up-regulates critical genes in neural crest development and is responsible for the observed phenotype of Ewing's family of tumors. Cancer Res. 2005; 65: 4633-4644.
56. Lessnick SL, Dacwag CS, Golub TR. The Ewing's sarcoma oncoprotein EWS/FLI induces a p53-dependent growth arrest in primary human fibroblasts. Cancer Cell. 2002; 1: 393-401.
57. Lipinski M, Braham K, Philip I, Wiels J, Philip T, Goridis C, Lenoir GM, Tursz T. Neuroectoderm-associated antigens on Ewing's sarcoma cell lines. Cancer Res. 1987; 47: 183-187.
58. Lipinski M, Hirsch MR, Deagostini-Bazin H, Yamada O, Tursz T, Goridis C. Characterization of neural cell adhesion molecules (NCAM) expressed by Ewing and neuroblastoma cell lines. International journal of cancer Journal international du cancer. 1987; 40: 81-86.
59. Rorie CJ, Thomas VD, Chen P, Pierce HH, O'Bryan JP, Weissman BE. The Ews/Fli-1 fusion gene switches the differentiation program of neuroblastomas to Ewing sarcoma/peripheral primitive neuroectodermal tumors. Cancer Res. 2004; 64: 1266-1277.
60. Staege MS, Hutter C, Neumann I, Foja S, Hattenhorst UE, Hansen G, Afar D, Burdach SE. DNA microarrays reveal relationship of Ewing family tumors to both endothelial and fetal neural crest-derived cells and define novel targets. Cancer Res. 2004; 64: 8213-8221.
61. Lin PP, Pandey MK, Jin F, Xiong S, Deavers M, Parant JM, Lozano G. EWS-FLI1 induces developmental abnormalities and accelerates sarcoma formation in a transgenic mouse model. Cancer Res. 2008; 68: 8968-8975.
62. Lee G, Kim H, Elkabetz Y, Al Shamy G, Panagiotakos G, Barberi T, Tabar V, Studer L. Isolation and directed differentiation of neural crest stem cells derived from human embryonic stem cells. Nature biotechnology. 2007; 25: 1468-1475.
63. Takashima Y, Era T, Nakao K, Kondo S, Kasuga M, Smith AG, Nishikawa S. Neuroepithelial cells supply an initial transient wave of MSC differentiation. Cell. 2007; 129: 1377-1388.
64. Sankar S, Gomez NC, Bell R, Patel M, Davis IJ, Lessnick SL, Luo W. EWS and RE1-Silencing Transcription Factor Inhibit Neuronal Phenotype Development and Oncogenic Transformation in Ewing Sarcoma. Genes Cancer. 2013; 4: 213-223.
65. Volchenboum SL, Andrade J, Huang L, Barkauskas DA, Krailo M, Womer RB, Ranft A, Potratz J, Dirksen U, Triche T, Lawlor E. Gene expression profiling of Ewing sarcoma tumors reveals the prognostic importance of tumor-stromal interactions: a report from the Children's Oncology Group. J Path: Clin Res. 25 Jan 2015 [Epub ahead of print].
66. Anders S, Huber W. Differential expression analysis for sequence count data. Genome biology. 2010; 11: R106.

EWS/FLI utilizes NKX2-2 to repress mesenchymal features of ewing sarcoma

Supplementary Material

Table S1: List of NKX2-2 Repressed and Activated Gene Targets. We found that NKX2-2 repressed 189 and activated 49 genes at fold change ≥ 1.5 ($|\log_2 T/C| \geq 0.585$) and maximum DESeq FDR ≥ 50. "T/C" denotes the ratio of reads between "treatment" (NKX2-2 shRNA) and "control" (control shRNA). Genes in boldface are also EWS/FLI-regulated, i.e. genes that are in the Venn diagram intersections (Fig. 1c).

Repressed Genes			
Ensembl ID	**Gene Symbol**	**Max DESeq FDR**	**$\lvert Log_2(T/C) \rvert$**
ENSG00000175899	**A2M**	824.2042	2.5672
ENSG00000171201	SMR3B	839.0181	2.4857
ENSG00000130203	**APOE**	638.7277	2.2606
ENSG00000109846	**CRYAB**	750.5163	2.0917
ENSG00000113083	**LOX**	650.2720	2.0691
ENSG00000120708	**TGFBI**	447.5006	1.8439
ENSG00000182492	**BGN**	397.8915	1.7014
ENSG00000168542	**COL3A1**	388.0310	1.6943
ENSG00000100292	**HMOX1**	348.7940	1.6022
ENSG00000140092	**FBLN5**	287.2886	1.4978
ENSG00000106333	**PCOLCE**	277.2993	1.4858
ENSG00000164220	**F2RL2**	224.5895	1.3074
ENSG00000181104	**F2R**	197.7093	1.3003
ENSG00000163017	ACTG2	186.1635	1.2566
ENSG00000224729	**RP13-530H6.2**	198.2907	1.2327
ENSG00000166426	CRABP1	177.9007	1.2267
ENSG00000152377	**SPOCK1**	194.4080	1.2238
ENSG00000050165	**DKK3**	194.3323	1.2094
ENSG00000162998	FRZB	177.4267	1.1972
ENSG00000163661	**PTX3**	161.1237	1.1891
ENSG00000105270	**CLIP3**	173.1340	1.1832
ENSG00000122786	**CALD1**	197.7093	1.1795
ENSG00000174938	**SEZ6L2**	177.9007	1.1714
ENSG00000113721	**PDGFRB**	159.8752	1.1524
ENSG00000138080	**EMILIN1**	163.2299	1.1487

ENSG00000255887	HTR4	148.7123	1.1307
ENSG00000132718	**SYT11**	145.7101	1.1229
ENSG00000140682	**TGFB1I1**	178.7892	1.1204
ENSG00000001036	**FUCA2**	135.8940	1.1032
ENSG00000163297	**ANTXR2**	145.0749	1.0982
ENSG00000137558	PI15	135.0315	1.0911
ENSG00000084636	**COL16A1**	154.8618	1.0823
ENSG00000170445	**HARS**	116.6256	1.0579
ENSG00000140416	**TPM1**	162.9830	1.0578
ENSG00000159840	**ZYX**	146.2752	1.0574
ENSG00000147100	**SLC16A2**	129.2495	1.0493
ENSG00000163359	**COL6A3**	154.8618	1.0387
ENSG00000185585	**OLFML2A**	139.5245	1.0355
ENSG00000172020	**GAP43**	138.2877	1.0349
ENSG00000091129	**NRCAM**	131.3168	1.0223
ENSG00000163346	**PBXIP1**	118.8992	1.0092
ENSG00000130176	**CNN1**	157.1690	1.0060
ENSG00000175868	CALCB	97.6286	1.0018
ENSG00000007062	PROM1	119.5708	0.9975
ENSG00000143341	HMCN1	107.9254	0.9945
ENSG00000100095	SEZ6L	104.3363	0.9831
ENSG00000172638	**EFEMP2**	122.1316	0.9617
ENSG00000113140	**SPARC**	113.8953	0.9529
ENSG00000100968	NFATC4	95.6476	0.9523
ENSG00000148677	**ANKRD1**	144.9075	0.9509
ENSG00000174099	**MSRB3**	119.5708	0.9492
ENSG00000119630	**PGF**	112.9963	0.9484
ENSG00000180573	HIST1H2AC	95.3523	0.9442
ENSG00000142871	**CYR61**	122.6468	0.9414
ENSG00000141338	ABCA8	102.8714	0.9372
ENSG00000120896	**SORBS3**	107.5048	0.9319
ENSG00000117228	**GBP1**	98.6774	0.9256
ENSG00000115414	**FN1**	93.2659	0.9066
ENSG00000171195	MUC7	108.4639	0.9031
ENSG00000163395	**IGFN1**	89.1615	0.8949
ENSG00000174807	**CD248**	97.7315	0.8923

ENSG00000026297	**RNASET2**	84.3447	0.8848
ENSG00000112769	**LAMA4**	92.0180	0.8815
ENSG00000213694	**S1PR3**	93.4723	0.8723
ENSG00000164488	**DACT2**	91.3191	0.8670
ENSG00000123384	**LRP1**	94.8068	0.8653
ENSG00000123933	**MXD4**	92.1400	0.8647
ENSG00000109576	**AADAT**	88.8271	0.8565
ENSG00000232783	AC073135.3	86.1990	0.8549
ENSG00000132386	SERPINF1	79.2795	0.8540
ENSG00000103485	QPRT	80.5658	0.8507
ENSG00000211445	**GPX3**	95.0507	0.8500
ENSG00000136235	**GPNMB**	125.6224	0.8428
ENSG00000131724	**IL13RA1**	92.2947	0.8420
ENSG00000109323	**MANBA**	90.7411	0.8409
ENSG00000115718	PROC	81.4366	0.8408
ENSG00000168994	**C6orf145**	80.7035	0.8352
ENSG00000163485	**ADORA1**	92.1477	0.8341
ENSG00000164938	**TP53INP1**	79.2954	0.8321
ENSG00000171940	**ZNF217**	74.9894	0.8251
ENSG00000118733	OLFM3	74.4940	0.8250
ENSG00000126016	AMOT	79.1751	0.8215
ENSG00000144730	**IL17RD**	90.7412	0.8207
ENSG00000013016	**EHD3**	90.2576	0.8147
ENSG00000076706	**MCAM**	96.1121	0.8129
ENSG00000180998	GPR137C	62.2068	0.8104
ENSG00000133110	**POSTN**	93.8375	0.8089
ENSG00000164692	**COL1A2**	88.0884	0.8041
ENSG00000169231	**THBS3**	70.3029	0.8030
ENSG00000168280	**KIF5C**	67.2596	0.8029
ENSG00000155130	**MARCKS**	68.7284	0.8026
ENSG00000162490	**C1orf187**	88.9574	0.8025
ENSG00000168487	**BMP1**	78.8870	0.8007
ENSG00000119522	**DENND1A**	69.3145	0.8002
ENSG00000245532	**NEAT1**	61.6564	0.7993
ENSG00000168461	**RAB31**	77.1856	0.7985
ENSG00000176720	**BOK**	82.4016	0.7968

ENSG00000166750	**SLFN5**	66.4069	0.7968
ENSG00000170500	LONRF2	62.5051	0.7967
ENSG00000064042	LIMCH1	65.5743	0.7945
ENSG00000149212	SESN3	68.1630	0.7911
ENSG00000162493	PDPN	65.1762	0.7899
ENSG00000173698	GPR64	71.5143	0.7875
ENSG00000162804	**SNED1**	69.0734	0.7869
ENSG00000075223	**SEMA3C**	67.8865	0.7862
ENSG00000144455	**SUMF1**	65.5743	0.7844
ENSG00000169071	**ROR2**	75.8909	0.7837
ENSG00000256061	**DYX1C1-CCPG1**	68.4338	0.7803
ENSG00000134013	**LOXL2**	80.7819	0.7742
ENSG00000150593	PDCD4	63.3693	0.7726
ENSG00000166340	TPP1	80.7120	0.7698
ENSG00000007866	**TEAD3**	67.3072	0.7641
ENSG00000087303	**NID2**	67.6544	0.7616
ENSG00000166444	**ST5**	63.5447	0.7592
ENSG00000168016	TRANK1	72.5045	0.7586
ENSG00000090776	EFNB1	63.4265	0.7585
ENSG00000141756	**FKBP10**	68.4422	0.7580
ENSG00000138829	FBN2	58.2532	0.7577
ENSG00000168386	**FILIP1L**	69.6937	0.7573
ENSG00000179820	**MYADM**	65.5680	0.7567
ENSG00000135363	**LMO2**	57.9719	0.7542
ENSG00000137070	IL11RA	64.4975	0.7539
ENSG00000119655	**NPC2**	63.1146	0.7536
ENSG00000088882	**CPXM1**	66.3513	0.7523
ENSG00000197444	OGDHL	69.8468	0.7505
ENSG00000173548	**SNX33**	61.2146	0.7388
ENSG00000154262	ABCA6	62.7327	0.7380
ENSG00000107796	**ACTA2**	69.8468	0.7357
ENSG00000135406	PRPH	61.3089	0.7353
ENSG00000102032	RENBP	61.7957	0.7351
ENSG00000123200	ZC3H13	59.6177	0.7334
ENSG00000090238	YPEL3	60.3276	0.7327
ENSG00000154258	ABCA9	61.8086	0.7305

ENSG00000019549	**SNAI2**	72.7718	0.7304
ENSG00000132563	REEP2	59.5967	0.7296
ENSG00000229036	**RP1-20N2.6**	54.4579	0.7280
ENSG00000187714	SLC18A3	61.0677	0.7227
ENSG00000185924	**RTN4RL1**	57.4379	0.7204
ENSG00000115363	**FAM176A**	64.7503	0.7196
ENSG00000100196	**KDELR3**	62.9979	0.7189
ENSG00000129038	**LOXL1**	72.0864	0.7175
ENSG00000174233	**ADCY6**	56.6107	0.7171
ENSG00000173110	**HSPA6**	70.8810	0.7158
ENSG00000166147	**FBN1**	70.4821	0.7138
ENSG00000132205	**EMILIN2**	66.4069	0.7129
ENSG00000104325	DECR1	51.8177	0.7125
ENSG00000153208	MERTK	57.4382	0.7101
ENSG00000180596	HIST1H2BC	51.0862	0.7096
ENSG00000166033	**HTRA1**	66.6696	0.7074
ENSG00000073712	**FERMT2**	63.8742	0.7049
ENSG00000089169	RPH3A	58.0015	0.7037
ENSG00000103710	RASL12	52.0173	0.7024
ENSG00000163430	**FSTL1**	54.7960	0.6943
ENSG00000184500	**PROS1**	52.8782	0.6936
ENSG00000254087	**LYN**	53.2529	0.6934
ENSG00000180139	**RP11-399O19.5**	59.4507	0.6920
ENSG00000087245	**MMP2**	74.3663	0.6888
ENSG00000144668	**ITGA9**	55.5170	0.6885
ENSG00000137507	**LRRC32**	64.4975	0.6875
ENSG00000135424	ITGA7	54.2254	0.6854
ENSG00000035862	**TIMP2**	59.4507	0.6841
ENSG00000145703	IQGAP2	55.9574	0.6839
ENSG00000148926	**ADM**	54.9067	0.6836
ENSG00000136153	**LMO7**	69.2007	0.6835
ENSG00000075213	**SEMA3A**	53.0944	0.6815
ENSG00000024422	**EHD2**	70.2261	0.6797
ENSG00000146904	**EPHA1**	52.8476	0.6784
ENSG00000064666	**CNN2**	51.0883	0.6764
ENSG00000100097	**LGALS1**	56.0601	0.6757

ENSG00000123989	**CHPF**	59.5704	0.6753
ENSG00000109790	**KLHL5**	50.8233	0.6749
ENSG00000124749	COL21A1	51.7971	0.6745
ENSG00000168140	**VASN**	55.5914	0.6706
ENSG00000134531	**EMP1**	51.4953	0.6703
ENSG00000197712	**FAM114A1**	74.0854	0.6691
ENSG00000170558	**CDH2**	55.2606	0.6657
ENSG00000136859	**ANGPTL2**	64.4887	0.6649
ENSG00000145248	**SLC10A4**	54.7960	0.6649
ENSG00000179954	**SSC5D**	55.6596	0.6588
ENSG00000176046	**NUPR1**	54.9144	0.6544
ENSG00000064309	**CDON**	50.7290	0.6529
ENSG00000106366	**SERPINE1**	56.9858	0.6427
ENSG00000131981	**LGALS3**	52.5960	0.6402
ENSG00000011028	**MRC2**	56.4280	0.6401
ENSG00000158089	**GALNT14**	50.5565	0.6331
ENSG00000118523	**CTGF**	52.6271	0.6294
ENSG00000130635	**COL5A1**	52.9122	0.6276
ENSG00000163909	**HEYL**	51.0532	0.6096
ENSG00000149591	**TAGLN**	50.0557	0.5875
Activated Genes			
Ensembl ID	**Gene Symbol**	**Max DESeq FDR**	**$\lvert Log_2(T/C) \rvert$**
ENSG00000128245	YWHAH	221.7330	1.4394
ENSG00000158710	TAGLN2	157.9439	1.2271
ENSG00000064300	**NGFR**	146.8393	1.1719
ENSG00000049540	ELN	127.8538	1.1311
ENSG00000140497	SCAMP2	117.3317	1.0755
ENSG00000137309	HMGA1	108.8962	1.0253
ENSG00000166803	**KIAA0101**	104.7058	0.9707
ENSG00000009709	**PAX7**	86.6807	0.9616
ENSG00000101187	SLCO4A1	89.0895	0.9250
ENSG00000079215	**SLC1A3**	86.1420	0.9049
ENSG00000112759	**SLC29A1**	81.4337	0.8922
ENSG00000186867	**QRFPR**	87.2617	0.8907
ENSG00000135447	**PPP1R1A**	81.5021	0.8899

ENSG00000158195	WASF2	78.8870	0.8809
ENSG00000169894	**MUC3A**	84.3078	0.8776
ENSG00000124164	VAPB	77.2833	0.8664
ENSG00000085552	**IGSF9**	80.7035	0.8663
ENSG00000138061	CYP1B1	81.5021	0.8430
ENSG00000159167	STC1	73.5211	0.8410
ENSG00000117289	**TXNIP**	67.0722	0.8307
ENSG00000071655	MBD3	66.4069	0.8216
ENSG00000249906	**RP5-1029K10.2**	70.9345	0.8201
ENSG00000187867	**PALM3**	68.1630	0.7994
ENSG00000213390	**ARHGAP19**	66.9043	0.7947
ENSG00000081181	**ARG2**	66.3513	0.7900
ENSG00000166342	**NETO1**	66.8842	0.7828
ENSG00000173805	**HAP1**	65.5680	0.7654
ENSG00000198576	**ARC**	61.3460	0.7649
ENSG00000166974	MAPRE2	63.4265	0.7561
ENSG00000080819	CPOX	58.0015	0.7519
ENSG00000173890	**GPR160**	53.8457	0.7515
ENSG00000126785	RHOJ	54.9563	0.7467
ENSG00000172757	CFL1	53.0042	0.7441
ENSG00000054611	TBC1D22A	50.5441	0.7417
ENSG00000131238	PPT1	53.0363	0.7396
ENSG00000135446	CDK4	55.7100	0.7380
ENSG00000057294	**PKP2**	55.8437	0.7289
ENSG00000149269	PAK1	55.1639	0.7271
ENSG00000172236	**TPSAB1**	54.3280	0.7254
ENSG00000171766	**GATM**	54.9487	0.7203
ENSG00000072736	**NFATC3**	52.5705	0.7202
ENSG00000128594	**LRRC4**	52.9122	0.7202
ENSG00000129484	**PARP2**	53.2527	0.7194
ENSG00000168765	**GSTM4**	50.8257	0.7172
ENSG00000181744	C3orf58	54.6557	0.7170
ENSG00000113368	**LMNB1**	51.6650	0.7152
ENSG00000165495	**PKNOX2**	52.9258	0.7141
ENSG00000164362	**TERT**	51.2488	0.7124
ENSG00000165731	**RET**	52.0706	0.7109

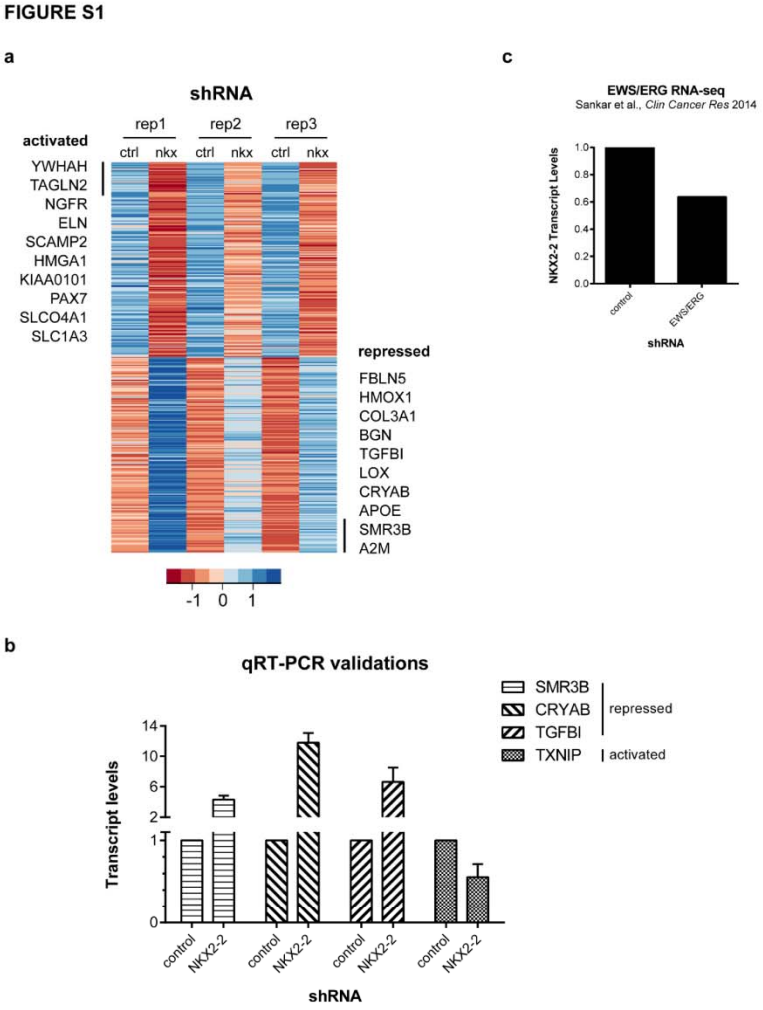

Figure S1: Key NKX2-2-regulated genes. (a) Heat map shows top 200 activated or repressed genes of NKX2-2 in A673 cells. The control shRNA and NKX2-2 shRNA lanes for each of three replicates are indicated. The top 10 genes in each set are enumerated. (b) qRT-PCR validation of select NKX2-2 target genes. (c) NKX2-2 is an activated target of EWS/ERG in TTC466 cells.

FIGURE S2

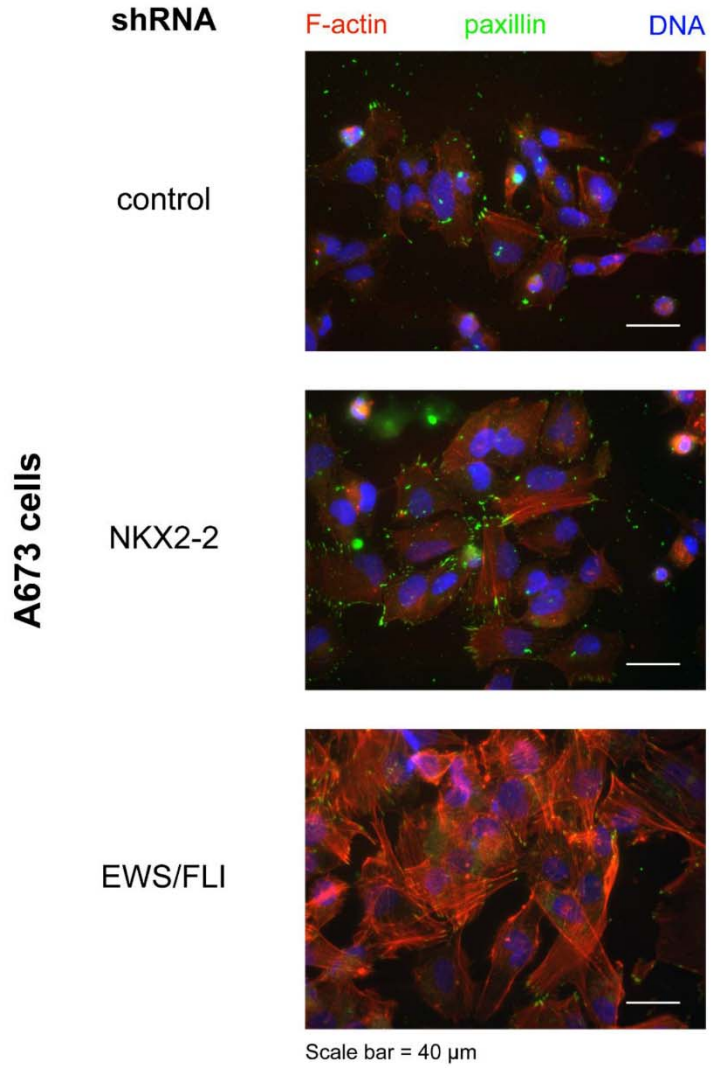

Figure S2: Immunofluorescence 40X fields of A673 cells harboring control, NKX2-2, or EWS/FLI shRNA. Merged images of IF staining for F-actin (red), paxillin (green), and DNA (blue) are shown.

FIGURE S3

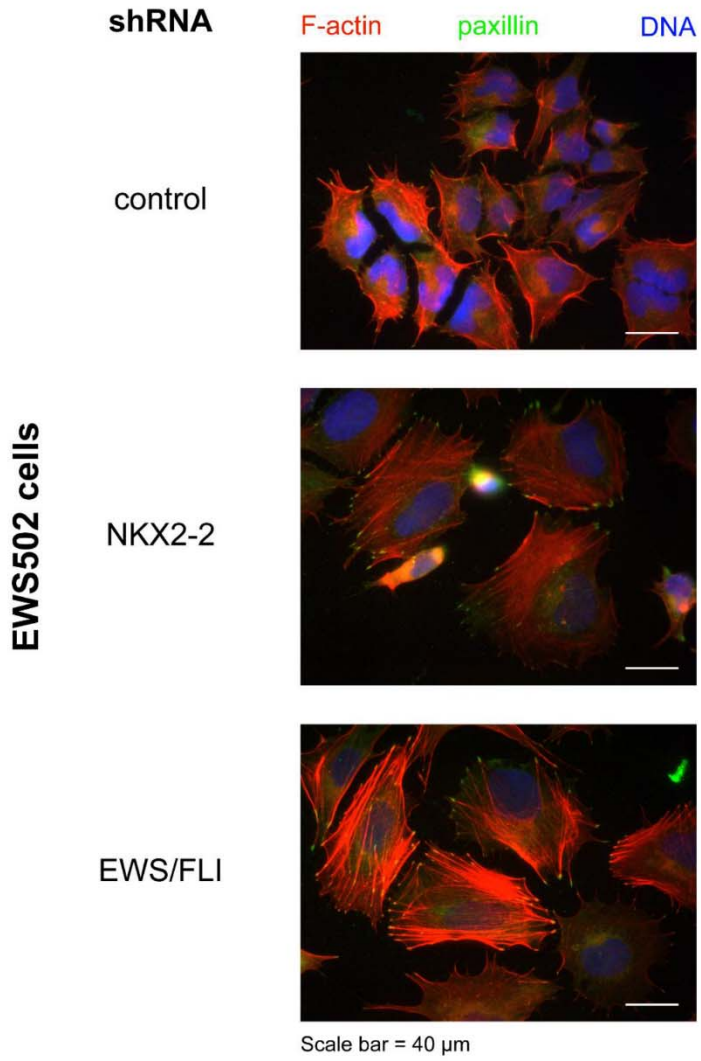

Figure S3: Immunofluorescence 40X fields of EWS502 cells harboring control, NKX2-2, or EWS/FLI shRNA. Merged images of IF staining for F-actin (red), paxillin (green), and DNA (blue) are shown.

FIGURE S4

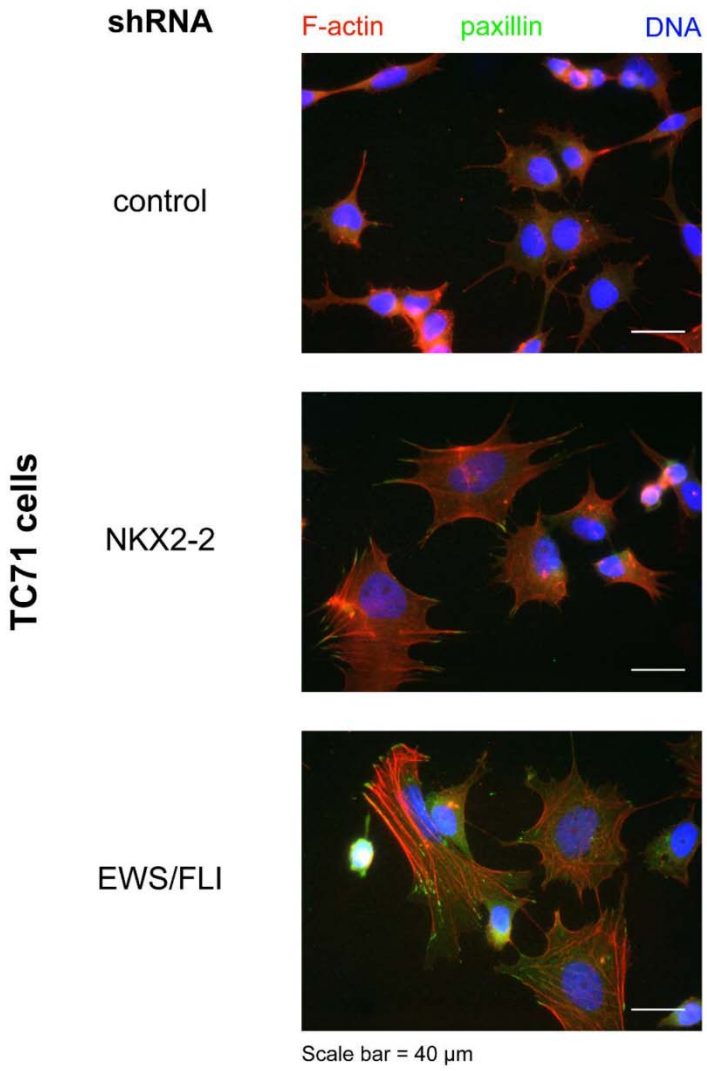

Figure S4: Immunofluorescence 40X fields of TC71 cells harboring control, NKX2-2, or EWS/FLI shRNA. Merged images of IF staining for F-actin (red), paxillin (green), and DNA (blue) are shown.

FIGURE S5

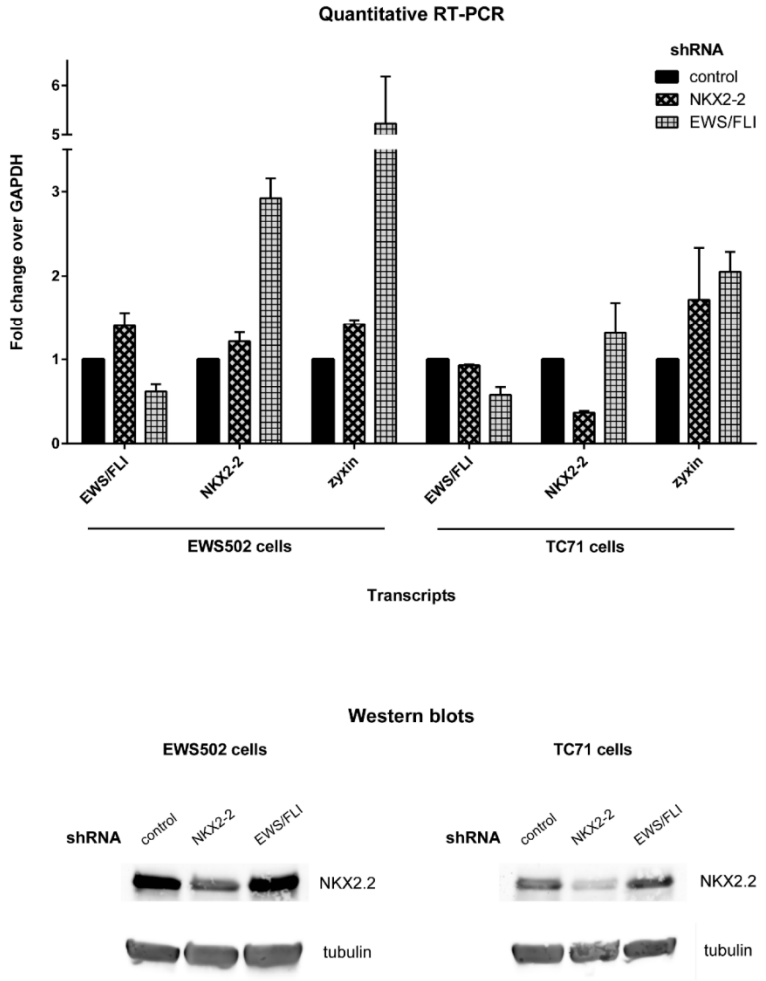

Figure S5: qRT-PCR and western blots of EWS502 and TC71 cells. *Top*, qRT-PCR results using EWS/FLI-, NKX2-2-, and zyxin-specific primer sets. Shown are fold-change values, normalized against GAPDH levels, for cells harboring control, NKX2-2 or EWS/FLI shRNA for either cell line. *Bottom*, NKX2.2 and tubulin protein levels for each knockdown condition in either cell line.

FIGURE S6

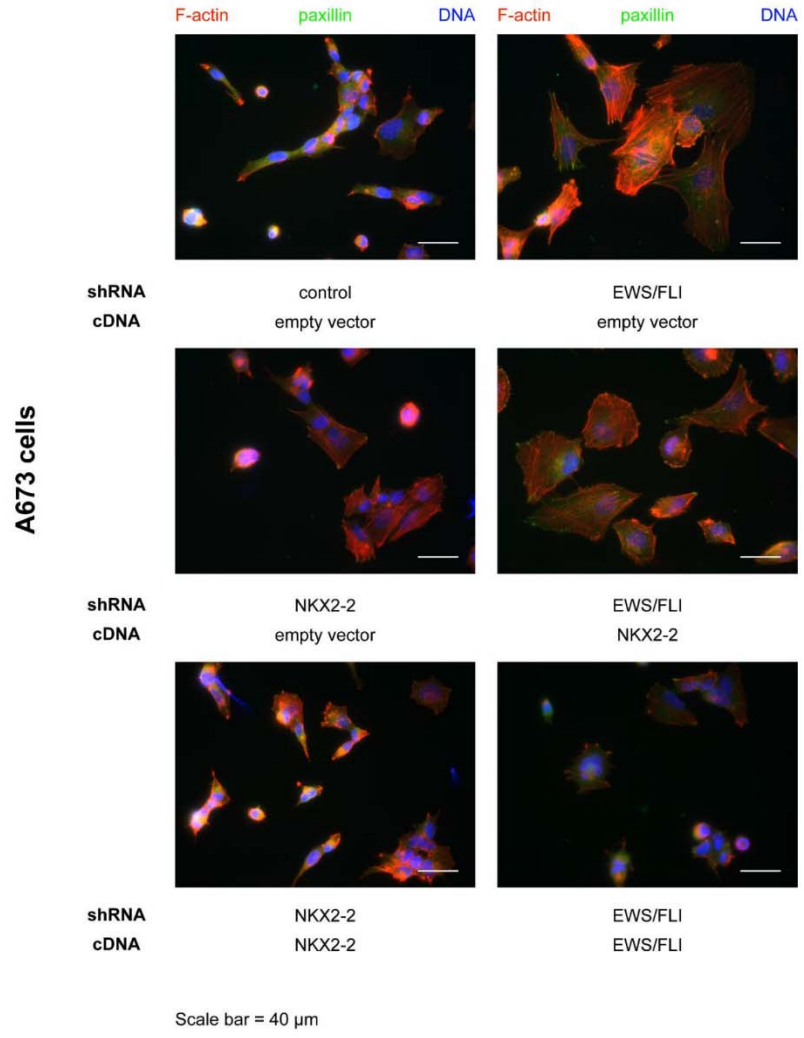

Figure S6: Immunofluorescence 40X fields of A673 knockdown-rescue cells. Cells harboring control, NKX2-2, or EWS/FLI shRNA, and empty vector (pMSCV-hygro) or cDNA for 3XFLAG::NKX2-2 or 3XFLAG::EWS/FLI, as indicated. Merged images of IF staining for F-actin (red), paxillin (green), and DNA (blue) are shown.

CHAPTER 3

NOVEL PROTEIN INTERACTIONS MEDIATED BY NKX2.2

John Fadul[1], Helena Lucente[1], Michael E. Engel[1,2,3], and Stephen L. Lessnick[1,2,3]

[1]Department of Oncological Sciences and the Huntsman Cancer Institute,
[2]Center for Children's Cancer Research, [3]Division of Pediatric Hematology/Oncology,
School of Medicine, University of Utah, Salt Lake City, Utah, USA

Abstract

Activation of the Notch pathway is inhibitory to the proliferation of Ewing sarcoma cells. To investigate the possible role of NKX2.2 in this growth inhibition, we asked whether NKX2.2 and the Notch transcriptional switch protein MTG16 are found in the same repressor complex. Here we show that NKX2.2 and MTG16 participate in a novel protein-protein interaction. Using domain deletion mutants of both proteins, we mapped this interaction on the transcriptional activation domain (TAD) of NKX2.2 and on the PST2 and NHR2 domains of MTG16. Unexpectedly, our co-immunoprecipitation studies also indicated that abolishing the DNA binding property of NKX2.2 either by the N178Q mutation or a full homeodomain deletion allows it to bind MTG16 with a much higher affinity. Furthermore, we found that NKX2.2 forms a homo-oligomer the assembly of which is similarly TAD-dependent. Lastly, we show that Notch1 competes with the NKX2.2 for MTG16 binding. While low expression levels for MTG16 in Ewing sarcoma cells may hamper the investigation of a potential NKX2.2-MTG16-controlled complex during Notch-induced growth inhibition, our work proposes that functional binding of these two proteins is possible in the proper cellular context and may be tractable in a pancreatic β-islet system. Moreover, we demonstrate that the NKX2.2 TAD is a competent protein binding motif. Whether the heterotypic and/or homotypic TAD-mediated interactions suppress direct transcriptional activation by NKX2.2, and whether different members of the NK2 and MTG families also interact, are interesting questions and are suggested prospects for future studies.

Introduction

NKX2.2 is a member of the evolutionarily ancient NK family of DNA-binding transcription factors. It has various functions that include specification of V3 interneurons in the central nervous system, control of oligodendrocyte development,

specification of insulin-producing β-islet cells in the pancreas, etc. [1-15]. Like other members of this family, NKX2.2 harbors a homeodomain (HD), which facilitates binding to specific target sequences in the genome, as well as the *tinman* (TN) domain (Fig. 3.1). Functional inactivation of *tin* in the fly or knockout of Nkx2.5 in the mouse—orthologous proteins that bear the TN domain—leads to abnormal heart development and early embryonic death [16]. TN has been shown to effect transcriptional repression, primarily through recruitment of Gro/TLE co-repressors and histone deacetylases (HDACs) [17]. Presumably, HDACs remove activating histone acetyl marks from surrounding histones, leading to compaction of the local epigenetic landscape and reduced access to transcription factors. NKX2.2, in addition, harbors the specific domain (SD), which is present in other NK2 family members, and the transcriptional activation domain (TAD) (Fig. 3.1) [16, 18]. Using luciferase reporter assays, Watada and colleagues demonstrated that a full deletion of, or a double A204E/L208E mutation in, the SD unmasks a C-terminal domain that effects transcriptional activation (i.e., the TAD) [18]. NKX2.2 and other NK2-class transcription factors have been shown to both transcriptionally repress and activate targets, though less certain is what governs switching between these two modes [7, 10, 11, 13, 18-20].

Previously it was demonstrated that activation of the Notch signaling pathway elicits growth inhibition in Ewing sarcoma cell lines. In particular, ectopic expression of the Notch ligand JAG1 or of the intracellular domains of Notch1 (N1-ICD), Notch2, or Notch3 in the Ewing sarcoma cell lines TC252 and SK-N-MC ablated cell proliferation completely [21]. It was unclear in this study whether cell growth was arrested or whether cells underwent necrosis or apoptosis. However, the effect of Notch activation was very interesting, and we resolved to determine how such growth inhibition is achieved mechanistically.

One way that NKX2.2 can impose an effect on Notch-induced growth inhibition is through MTG16 (myeloid translocation gene on chromosome 16). MTG16, alternatively named ETO2 or CBFA2T3, itself participates in the chromosomal translocation t(16;21)(q24;q22) that drives acute myeloid leukemia (AML) [22]. In the absence of an activating signal, Notch transcriptional targets are in a repressed state: DNA-bound CSL recruits MTG16, co-repressors, and HDACs. Upon binding of a cognate ligand, sequential protease cleavages of the Notch1 receptor occur, releasing N1-ICD from the plasma membrane and into the nucleus, where it binds CSL, knocks off MTG16 and associated co-repressors, and recruits mastermind-like (MAML) and co-activators. Thus, MTG16 serves as the switch between the repressed and activated states of Notch targets [23]. Using a series of co-immunoprecipitation experiments utilizing serial domain deletion mutants of MTG16 (Fig. 3.2), Engel and colleagues demonstrated that MTG16 binds CSL via the NHR3 domain and N1-ICD via the PST1 domain; importantly, N1-ICD was shown to disrupt the MTG16-CSL interaction [23]. Thus, we decided to pursue a candidate approach and investigate whether these interactions define a framework in which NKX2.2 and MTG16 participate in a complex that is disassembled by a Notch signal, leading to Ewing sarcoma growth inhibition.

Results

Previously it was shown that MTG16 serves as the switch between the repressed and activated states of Notch target promoters. Specifically, it was demonstrated that MTG16 binds N1-ICD [23]. We reasoned that NKX2.2 may participate in the same repressive, MTG16-harboring complex. We enforced co-expression of Flag-tagged NKX2.2 and myc-tagged MTG16 in HEK293-EBNA cells. Co-immunoprecipation studies from whole cell protein lysates revealed that NKX2.2 and MTG16 indeed physically interact (Fig. 3.3a). We next mapped this interaction using the domain deletion mutants

of NKX2.2 [24]. While deletions of TN or SD are dispensable for the interaction, any mutant with the TAD deleted (i.e., ΔTAD, ΔSD-TAD, and TN-HD) resulted in abrogation of the interaction (Fig. 3.3a). We therefore concluded that the NKX2.2-MTG16 interaction is facilitated by the TAD. Unexpectedly, we found that the point mutant N178Q pulled down MTG16 with dramatically higher affinity than wild-type or indeed any other mutant (Fig. 3.3a). This put forward two possibilities. One, the substitution of asparagine with glutamine at position 178 causes a conformational change that allows NKX2.2 to unravel and expose the MTG16 binding surface on the TAD. We reasoned that this is improbable owing to the minimal structural change with that substitution. More likely, NKX2.2 switches between "closed" and "open" conformations depending on the state of DNA binding. We reasoned that a different DNA binding mutant should phenocopy N178Q if the second possibility is true. To this end, we cloned a full deletion of the homeodomain (ΔHD, Fig. 3.1). Indeed, ΔHD pulls down MTG16 with the same high affinity as N178Q (Fig. 3.3a).

We next mapped the interaction on MTG16 using myc-tagged serial domain deletion mutants (Fig. 3.2; Fig. 3.3b,c). When we pulled down immunocomplexes using α-Flag and blotted for myc, all of the ΔC mutants showed an interaction, except MTG16$^{\Delta 6C}$ and MTG16$^{\Delta 7C}$ (Fig. 3.3b). These NKX2.2-binding-deficient mutants both lack the PST2 domain (Fig. 3.2), suggesting that the NKX2.2-MTG16 interaction is mediated by PST2. However, immunoprecipitations using the ΔN mutant series revealed that MTG16$^{\Delta 7N}$, which lacks the PST2 domain, is capable of binding, while MTG16$^{\Delta 8N}$, which lacks the contiguous PST2 and NHR2 domains, is not (Fig. 3.2; Fig. 3.3c). If PST2 is the lone mediator of NKX2.2 binding, we would predict that MTG16$^{\Delta 7N}$ abolishes the interaction. Therefore, it appears that PST2 and NHR2 comprise an interface to which NKX2.2 binds. This model is consistent with both MTG16$^{\Delta 5C}$ and MTG16$^{\Delta 7N}$ being capable of NKX2.2 binding (Fig. 3.2; Fig. 3.3b,c). MTG16 mutants with smaller deletions

at or near the PST2-NHR2 boundary may help define the minimal region able to bind NKX2.2, and is an interesting aim for future studies.

Another prediction from these data is that the HD somehow occludes the MTG16 binding surface on the TAD; this model is consistent with the higher MTG16 affinity of N178Q and ΔHD compared to wild-type NKX2.2. One mechanism by which this might occur is if NKX2.2 binds itself. We therefore sought to determine whether NKX2.2 oligomerization occurs. To this end we cloned the wild-type and mutant constructs of NKX2.2 to express an N-terminal hemagglutinin (HA) tag (Fig. 3.1). We co-expressed 3xFlag::NKX2.2 and HA::NKX2.2 in HEK293-EBNA cells and isolated protein. Using these whole cell lysates, we again pulled down with α-Flag and blotted with HA. Indeed, we observed that the differently tagged species of NKX2.2 interact with each other, demonstrating oligomerization (Fig. 3.4a). To map this interaction, we co-expressed 3xFlag::NKX2.2 and either wild-type or mutant HA::NKX2.2. Interestingly, the TAD again is indispensable for this homotypic interaction (Fig. 3.4a). To ensure that the result is not an artifact, we imposed the expression of 3xFlag::ΔTAD against the full complement of HA-tagged constructs. Expectedly, when we pulled down immunocomplexes with α-Flag, none of the HA constructs indicated any interaction (Fig. 3.4b). We therefore concluded that the TAD facilitates homo-oligomerization of NKX2.2. Interestingly, mouse Nkx2.5 has been previously demonstrated to form dimers both on and off DNA, and to contact proximal palindromic binding sites in the promoter of the atrial natriuretic factor (ANF) gene, a known direct target. It was demonstrated that regions in both the HD and in the C-terminal domain (i.e., parallel to the NKX2.2-TAD) are required for homodimerization on DNA [25]. Subsequent studies elucidated the crystal structure of the Nkx2.5-HD bound to the ANF promoter and, while only the HD and not the full-length protein was crystallized, the authors posit that such a conformation would allow the C-termini of two Nkx2.5 molecules to physically interact

and form a dimer [26]. This is consistent with our observation that the TAD, which is the most C-terminal domain of NKX2.2, is absolutely required for homo-oligomerization. Whether NKX2.2 in Ewing sarcoma cells forms a dimer or has more component subunits, and whether the homo-oligomeric form is DNA-bound, are yet to be determined. It is worthwhile to note that the NHR2 domain of MTG16 and of the related MTG8 and MTGR1 proteins facilitates homotetramerization [27].

We next explored the possibility that N1-ICD disrupts the NKX2.2-MTG16 complex, in a manner parallel to its disruption of the MTG16-CSL complex [23]. To address this question, we imposed the expression of increasing levels of N1-ICD on the NKX2.2-MTG16 interaction. We expected to see that the NKX2.2-MTG16 interaction would dose-dependently decrease with increasing N1-ICD expression, and this is indeed the case (Fig. 3.5a). Importantly, MTG16$^{\Delta 2N}$—which lacks the PST1 domain that mediates N1-ICD binding—is incapable of disrupting the NKX2.2-MTG16 complex (Fig. 3.2; Fig. 3.5a) [23]. This suggests that it is specifically the binding of N1-ICD to MTG16 that knocks NKX2.2 off the complex.

Discussion

Concurrent experiments at the time indicated that expression levels of MTG16, MTG8, and MTGR1 are very low in A673 cells and other Ewing sarcoma cell lines (data not shown and ref. [28]). This does not necessarily preclude the assembly of an NKX2.2-MTG6-controlled repressor complex in our system of interest, but we surmise that its experimental confirmation will be technically very difficult. However, there is a possibility that such a complex forms and is functional in a pancreatic β-islet system. We have preliminary evidence that MTG16 is expressed and is amenable to immunoprecipitation in βTC6 cells, a murine pancreatic insulinoma cell line derived from β-islet cells (Fig. 3.5b). NKX2.2 is also expressed in these cells [13], giving rise to

the question of whether an endogenous NKX2.2-MTG16 complex exists in this system. If such a complex does exist and is stable, the question of the biological significance of the NKX2.2-MTG16 interaction—the biggest gap in our current work—can finally be addressed. We have identified many lines of investigation stemming from our data. In particular, does NKX2.2-MTG16 recruit Gro/TLE co-repressors and HDACs at previously identified NKX2.2 direct transcriptional targets in β-islet cells? Is repression mediated through changes in the local epigenetic landscape? Does Notch activation figure in β-islet cell specification? Importantly, β-islet cells may serve as a paradigm in which to further investigate the role NKX2.2 in mediating cell specification and differentiation, as has been shown in various contexts [2, 4, 5, 9, 10, 13, 15, 28].

Although at this time we have not worked out the biological significance of the NKX2.2-MTG16 interaction, our current work makes significant contributions to the understanding of protein interactions mediated by NKX2.2. Firstly, to the best of our knowledge, the interaction of NKX2.2 and MTG16 has not been reported before. MTG16 is a scaffolding protein that has numerous protein binding interfaces. The possibility that NKX2.2 recruits MTG16 to amplify its ability to recruit co-repressors to DNA and cause direct transcriptional repression is very interesting and needs to be experimentally validated. The elucidation of biochemical and stoichiometric details is also vastly important. We need to answer whether the NKX2.2-MTG16 interaction is direct or mediated by other proteins, and how many NKX2.2 and MTG16 subunits are assembled on promoters for transcriptional repression.

Secondly, we discovered that NKX2.2 is able to oligomerize with itself—another novel interaction. This is consistent with reports of the related mouse protein Nkx2.5 forming DNA-bound dimers [25, 26]. The finding brings forth many interesting questions, such as whether these NKX2.2 oligomers are DNA-bound. More pointedly, is oligomerization a mechanism by which NKX2.2 activity can be regulated post-

translationally? Because this is a homotypic interaction, one could potentially ask these questions in any cellular context wherein NKX2.2 is expressed: Ewing sarcoma, β-islet cells, or developing interneurons and oligodendrocytes.

Thirdly, we have demonstrated that the TAD is a competent protein-binding motif, both in heterotypic and homotypic interactions. Interestingly, the mouse Nkx2.5 dimer previously identified also forms contacts partly via the C-terminal domain, which is the TAD in NKX2.2. However, we have not asked specifically whether the HD contributes to NKX2.2 homo-oligomerization, as it does in Nkx2.5 dimers [25, 26]. In addition, our data bring forth the possibility that proteins binding to TAD may suppress direct transcriptional activation by NKX2.2, and may help explain why deletion of SD allows activation to occur [18]. Furthermore, since both mouse Nkx2.5 and human NKX2.2 form oligomers, we hypothesize that this is a generalizable feature of NK2 class transcription factors. Taking this hypothesis further, and considering that TAD mediates heterotypic interactions as well and that the MTG proteins are very structurally similar, one might predict that any TAD-bearing NK2-class transcription factor and MTG family member may possibly interact. In summary, our current study identifies novel protein-protein interactions of NKX2.2, presents preliminary data that such interactions are possible and functional in other cellular contexts, and proposes future aims for the investigation of the biological significance of NKX2.2 binding with MTG16 and homo-oligomerization.

Materials and Methods

Cloning of cDNA constructs

The cloning strategies for myc::MTG16 (pCMV5), serial domain deletion mutants of MTG16 from either the N- or C-terminus, and Flag::N1-ICD (pCMV5) have been previously described [23]. The cloning strategies for 3xFlag::NKX2.2 (pQCXIN) and

domain deletion mutants of NKX2.2 have also been previously described [24]. Briefly, the 3xFlag::ΔHD-NKX2.2 (pQCXIN) was generated using a two-step sewing PCR with the following primers, all in 5' to 3' orientation:

FlagNKX_NotI.F: AGCTGCGGCCGCGCCGCCGCCATGGACTACAAAGACCATGACGGTG
delHDfir.R: CGGGGTCTCCTTGTCATTGTCCGGTGACTCGTCGGCCGAGG
delHDsec.F: GGACAATGACAAGGAGACCCCGAAAGGTATGGAGGTGACGCCCC
FlagNKX_BamHI.R: AGCTGGATCCTCACCAAGTCCACTGCTGGGC

PCR products were visualized using ethidium bromide on 1% agarose, then the expected amplicons were excised and gel-purified using a QIAquick Gel Extraction Kit (Qiagen). The amplicons and pQCXIN were *Not*I- and *Bam*HI-restricted and ligated with T4 DNA ligase (New England Biosciences). Using standard techniques, ligation products were used to transform chemically competent DH5α *E. coli*, clones were tested for the cDNA in correct orientation, and DNA sequence was confirmed. The HA-tagged wild-type and domain deletion NKX2.2 constructs were PCR-amplified from their Flag-tagged counterparts in pQCXIN [24] using the following primers, , all in 5' to 3' orientation:

Forward: AGCTGCGGCCGCGCCGCCGCCATGTACCCATACGATGTTCCAGATTACGC
TACCGGTTCGCTGACCAACACAAAGACGGG
Reverse: AGCTGGATCCTCACCAAGTCCACTGCTGGGC
delTAD_Reverse: AGCTGGATCCCGCGTGACATGGTTTGCCGTC

Amplicons were purified and subcloned into *Not*I- and *Bam*HI-restricted pQCXIH (Clontech) using strategies described above.

Cell line and transfections

HEK293 cells expressing the Epstein-Barr virus nuclear antigen (EBNA) were grown in neomycin selection using standard techniques. The day before transfection, 1 x 10^7 HEK293-EBNA cells were seeded into 10-cm tissue culture dishes. The transfection cocktail consisted of: 10 μg of each construct, 30 μL TransIT-LT1 Transfection Reagent (Mirus) per 10 μg DNA, and 2 mL Opti-MEM I Reduced Serum Medium (Life Technologies). The transfection cocktail was mixed by inverting and left to incubate at room temperature for 20 min. The nutrient media from the cells was aspirated and replaced with 3 mL of the following media: 10% fetal bovine serum (Life Technologies), 1% penicillin-streptomycin-glutamine (Life Technologies), and 100 μM sodium pyruvate (Life Technologies) in Dulbecco's Modified Eagle's Medium (Corning). The transfection mix was pipetted dropwise into the dish and left to incubate at 37°C and 5% CO_2 for 48 h.

Co-Immunoprecipitation

After incubation, the media was aspirated. Working quickly on ice, cells were washed twice with ice-cold PBS and harvested using a cell lifter. Cells were resuspended in 1 mL phosphoprotecting lysis buffer (PPLB) with protease inhibitors added immediately before lysis, and transferred to chilled 1.5-mL microcentrifuge tubes. The cell suspension was sonicated on ice for 20 s (10 cycles of 1 s “on” and 1 s “off”) at 5 W using a Misonix Sonicator 3000 fitted with a microtip probe, then rotated for 30 min at 4°C. Total cell protein lysates were centrifuged at 13000 rpm for 30 min at 4°C. Clarified extracts were transferred to fresh tubes. A 75-μL aliquot was reserved and resuspended with an equal volume of 2x SDS gel loading buffer with DTT. The protein lysates were pre-cleared with 30 μL of sheep anti-mouse IgG Dynabeads M-280 (Life Technologies) for 1 h at 4°C with rotation. The beads were collected using a magnetic tube rack, then the lysates were transferred to tubes contaning 3 μg mouse α-Flag M2 antibody (Sigma).

The tubes were rotated for 5 min at 4°C to distribute the antibody, then incubated on ice in the cold room for 90 min. The immunocomplexes were precipitated with 30 µL of sheep α-mouse IgG Dynabeads for 1 h at 4°C with rotation. Beads were collected and the supernatants disposed. Beads were washed three times with 750 µL PPLB without protease inhibitors, each time for 2 min at 4°C with rotation. Beads were collected and and resuspended in 65 µL 2x SDS gel loading buffer, boiled for 10 min, and stored at -80°C or prepared for western blotting. This protocol was adapted from [23].

Antibodies and western blotting

Western blotting was performed using standard techniques. We used the following commercially available primary antibodies: rabbit anti-HA (Abcam) and mouse α-tubulin (Calbiochem). The R332 and R333 rabbit α -MTG16 antibodies were kind gifts from Michael Engel. We used the following HRP-conjugated secondary antibodies: mouse α-Flag M2 (Sigma), donkey α-rabbit IgG (GE Healthcare), sheep α-mouse IgG (GE Healthcare).

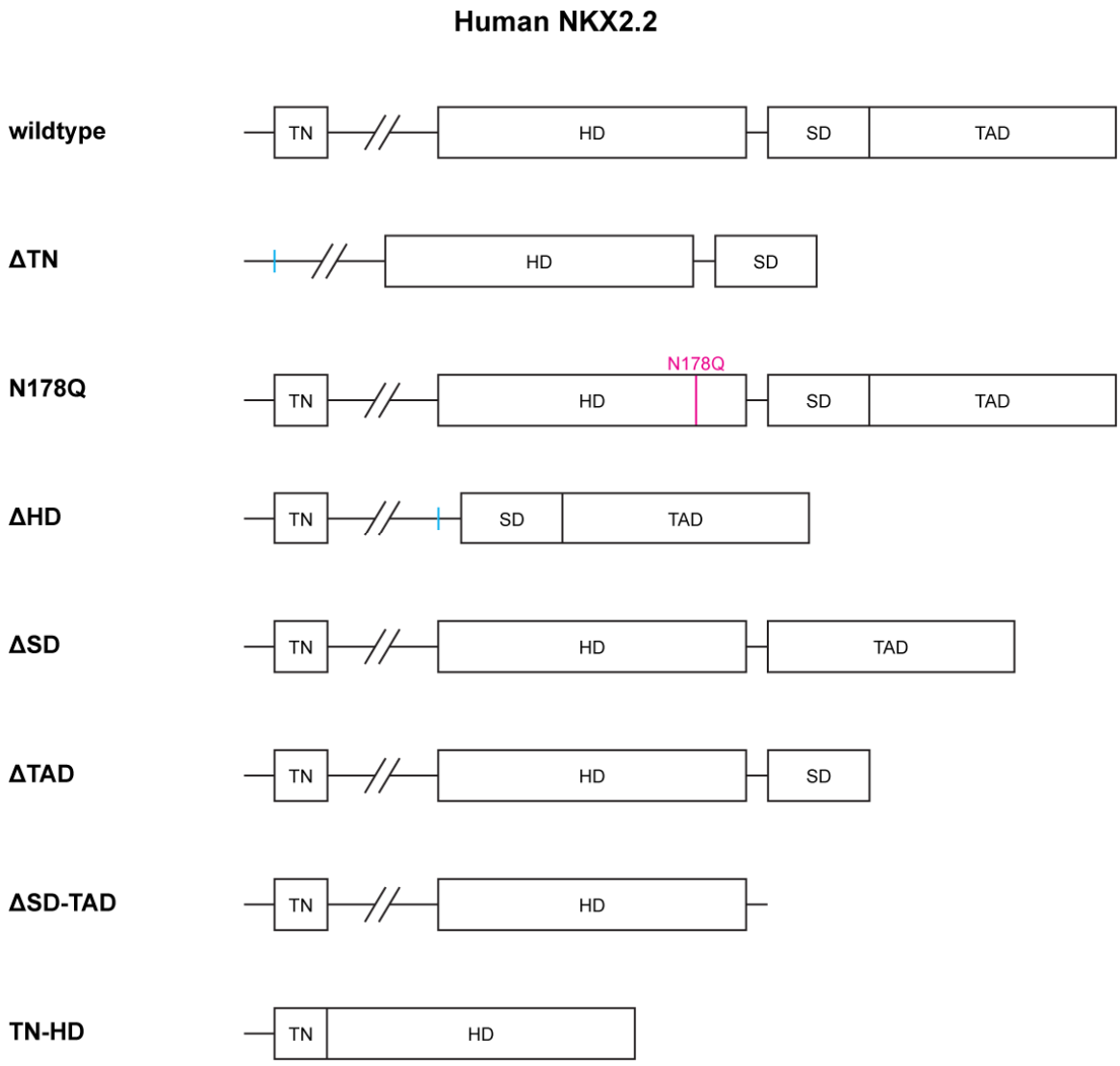

Figure 3.1. Domain organization of wild-type and mutant human NKX2.2. The functional domains *tinman* (TN), homeodomain (HD), specific domain (SD), and transcriptional activation domain (TAD), as well as linker regions, are drawn to scale from the N to the C terminus. For illustration purposes, the linker between TN and HD is drawn at a quarter of its length. The DNA binding point mutant N178Q is indicated in magenta. Small vertical bars in cyan indicate a domain deletion between flanking linkers. The N-terminal 3xFlag or HA tags are not illustrated.

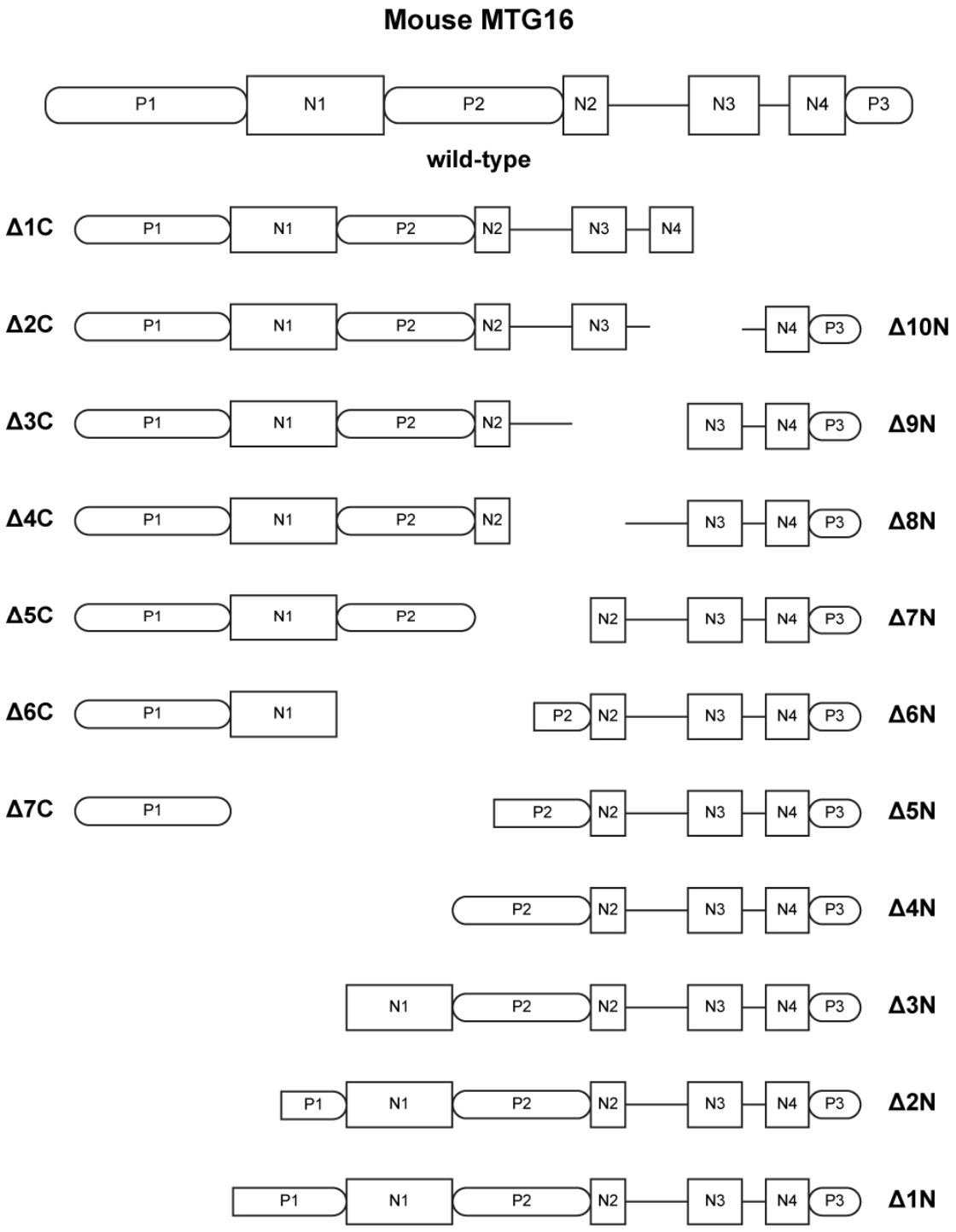

Figure 3.2. Domain organization of wild-type and mutant mouse MTG16. The three PST (P) and four NHR (N) domains, as well as linker regions, are drawn to scale. ΔC and ΔN mutants are successive deletions from the C or N terminus, respectively. The N-terminal myc tag is not illustrated. The exact boundaries of the deletions are detailed elsewhere [23].

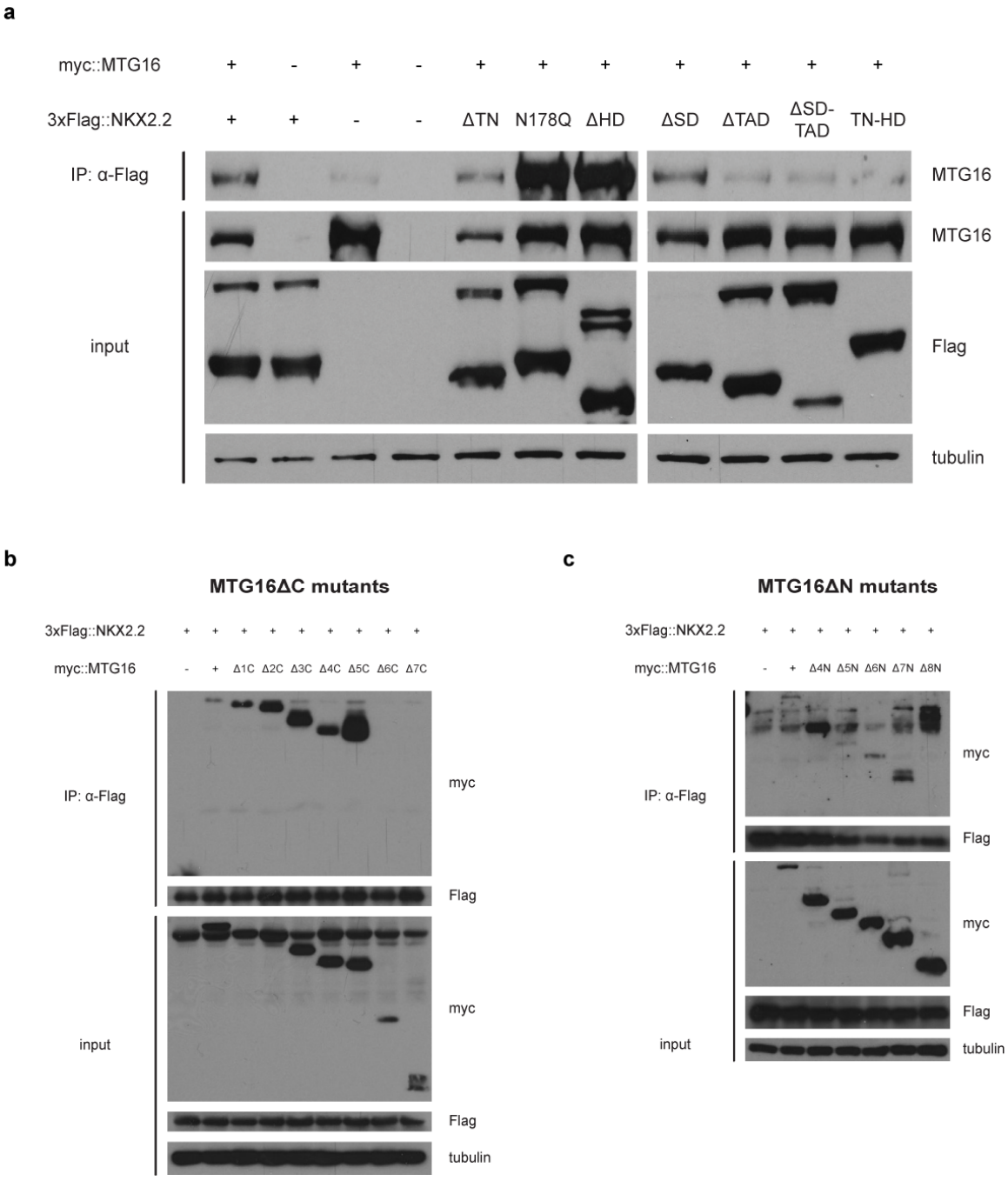
a
myc::MTG16
3xFlag::NKX2.2
ΔTN
N178Q
ΔHD
ΔSD
ΔTAD
ΔSD-TAD
TN-HD
IP: α-Flag
MTG16
input
Flag
tubulin
b
MTG16ΔC mutants
Δ1C Δ2C Δ3C Δ4C Δ5C Δ6C Δ7C
myc
c
MTG16ΔN mutants
Δ4N Δ5N Δ6N Δ7N Δ8N

Figure 3.3. NKX2.2 and MTG16 participate in a novel protein interaction that is mappable on both proteins.
(a) NKX2.2 and MTG16 bind using a co-immunoprecipitation assay in a TAD-dependent fashion. Wild-type or mutant 3xFlag::NKX2.2 or empty pQCXIN vector and myc::MTG16 or empty pCMV5 vector were used to transfect HEK293-EBNA cells, as indicated. Whole cell lysates (input) or immunocomplexes precipitated with α-Flag antibody were run in SDS-PAGE and blotted for MTG16 (R333), Flag, or tubulin. The asterisk denotes the high MW species of each NKX2.2 variant. (b,c) The NKX2.2-MTG16 interaction requires the PST2 domain of MTG16. Expression of 3xFlag::NKX2.2 was imposed on wild-type or mutant myc::MTG16 or empty pCMV5 vector. Input or immunocomplexes precipitated with α-Flag antibody were run in SDS-PAGE and blotted for myc, Flag, GFP, or tubulin. Shown are co-immunoprecipitation mapping experiments using the ΔC (left, b) or ΔN (right, c) MTG16 mutant series.

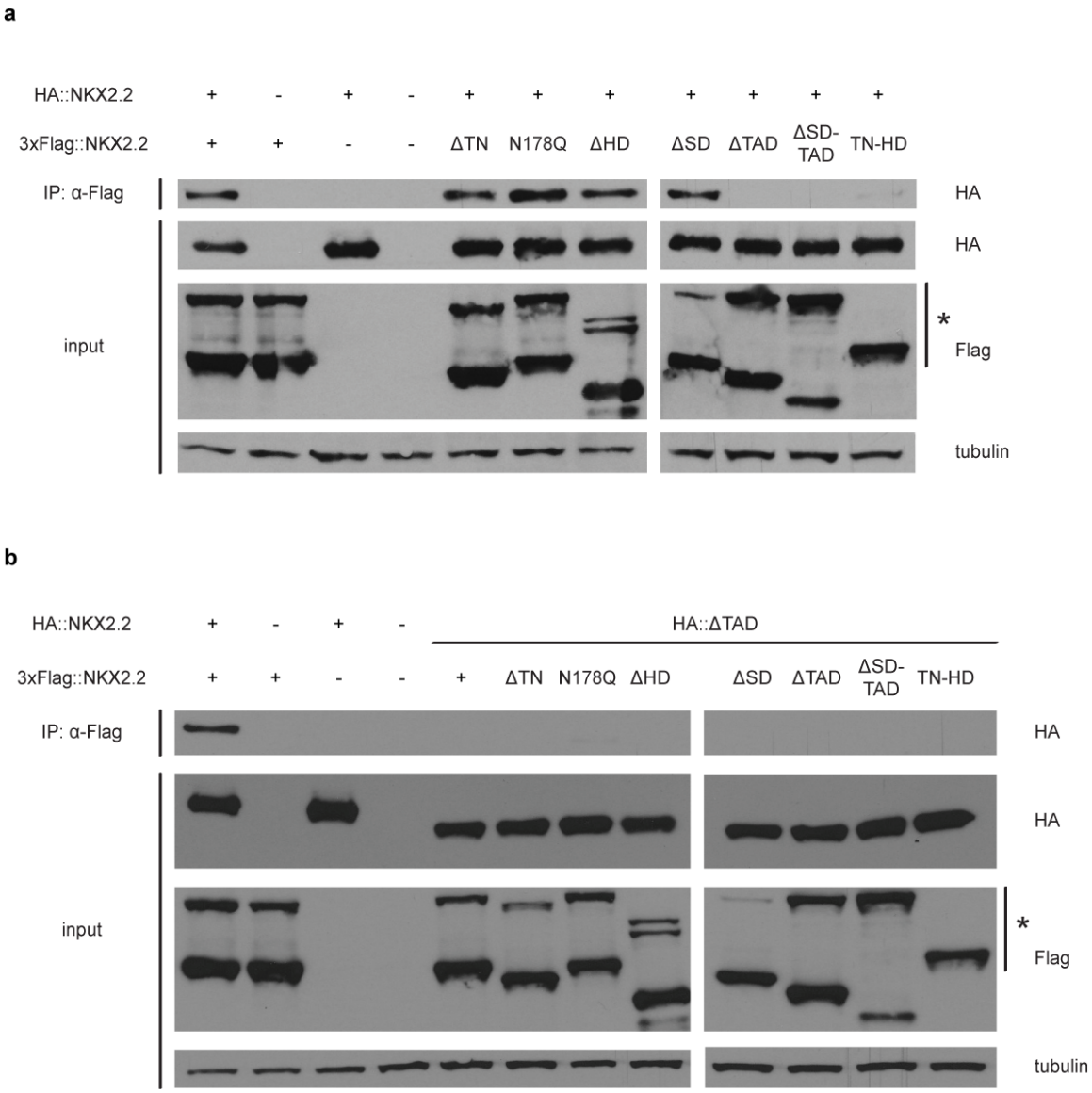

Figure 3.4. NKX2.2 forms a homo-oligomer using TAD.
(a) NKX2.2 forms a TAD-dependent homo-oligomer. Differently tagged species of wild-type or mutant NKX2.2 (HA-tag in pQCXIH, 3xFlag-tag in pQCXIN) or empty vector were used to transfect HEK293-EBNA cells, as indicated. Co-immunoprecipitations are as in Fig. 3.3a. The asterisk denotes the high MW species of each NKX2.2 variant. (b) TAD deletion abrogates homo-oligomerization. HA::ΔTAD expression was imposed on wild-type or mutant 3xFlag::NKX2.2. Co-immunoprecipitations are as in Fig. 3.3a. The asterisk denotes the high MW species of each NKX2.2 variant.

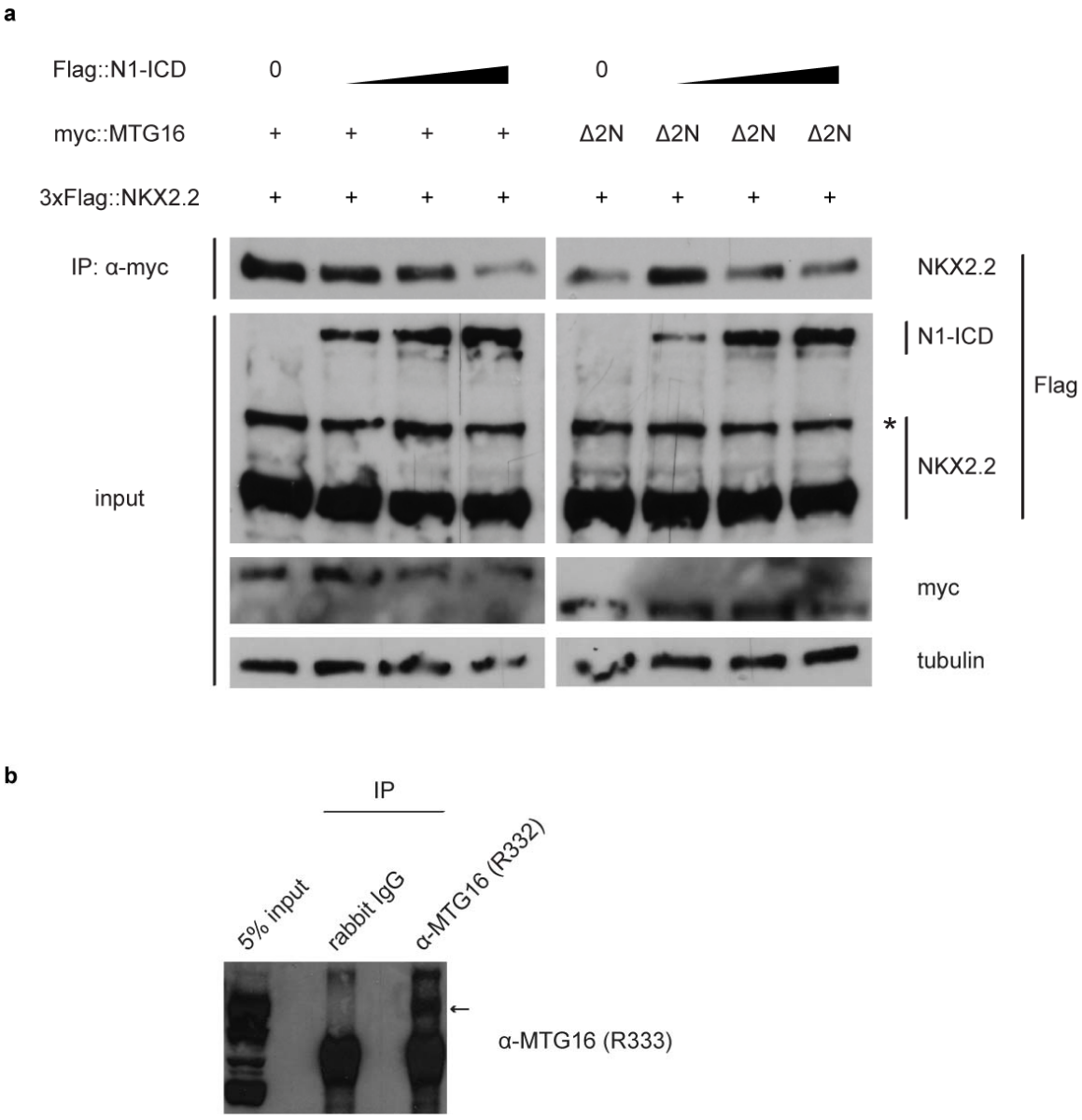

Figure 3.5. NKX2.2 and Notch1 intracellular domain compete for MTG16 binding.

(a) Expression of increasing levels of the Flag::N1-ICD construct was imposed upon constant levels of 3xFlag::NKX2.2 and either myc::MTG16 or myc::MTG16$^{\Delta 2N}$. Input or immunocomplexes precipitated with α-Flag antibody were run in SDS-PAGE and blotted for Flag, myc, or tubulin. The asterisk denotes the high MW species of NKX2.2. (b) MTG16 is expressed and is amenable to immunoprecipitation in murine βTC6 cells. Shown are 5% input whole cell lysate and rabbit IgG- or α-MTG16 (R332)-immunoprecipitated complexes blotted with a different α-MTG16 antibody (R333). The arrow indicates a band of expected size for mouse MTG16.

References

1. Briscoe J, Sussel L, Serup P, Hartigan-O'Connor D, Jessell TM, Rubenstein JL, et al. Homeobox gene Nkx2.2 and specification of neuronal identity by graded Sonic hedgehog signalling. Nature. 1999;398(6728):622-7.

2. Holz A, Kollmus H, Ryge J, Niederkofler V, Dias J, Ericson J, et al. The transcription factors Nkx2.2 and Nkx2.9 play a novel role in floor plate development and commissural axon guidance. Development. 2010;137(24):4249-60.

3. McMahon AP. Neural patterning: the role of Nkx genes in the ventral spinal cord. Genes Dev. 2000;14(18):2261-4.

4. Qi Y, Cai J, Wu Y, Wu R, Lee J, Fu H, et al. Control of oligodendrocyte differentiation by the Nkx2.2 homeodomain transcription factor. Development. 2001;128(14):2723-33.

5. Tochitani S, Hayashizaki Y. Nkx2.2 antisense RNA overexpression enhanced oligodendrocytic differentiation. Biochem Biophys Res Commun. 2008;372(4):691-6.

6. Anderson KR, Torres CA, Solomon K, Becker TC, Newgard CB, Wright CV, et al. Cooperative transcriptional regulation of the essential pancreatic islet gene NeuroD1 (beta2) by Nkx2.2 and neurogenin 3. J Biol Chem. 2009;284(45):31236-48.

7. Anderson KR, White P, Kaestner KH, Sussel L. Identification of known and novel pancreas genes expressed downstream of Nkx2.2 during development. BMC Dev Biol. 2009;9:65.

8. Cissell MA, Zhao L, Sussel L, Henderson E, Stein R. Transcription factor occupancy of the insulin gene in vivo. Evidence for direct regulation by Nkx2.2. J Biol Chem. 2003;278(2):751-6.

9. Desai S, Loomis Z, Pugh-Bernard A, Schrunk J, Doyle MJ, Minic A, et al. Nkx2.2 regulates cell fate choice in the enteroendocrine cell lineages of the intestine. Dev Biol. 2008;313(1):58-66.

10. Doyle MJ, Loomis ZL, Sussel L. Nkx2.2-repressor activity is sufficient to specify alpha-cells and a small number of beta-cells in the pancreatic islet. Development. 2007;134(3):515-23.

11. Doyle MJ, Sussel L. Nkx2.2 regulates beta-cell function in the mature islet. Diabetes. 2007;56(8):1999-2007.

12. Hill JT, Anderson KR, Mastracci TL, Kaestner KH, Sussel L. Novel computational analysis of protein binding array data identifies direct targets of Nkx2.2 in the pancreas. BMC Bioinformatics. 2011;12:62.

13. Papizan JB, Singer RA, Tschen SI, Dhawan S, Friel JM, Hipkens SB, et al. Nkx2.2 repressor complex regulates islet beta-cell specification and prevents beta-to-alpha-cell reprogramming. Genes Dev. 2011;25(21):2291-305.

14. Raum JC, Gerrish K, Artner I, Henderson E, Guo M, Sussel L, et al. FoxA2, Nkx2.2, and PDX-1 regulate islet beta-cell-specific mafA expression through conserved sequences located between base pairs -8118 and -7750 upstream from the transcription start site. Mol Cell Biol. 2006;26(15):5735-43.

15. Sussel L, Kalamaras J, Hartigan-O'Connor DJ, Meneses JJ, Pedersen RA, Rubenstein JL, et al. Mice lacking the homeodomain transcription factor Nkx2.2 have diabetes due to arrested differentiation of pancreatic beta cells. Development. 1998;125(12):2213-21.

16. Harvey RP. NK-2 homeobox genes and heart development. Dev Biol. 1996;178(2):203-16.

17. Muhr J, Andersson E, Persson M, Jessell TM, Ericson J. Groucho-mediated transcriptional repression establishes progenitor cell pattern and neuronal fate in the ventral neural tube. Cell. 2001;104(6):861-73.

18. Watada H, Mirmira RG, Kalamaras J, German MS. Intramolecular control of transcriptional activity by the NK2-specific domain in NK-2 homeodomain proteins. Proc Natl Acad Sci U S A. 2000;97(17):9443-8.

19. Choi CY, Lee YM, Kim YH, Park T, Jeon BH, Schulz RA, et al. The homeodomain transcription factor NK-4 acts as either a transcriptional activator or repressor and interacts with the p300 coactivator and the Groucho corepressor. J Biol Chem. 1999;274(44):31543-52.

20. Yu Z, Syu LJ, Mellerick DM. Contextual interactions determine whether the Drosophila homeodomain protein, Vnd, acts as a repressor or activator. Nucleic Acids Res. 2005;33(1):1-12.

21. Bennani-Baiti IM, Aryee DN, Ban J, Machado I, Kauer M, Muhlbacher K, et al. Notch signalling is off and is uncoupled from HES1 expression in Ewing's sarcoma. J Pathol. 2011;225(3):353-63.

22. Gamou T, Kitamura E, Hosoda F, Shimizu K, Shinohara K, Hayashi Y, et al. The partner gene of AML1 in t(16;21) myeloid malignancies is a novel member of the MTG8(ETO) family. Blood. 1998;91(11):4028-37.

23. Engel ME, Nguyen HN, Mariotti J, Hunt A, Hiebert SW. Myeloid translocation gene 16 (MTG16) interacts with Notch transcription complex components to integrate Notch signaling in hematopoietic cell fate specification. Mol Cell Biol. 2010;30(7):1852-63.

24. Owen LA, Kowalewski AA, Lessnick SL. EWS/FLI mediates transcriptional repression via NKX2.2 during oncogenic transformation in Ewing's sarcoma. PLoS One. 2008;3(4):e1965.

25. Kasahara H, Usheva A, Ueyama T, Aoki H, Horikoshi N, Izumo S. Characterization of homo- and heterodimerization of cardiac Csx/Nkx2.5 homeoprotein. J Biol Chem. 2001;276(7):4570-80.

26. Pradhan L, Genis C, Scone P, Weinberg EO, Kasahara H, Nam HJ. Crystal structure of the human NKX2.5 homeodomain in complex with DNA target. Biochemistry. 2012;51(32):6312-9.

27. Liu Y, Cheney MD, Gaudet JJ, Chruszcz M, Lukasik SM, Sugiyama D, et al. The tetramer structure of the Nervy homology two domain, NHR2, is critical for AML1/ETO's activity. Cancer Cell. 2006;9(4):249-60.

28. Fadul J, Bell R, Hoffman LM, Beckerle M, Engel ME, Lessnick SL. EWS/FLI utilizes NKX2-2 to repress mesenchymal features of Ewing sarcoma. Genes Cancer. 2015;6(3-4):129-43.

CHAPTER 4

CONCLUSION AND FUTURE DIRECTIONS

The work presented in this doctoral dissertation represents a logical and necessary continuity in the work of our laboratory on the function of NKX2-2 in Ewing sarcoma. Previously, our group identified NKX2.2 as a critical upregulated gene in Ewing sarcoma and demonstrated that it is a distinguishing marker for this pediatric cancer among look-alike SRBCTs [1]. Furthermore, it was demonstrated that transcriptional repression, DNA binding, and suppression of transcriptional activation were functions that were necessary for NKX2-2 to maintain the transformed phenotype. Through microarray transcriptional profiling, it was shown that NKX2-2 mediates a significant portion of the EWS/FLI-regulated universe of transcriptional targets, and that the pan-HDAC inhibitor vorinostat fully reverses the NKX2-2 program, suggesting that histone deacetylation is a chief mechanism by which NKX2-2 regulates its targets [2].

In this current work, we took two separate but related approaches to fully define the role of NKX2-2 in Ewing sarcomagenesis. In the first approach, detailed in Chapter 2 [3], we performed NKX2-2 transcriptional profiling in the Ewing sarcoma cell line A673 using RNA-seq, both to overcome the biases of microarrays and to facilitate direct comparisons with other deep sequencing efforts in our lab. What we found was extremely interesting: NKX2-2 represses genes critical for cell adhesion and ECM organization. Through immunofluorescence studies, cell adhesion and migration assays, and assessment of zyxin levels, we demonstrated that, much like EWS/FLI depletion [4, 5], NKX2-2 loss imbues Ewing sarcoma cells with mesenchymal characteristics. Importantly, we found that NKX2-2 and ZEB2 control anti-mesenchymalization and anti-epithelialization programs, respectively, in this cancer [3].

This finding mirrors some of the identified roles of NKX2.2, especially with respect to developmental arrest and differentiation. For example, NKX2.2 binds and represses the promoter of *Arx* in mouse βTC6 cells. If the NKX2.2-TN repressor domain is mutated, *Arx* becomes misexpressed in β-cells. This leads to reduced expression of β-

cell-specific factors and increased expression of α-cell-specific factors, suggesting β- to α-cell reprogramming. The effect is completely neutralized by deleting *Arx*, suggesting that re-differentiation is dependent upon NKX2-2 repression of this gene [6]. In a similar fashion, deletion of *Nkx2.2* in mice generates somatic motor neurons where V3 interneurons should have developed. This ventral expansion suggests that V3 progenitor cells have the capacity for motor neuron development that is inhibited by Nkx2.2 expression [7]. In gliomas, it has been demonstrated that decreasing NKX2-2 levels is correlated with cancer progression. In particular, NKX2-2 inhibits the self-renewal ability of glioma-initiating cells by promoting oligodendroglial differentiation [8]. This is in contrast with the role of NKX2-2 in Ewing sarcoma, wherein it inhibits differentiation; nonetheless, in either case, weak levels of NKX2-2 seem to promote tumor progression, echoing the importance of cellular context in carcinogenesis.

There are many questions left unanswered. First, we need to define the direct transcriptional targets of NKX2-2. We have attempted this before using two chromatin immunoprecipitation (ChIP)-based strategies: an endogenous ChIP using a NKX2.2-specific antibody and streptavidin ChIP using biotinylated, exogenous NKX2.2. While I can show in either strategy that endogenous or exogenous NKX2.2 can be pulled down efficiently and specifically, our RNA-seq data revealed no bona fide targets. One difficulty is the absence of confirmed direct NKX2.2 targets in Ewing sarcoma that could serve as positive controls during optimization. The consensus sequence of NKX2.2, T(T/C)AAGT(A/G)(C/G)TT, determined using a PCR-based enrichment strategy [9], was confirmed by our group to be bound in vitro by all our NKX2.2 constructs (Fig. 3.1), except the DNA-binding mutant N178Q [2]. Through bioinformatic analysis of protein-binding microarrays and electrophoretic mobility shift assays, a binding site containing an alternative “GAGT” core (instead of “AAGT”) was also predicted and confirmed [10]. Since we already have the RNA-seq data, one thought is to survey the promoters of

identified NKX2-2-regulated targets for these consensus sites to find candidate genes for positive controls. Finding the direct target loci of NKX2.2 in Ewing sarcoma will allow us to ask many questions: does NKX2.2 recruit Gro/TLE co-repressors and HDACs to these regions and alter histone acetylation marks, as has been previously demonstrated in a pancreatic β-islet cell line [6]? Does ΔSD or a potential double deletion ΔTN-ΔSD drive transcriptional activation of an otherwise repressed target gene? Furthermore, it would be interesting to ascertain whether any of the repressed ECM genes, such as several collagen subtypes, identified by RNA-seq are direct targets. While we have demonstrated the importance of cell adhesion to the repressed mesenchymal program in Ewing sarcoma cells, we have not directly addressed the significance of repressing ECM organization. Interestingly, while Ewing sarcoma SK-ES-1 cells adhered to fibronectin or laminin substrates [11], they did not adhere to substrates supplemented with collagen I, III, or IV [12]. We need to confirm this in a panel of Ewing cell lines and ask whether de-repression of collagen genes affects adhesion and, possibly, transformation and metastasis. Importantly, the composition of the surrounding ECM might play a role in distal site "decision-making" during the metastatic process. Lastly, since the stratification of patient survival using NKX2-2 expression levels only approached significance ($p=0.07$; Fig. 2.7), we need to survey other available datasets to see whether this trend holds.

One prediction that could be made from the quantified immunofluorescence data is that, because we make our observations on polyclonal populations of shRNA-infected cells, the specific level of NKX2-2 or EWS/FLI in a particular cell dictates how "mesenchymalized" that cell is. Since lower NKX2-2 expression levels in tumors indicate a poor prognosis (Fig. 2.7), our in vitro data may have repercussions on patient survival. An interesting route of investigation is to perform single-cell RNA-seq from Ewing sarcoma samples. Such a survey will give us an idea of the level of heterogeneity with

respect to NKX2-2 expression, and perhaps shed light on what percentage of the tumor has an enhanced capacity to escape and migrate at baseline.

A possibility that has previously been suggested is that Ewing sarcoma cells may toggle expression of EWS/FLI and/or ZEB2 to accentuate mesenchymal or epithelial traits [13]. I propose here that NKX2-2 levels might also be toggled through EWS/FLI to drive transient re-differentiation into a cell type with manifest mesenchymal characteristics and to promote migration to a distal site. To investigate this, different fluorescent reporters may be engineered, through CRISPR-Cas9, into the endogenous NKX2-2 and ZEB2 loci. In this way, Ewing sarcoma cells xenografted into mice using the intratibial model may be monitored as they form the primary tumor, travel through the bloodstream, and establish a secondary site. The challenge here is catching the Ewing sarcoma cells during transit. While there is evidence that EWS/FLI induces CD99 expression, this seems to be a weak regulation [14]. Perhaps migrating Ewing sarcoma cells can be captured in the bloodstream using CD99, and the ratio of NKX2-2 to ZEB2 expression (i.e., fluorescence) may serve as the readout for whether the cell is more mesenchymal or more epithelial.

In the second part of my dissertation, with the understanding that NKX2-2 depends on other factors to perform its transcriptional roles, we asked who the NKX2.2 interaction partners are. Though not described in this manuscript, we addressed this question using an unbiased strategy. I expressed the abovementioned biotinylated 3xFlag::NKX2.2 construct in Ewing sarcoma A673 cells and performed tandem affinity purification, first with streptavidin, then with a Flag antibody [15]. Our mass spectrometry experiment did not identify any Gro/TLE family proteins or HDACs—protein interaction partners that we were expecting to see. As a result, we undertook a candidate approach that involved MTG16; the work comprises Chapter 3 of this dissertation. In summary, we identified two novel protein-protein interactions: NKX2.2

with MTG16, and NKX2.2 with itself. Both binding events are facilitated by the NKX2.2-TAD, suggesting that this domain is a competent protein-binding motif. While low expression levels of MTG16 prevented our further investigation of this complex in Ewing sarcoma cells, we and other groups demonstrated that NKX2.2 [6] and MTG16 (Fig. 3.5) are expressed at sufficient levels and are amenable to immunoprecipitation in βTC6 cells.

It has been previously suggested that pancreatic differentiation borrows many aspects of neural development, despite these two tissues originating from different germ layers (endoderm and ectoderm, respectively). The pancreas and the brain overlap significantly in many aspects, such as cellular physiology, gene expression, and modulation by the same transcription factors [16]. The demonstration that one such transcription factor, NKX2.2, has the capacity to interact with novel proteins through its TAD might allow us to ask broader questions about development and evolution. A possible future experiment might be to use the NKX2.2-TAD as a bait to identify protein interaction partners in Ewing sarcoma, developing β-islet cells, and neural progenitors. Are there any similarities in the interactomes of these different cell types? Do different TAD-harboring NK2 factors pull down different proteins? Surveying the interactions of proteins that co-evolved to function in the same complexes and pathways may give information that is as critical as defining the epistatic relationships of transcription factors and their targets. It is tempting to speculate that the developmental role of NKX2-2 in Ewing sarcoma might give clues to the function of a possible NKX2.2-controlled complex in the development of other tissues, such as the pancreas.

Unquestionably, the way forward is to be able to target Ewing sarcoma cells effectively and specifically. A small molecule inhibitor of LSD1, HCI2509, was developed in the laboratory of Sunil Sharma in collaboration with our group here at the Huntsman Cancer Institute. Ewing sarcoma cells treated with HCI2509 mimic the transcriptional

profile of EWS/FLI knockdown. Moreover, HCI2509 reduces colony formation in soft agar, increases caspase activity, and reduces the volume of tumor xenografts in nude mice, leading to greater survival [17]. Interestingly, treatment with the LSD1 inhibitor also causes Ewing sarcoma cells to display mesenchymal features in a dose-dependent manner. The cells do eventually die, presumably from blockage of LSD1-dependent EWS/FLI function [17]. It will be critical to ensure that, in the timeframe between the cells manifesting mesenchymal characteristics and cell death, Ewing sarcoma cells do not gain sufficient migratory capabilities to allow for tumor escape, transit, and establishment of a viable metastatic site. Perhaps a strategy to simultaneously target tumor cells with HCI2509 and with the miR-200 cluster to both inhibit LSD1 function and promote epithelialization through downregulation of ZEB2, respectively, may prove to be therapeutically useful. Importantly, our studies of the transcription factors EWS/FLI, ZEB2, and NKX2-2 have helped us understand the plasticity of Ewing sarcoma cells and may aid in the fine-tuning of treatment strategies currently being developed.

References

1. Smith R, Owen LA, Trem DJ, Wong JS, Whangbo JS, Golub TR, et al. Expression profiling of EWS/FLI identifies NKX2.2 as a critical target gene in Ewing's sarcoma. Cancer Cell. 2006;9(5):405-16.

2. Owen LA, Kowalewski AA, Lessnick SL. EWS/FLI mediates transcriptional repression via NKX2.2 during oncogenic transformation in Ewing's sarcoma. PLoS One. 2008;3(4):e1965.

3. Fadul J, Bell R, Hoffman LM, Beckerle M, Engel ME, Lessnick SL. EWS/FLI utilizes NKX2-2 to repress mesenchymal features of Ewing sarcoma. Genes Cancer. 2015;6(3-4):129-43.

4. Chaturvedi A, Hoffman LM, Welm AL, Lessnick SL, Beckerle MC. The EWS/FLI oncogene drives changes in cellular morphology, adhesion, and migration in Ewing sarcoma. Genes Cancer. 2012;3(2):102-16.

5. Chaturvedi A, Hoffman LM, Jensen CC, Lin YC, Grossmann AH, Randall RL, et al. Molecular dissection of the mechanism by which EWS/FLI expression compromises actin cytoskeletal integrity and cell adhesion in Ewing sarcoma. Mol Biol Cell. 2014;25(18):2695-709.

6. Papizan JB, Singer RA, Tschen SI, Dhawan S, Friel JM, Hipkens SB, et al. Nkx2.2 repressor complex regulates islet beta-cell specification and prevents beta-to-alpha-cell reprogramming. Genes Dev. 2011;25(21):2291-305.

7. Briscoe J, Sussel L, Serup P, Hartigan-O'Connor D, Jessell TM, Rubenstein JL, et al. Homeobox gene Nkx2.2 and specification of neuronal identity by graded Sonic hedgehog signalling. Nature. 1999;398(6728):622-7.

8. Muraguchi T, Tanaka S, Yamada D, Tamase A, Nakada M, Nakamura H, et al. NKX2.2 suppresses self-renewal of glioma-initiating cells. Cancer Res. 2011;71(3):1135-45.

9. Watada H, Mirmira RG, Kalamaras J, German MS. Intramolecular control of transcriptional activity by the NK2-specific domain in NK-2 homeodomain proteins. Proc Natl Acad Sci U S A. 2000;97(17):9443-8.

10. Hill JT, Anderson KR, Mastracci TL, Kaestner KH, Sussel L. Novel computational analysis of protein binding array data identifies direct targets of Nkx2.2 in the pancreas. BMC Bioinformatics. 2011;12:62.

11. Vlodavsky I, Gospodarowicz D. Respective roles of laminin and fibronectin in adhesion of human carcinoma and sarcoma cells. Nature. 1981;289(5795):304-6.

12. Vlodavsky I, Lui GM, Gospodarowicz D. Morphological appearance, growth behavior and migratory activity of human tumor cells maintained on extracellular matrix versus plastic. Cell. 1980;19(3):607-16.

13. Wiles ET, Bell R, Thomas D, Beckerle M, Lessnick SL. ZEB2 represses the epithelial phenotype and facilitates metastasis in Ewing sarcoma. Genes Cancer. 2013;4(11-12):486-500.

14. Rocchi A, Manara MC, Sciandra M, Zambelli D, Nardi F, Nicoletti G, et al. CD99 inhibits neural differentiation of human Ewing sarcoma cells and thereby contributes to oncogenesis. J Clin Invest. 2010;120(3):668-80.

15. Kim J, Cantor AB, Orkin SH, Wang J. Use of in vivo biotinylation to study protein-protein and protein-DNA interactions in mouse embryonic stem cells. Nat Protoc. 2009;4(4):506-17.

16. Arntfield ME, van der Kooy D. beta-Cell evolution: How the pancreas borrowed from the brain: The shared toolbox of genes expressed by neural and pancreatic endocrine cells may reflect their evolutionary relationship. Bioessays. 2011;33(8):582-7.

17. Sankar S, Theisen ER, Bearss J, Mulvihill T, Hoffman LM, Sorna V, et al. Reversible LSD1 inhibition interferes with global EWS/ETS transcriptional activity and impedes Ewing sarcoma tumor growth. Clin Cancer Res. 2014;20(17):4584-97.